REPORT DOCUMENTATION PAGE

Form Approved
OMB No. 074-0188

1. AGENCY USE ONLY (Leave blank)	2. REPORT DATE	3. REPORT TYPE AND DATES COVERED
	September 2003	Final (15 Aug 2000 - 15 Aug 2003)

4. TITLE AND SUBTITLE
Biochemical Studies and Optical Digitizer Development for Enhanced Orthopedic Footwear

5. FUNDING NUMBERS
DAMD17-00-1-0577

6. AUTHOR(S)
Vern L. Houston, Ph.D.

20040421 058

7. PERFORMING ORGANIZATION NAME(S) AND ADDRESS(ES)
Veterans Administration New York Harbor
Healthcare System
New York, NY 10010

E-Mail: vern.houston@med.nyu.edu

8. PERFORMING ORGANIZATION REPORT NUMBER

9. SPONSORING / MONITORING AGENCY NAME(S) AND ADDRESS(ES)
U.S. Army Medical Research and Materiel Command
Fort Detrick, Maryland 21702-5012

10. SPONSORING / MONITORING AGENCY REPORT NUMBER

11. SUPPLEMENTARY NOTES
Original contains color plates: ALL DTIC reproductions will be in black and white

12a. DISTRIBUTION / AVAILABILITY STATEMENT
Approved for Public Release; Distribution Unlimited

12b. DISTRIBUTION CODE

13. ABSTRACT (Maximum 200 Words)

Properly fitting, functional footwear is paramount for preventing foot/ankle discomfort and injury, and maintaining mobility of military personnel and veterans. Custom designed and manufactured orthopedic footwear is an essential component in treatment and rehabilitative care of persons with neuromusculoskeletal foot/ankle pathologies, biomechanical disorders and injuries, and systemic disorders, such as Diabetes Mellitus and peripheral vascular disease, complications from which affect the feet and ankles. Orthopedic footwear design is still based on pedorthists' subjective judgments, so the degree of fit and function attained and the quality of footwear produced are inconsistent, and highly dependent upon the level of training, experience, and skill of the pedorthist involved. The objective of this project was to develop quantitative methods for effective, expeditious, repeatable, and consistent design and manufacture of well-fitting, comfortable, and functional orthopedic footwear. To accomplish this: (1) a 3-D optical digitizer capable of rapidly and accurately scanning peoples' feet and ankles in natural and prescribed alignments, in partial and full weight bearing states, with preservation of anatomical fiduciary landmarks' spatial location, was developed; and in concert (2) biomechanical studies were performed: (i) to derive measures quantifying footwear fit; (ii) to derive quantitative design specifications for footwear orthopedic components and modifications; and (iii) to determine the mechanical characteristics of insole materials and designs.

14. SUBJECT TERMS
Pedorthics. Foot. Shoes. Biomechanics. 3-D digitization, Computer-Aided Design and Manufacture

15. NUMBER OF PAGES
62

16. PRICE CODE

17. SECURITY CLASSIFICATION OF REPORT	18. SECURITY CLASSIFICATION OF THIS PAGE	19. SECURITY CLASSIFICATION OF ABSTRACT	20. LIMITATION OF ABSTRACT
Unclassified	Unclassified	Unclassified	Unlimited

AD_____

Award Number: DAMD17-00-1-0577

TITLE: Biochemical Studies and Optical Digitizer Development for Enhanced Orthopedic Footwear

PRINCIPAL INVESTIGATOR: Vern L. Houston, Ph.D.

CONTRACTING ORGANIZATION: Veterans Administration New York Harbor Healthcare System
New York, NY 10010

REPORT DATE: September 2003

TYPE OF REPORT: Final

PREPARED FOR: U.S. Army Medical Research and Materiel Command
Fort Detrick, Maryland 21702-5012

Table of Contents

Introduction — Properly fitting and functioning footwear is essential for prevention of foot and ankle injuries, and for maintenance of maximum mobility of military personnel, veterans, and persons in the civilian population. This is especially true for women, who have historically been plagued with foot and ankle problems caused by ill-fitting footwear. In studies of US military personnel, it was found that female personnel suffer a disproportionately high incidence of musculoskeletal injuries during basic training compared to their male counterparts (as high as 10:1). Ill-fitting, inadequately functioning footwear was found to be a principal factor causing this high incidence of trauma [Ross and Woodward 1994; Reinker and Ozburne 1979]. Correspondingly, the American Orthopaedic Foot and Ankle Society reported in 1993 that of 356 women surveyed in the United States, 20 to 60 years of age, without a history of traumatic injury, arthritis, or diabetes, 73% had suffered foot–ankle problems ranging from pain to deformities caused by ill-fitting footwear [Frey, et al. 1993, 1995]. Conversely, properly fitting and functional orthopedic footwear has been shown to be a crucial part of the rehabilitative treatment and care of persons suffering neuromusculoskeletal disorders, and/or systemic diseases, such as Diabetes Mellitus and arthritis, that adversely affect the feet and ankles, [D'Ambrosia 1987; Riddle and Freeman 1988; Rodgers and Cavanagh 1989; Boulton et al. 1993; Boulton 1998; Coleman 1993; Gould 1982; Janisse 1998, 1993; Moncur and Shields 1983; Tovey and Moss 1987; Wosk and Voloshin 1985; Mueller 1999; Kelly, et al. 2000]. In such cases well-fitting, functional, comfortable footwear can be the difference between independent, unaided mobility, and forced reliance upon crutches, or confinement to a wheelchair, or for patients with chronic diabetes and peripheral vascular disease, prevention of pedal ulceration, necrosis, gangrene, and consequent amputation, Figure 1.

Unfortunately, design and manufacture of (orthopedic) footwear has remained a slow, laborious, almost exclusively subjective process. Use of quantitative information in design, construction, and fitting of footwear is limited, typically involving no more than heel-to-toe length and metatarsal ball width measurements. Consequently, the quality of footwear design, manufacture, and fit is highly dependent upon the level of training, experience, and skill of the pedorthist(s) involved. The level of pedorthic care patients receive thus varies immensely across the United States and around the World. This is underscored by results from VA NYHHS Rehabilitation Engineering studies which showed that variations as high as 58% may be encountered in the values of pedal segmental volumes, cross-sectional areas, and linear and circumferential dimensions clinically measured and recorded by different practitioners for the same subject; and variations of 24% and more are encountered in measurements repeatedly taken of the same subject by a given pedorthist/orthotist/prosthetist [Houston, et al. 1998a]. These inter- and intra-practitioner variations and errors in characterization of the geometry of patients' feet and ankles significantly increase the amount of work and time required, both by the pedorthist and by the patient, enduring numerous trial-and-error design/production/fitting iterations, before "acceptably" fitting, "tolerably" comfortable, and "reasonably" functional footwear is finally obtained. More exacting, quantitative measurements and instrumentation to more accurately characterize pedal geometry, morphology, and biomechanical function are needed. Furthermore, few, if any, controlled, quantitative investigations have been reported in which quantitative specifications and design principles for orthopedic footwear, footwear components and modifications, have been presented. Research is thus needed that will contribute to the development of improved, standard procedures and equipment enabling effective, efficient, expeditious, and consistent design and manufacture of better fitting, more functional and comfortable footwear for US military personnel, veterans, and civilians.

The objective of this project was to develop knowledge, equipment, and procedures that will contribute to the quantitative design and manufacture of well-fitting, comfortable, and functional orthopedic footwear. A 3-D optical digitizer was developed that can rapidly, accurately, repeatably, and consistently digitize peoples' feet and ankles in natural and prescribed orthopedic alignments, in partial and full weight bearing states, registering the spatial location of fiduciary anatomical landmarks, the data from which can be imported into a pedorthic CAD/CAM system for design and manufacture of custom (orthopedic) footwear. In addition, biomechanical studies were conducted: (i) to derive measures quantifying footwear fit (especially for assessment of the fit of footwear for female military personnel); (ii) to derive quantitative design specifications for orthopedic footwear components and modifications; and (iii) to characterize the mechanical properties and performance of footwear insole materials.

Research Performed

The project research was divided into six constituent tasks: (1) Pedorthic Optical Digitizer Development; (2) Quantification of Footwear Fit; (3) Assessment of Military Footwear/Last Design and Fit; (4) Footwear Biomechanical Studies; (5) Footwear Material Mechanical Testing; and (6) Summary Analysis and Documentation of Results.

Pedorthic Optical Digitizer Development — Specifications for a pedorthic optical digitizer were prepared, estimates were solicited, and a contract for procurement of the requisite components was issued in the first year of the project. The components were received at the beginning of the second year of the project. They were subsequently assembled, calibrated in situ, and laboratory tested with a range of geometric phantoms. Work on development of software for control of the digitizer, and for measurement acquisition, processing, and storage was conducted over the duration of the project. Development of software for import of the optical scan measurements into the VA Pedorthic CAD/CAM System [Houston, et al. 1998b] for visualization and analysis of the measurement data, and for use in design and manufacture of custom orthopedic footwear, was performed in the second and third project years. The ALDIR software developed by the investigators in their Prosthetics–Orthotics research for detection, identification, and registration of the spatial locations of fiduciary anatomical landmarks, was also adapted and tested in the second and third project years.

The pedorthic digitizer developed, Figure 2, consists of three scan heads (two dorsal heads and a single plantar head), mounted on synchronized, servo motor driven, horizontal translation rails, controlled by a personal computer, which also serves as the measurement acquisition, processing, and storage platform. The two dorsal scan heads each contain a 15 milliwatt, 632.8 nm wavelength (near–infrared), helium–neon laser. The plantar scan head contains a 780 nm wavelength (infrared) laser, that is invisible to the two dorsal heads. In addition, each scan head also contains two 740x480 pixel charge coupled device (CCD) cameras (one for capture of spatial range information and the other for capture of color (RGB) information), a prism, mirrors, and associated optoelectronics, housed circumferentially around the inside periphery of the head.

To digitize a person's foot and ankle, capturing its spatial geometry and surface topography, the person is positioned on the digitizer's walkway, standing between the support bars with his/her foot and ankle anatomically aligned and centered "as best as possible" in the 30 cm high x 30 cm wide x 50 cm long scannable spatial envelope between the medial and lateral scan heads, directly over the plantar scan head, while either: (i) suspended in a non-weight bearing state; or (ii) resting on a transparent, low reflectivity lucite platen in a semi-weight bearing state; or (iii) supported on a transparent platen in a full-weight bearing state. The medial scan head views the

mediodorsal aspect (including the arch) of the person's foot and ankle, from a perspective orthogonal to the sagittal plane through the heel and toes. The lateral scan head views the laterodorsal aspect of the foot and ankle, from a perspective orthogonal to the pedal heel–toe axis, but inclined at 22.5 deg above the horizontal to enable the dorsum of the foot to be captured. The plantar aspect of the foot is digitized by the plantar scan head through a transparent glass or plastic platen, upon which it is supported in partial or full weightbearing.

Upon initiation of scanning, light is emitted from the laser in each scan head and transmitted through the prism in the head's optical assembly, where it is refracted into a plane and transmited around the scan head perimeter to the opening in the housing, where it is projected radially outward onto the person's foot–ankle, Figure 3. The resulting constituent planar segments of light projected from each head onto the top, sides, and plantar surfaces of the foot and ankle, converge to generate a continuous vertical plane of light, incident 360 degrees around the foot. The laser light specularly reflected from the person's foot–ankle travels back to the heads, where it is in turn reflected via the scan head mirrors, back to the optical assembly, where it is focused onto the scan head cameras' CCD arrays. The mirrors in the scan heads are aligned so that the specularly reflected light is viewed by the cameras from ±22 deg perspectives on either side of the incident plane. The cameras in each scan head are electronically poled, and the addresses of the illuminated CCD pixels and their respective intensities are output to the digitizer computer. The signals from the contralateral and ipsilateral images are averaged when signals from both views are present, or passed through, if only one signal is present. This enables pedal contours that are hidden from one perspective, but seen by the other, such as in concavities around the malleoli, in tissue folds, and near hammer toes, to be captured and preserved. The resultant output signals from each camera are post-processed through empirical compensation filters to correct for nonlinearities in the respective scan head's optics. The corrected output signals, together with the respective poling information (i.e., CCD array illuminated pixel row and column addresses), are then mapped via a triangulation algorithm relating equivalent camera pixel optical origin and scan head location to the respective digitizer scan field (x,y,z) spatial coordinates of the foot–ankle surface.

As scanning proceeds, the heads are synchronously driven by the computer controller at the user selected (constant) speed along the horizontal translation rails. As the heads move along the rails from the crest of the heel to the distal border of the toes, vertical cross–sections of the person's foot–ankle are sequentially digitized. The surface contours over the person's foot–ankle are sampled at 30 frames per second at resolutions of better than or equal to 0.5 mm radially in 400 angular increments (from the cameras). The data acquired from the scan heads are then mathematically combined into 256 points, uniformly distributed around each pedal cross section. Where the data from the medial and lateral dorsal heads and the plantar head overlap, the measurements are smoothed using a moving average, least mean square filter to derive the best continuous estimate of the respective pedal cross–sectional contour. The incremental spacing between digitized cross–sections is determined by the speed at which the scan heads are driven along the translation rails. Speeds yielding incremental spacings of 0.5 mm to 5.0 mm, to within an accuracy of greater than ±0.1 mm, can be selected by the digitizer operator. For an incremental spacing between cross sections of 1.0 mm, 9 seconds are required to digitize 69,120 points over a person's foot–ankle that is 27 cm long.

Upon completion of the scan, the measurement data are displayed as a pixel image, allowing the operator to interactively select longitudinal and latitudinal borders, inside of which the data will be kept and outside of which it will be discarded. This allows the points in the scan field

containing little to no information about the foot and ankle, i.e., for which the signal-to-noise ratio is very small, to be discarded, so the size of the resulting measurement file that is post-processed through a bandpass filter to remove high frequency optical and electrical noise, and then saved, is minimal.

To identify anatomical fiduciary landmarks and patient specific ad hoc landmarks, the automated landmark detection, identification, and registration (ALDIR) software previously developed by the VA NYHHS Rehabilitation Engineering researchers in their Prosthetics–Orthotics research was adapted [Houston, et al. 1995, 1998b]. The landmark detection part of the algorithm was implemented as a two layer neural network with log–sigmoid neurons in a 120–25–1 I/O ratio, and the identification part of the algorithm was implemented as a maximum likelihood filter, to predict the identity of the respective "detected" markers relative to an anthropometric template, Figure 4. The scan head camera range data and landmark data are subsequently concatenated and stored in the scan subject subdirectory in the file format selected by the operator (typically the floating center, cylindrical coordinate format used in the VA Pedorthic CAD/CAM System, or the fixed center cylindrical coordinate format used in most prosthetics–orthotics CAD/CAM systems). From this subdirectory the measurements can be transmitted to a designated CAD workstation or central fabrication facility for footwear design and manufacture.

Pedal support platens, shaped to match orthopedic footwear plantar contours, were designed and prototypes fabricated from transparent, low refractive index Lucite, with 0.25 inch, 0.50 inch, and 0.625 inch heel heights, respectively, in a range of instep sizes. Laboratory tests measuring the platen's transmissivity and refractivity were performed, and an algorithm for compensation of scan image refraction was developed. Clinical tests with the prototype platens, showed significant measurement corruption from spurious signals from multiple reflections of the incident laser light, Figure 5. To circumvent these difficulties and minimize measurement errors, the laser in the plantar scan head was changed from a 632.8 nm near–infrared laser, to a 780 nm infrared laser, invisible to the two dorsal scan head cameras. In addition, the power of the plantar scan head laser was reduced by 50%, and the thickness of the support platens reduced to 6.25 mm to mitigate spurious, multiply reflected signals. A black silhouette was also generated and placed on the support platen along the lateral border of the subject's foot before scanning to reduce multiply reflected, refracted signals from the lateral dorsal head. With the introduction of these modifications, good quality, accurate scans of test subjects' feet–ankles were able to be obtained, Figure 6.

Quantification of Footwear Fit — To establish a reference for quantification of footwear fit, US military footwear Lasts for female personnel, and for male personnel for oxford style shoes, were obtained from the Defense Logistics Agency, Defense Personnel Service Center (DLA DPSC). 144 of these Lasts were digitized with the optical digitizer. The resulting digitized measurement files were compiled in the project computerized database, and entered into the Last Library of the VA Pedorthics CAD/CAM System. Comparative analysis of the resulting scans for a range of sizes, showed the Lasts to be algebraically scaled, Figure 7. Clinical experience has shown feet of normal, healthy individuals do not algebraically scale by more than ±2 sizes without significant error. The fact that DLA DPSC Lasts are algebraically scaled by more than two sizes may contribute to the improper fit of military footwear for many soldiers, especially female personnel, thus increasing their susceptibility to foot and ankle injury during basic training and active duty.

In addition to this work, summary statistics were tabulated from the medical and pedorthic records (including orthopedic Last style and dimensions, shoe modifications and upper patterns)

of 290 "representative" pedorthic patients' from the VA National Footwear Center. The resulting data was analyzed in the first project year to establish common regions of the foot–ankle with relative low load tolerance, and higher susceptibility to injury, biomechanical disorders, and neuromusculoskeletal pathologies, Table 1.

To quantify pedal/footwear dorsal interface stresses during stance and gait in "ill-fitting" versus "well-fitting" footwear, a Tekscan, Inc. IScan stress measurement system was procured. Calibration and laboratory testing of 27 IScan Model #6910 miniature FVR array transducers, however, failed to yield a single transducer with a sensel array with at least four of the nine elements measurable over the range of pressures encountered at the foot/shoe interface. Use of the IScan transducers to measure pedal dorsal stressess, therefore, was abandoned. In their place, single element Flexiforce, FVR transducers were procured, calibrated, and used to measure pedal dorsal interface pressures in synchrony with 960 element FScan transducers measuring pedal plantar pressures, in "well-fitting," and in "ill-fitting," footwear during stance and gait, Figure 8. Analysis of the resulting data showed minimal differences between dorsal pedal normal stresses in "uncomfortable/painful" shoes, and "comfortable" shoes. Specifically, the measured differences between pedal dorsal pressures deemed "uncomfortable" and those deemed "comfortable" was found to lie near or within the level of variability encountered between respective values in each class, measured in repeated gait trials. These findings substantiate results from the investigators' finite element modeling and analysis studies showing that, except in cases of catastrophic conditions when loads exceed the yield point and critical strength of tissues, and thus cause mechanical failure and trauma, differences between "comfortable" and "uncomfortable" stress and strain levels are minimal. Meaningful differences occur only with respect to the non-elastic, strain energy densities produced in the tissues by repetitive loading, Table 4. This implies that to avoid podalgia, fascitis, and pedal tissue trauma from repetitive mechanical loading, new footwear materials and designs are needed that distribute and dissipate strain energies, preventing them from being transferred to and dissipated in soft pedal tissues.

Assessment of Military Footwear Fit — To assess the fit of US Military footwear, 51 normal, healthy female subjects and 25 male subjects of military service age (18 to 45 years of age) were recruited, and scans, casts, and a set of 23 manual measurements, were acquired of their feet and ankles, Table 2. The parameters measured in the optical scans and those recorded manually comprise the metrics most commonly used in pedorthic Last grading, together with the principal pedal dimensions measured in the comprehensive anthropometric survey of the lower limbs of 867 US military personnel [Parham, et al. 1992]. A comparative analysis of the resulting data was performed to identify the regions that evidence good conformance, and those that exhibit poor compliance, between the subjects' feet and ankles and the respective US Military Lasts obtained from the DLA DPSC (and by extension the footwear manufactured from these Lasts that would be issued to the subjects under current military practice), Figures 9 and 10. Special attention was given to the measurements at the subjects' metatarsal heads (ball of the foot) and at their heels, as successfully fitting and functional footwear requires intimate compliance in these regions. (If footwear dimensions are too narrow at the ball, the repetitive stresses and strains incurred during gait will quickly result in podalgia and trauma. Similarly, if footwear dimensions are too narrow at the heel, the foot will be pushed forward in the shoe, impinging on the metatarsals and toes, also causing pain and trauma. If footwear is too wide at the ball and/or heel, a pseudoarthrosis will exist, the foot and ankle will not be properly supported, and the foot will slide anteroposteriorly and/or mediolaterally, decreasing the person's stability, and increasing his/her susceptibility to trauma.)

When the sizes of footwear available are limited, to obtain a fit that will accommodate the person's foot, the solution most often employed is to go up (or down) one or more sizes in length. This is far from ideal, however, and may give rise to additional complications further exacerbating the problem. As seen in Figure 11, the maximal ball width of US Military Lasts sized with respect to the heel-to-toe length of a person's foot (allowing approximately 7 mm clearance at the distal end of the toes) lies approximately $6*L_B$ mm anterior to the maximal ball width of the foot. This was found to occur for all of the subjects tested. Going to a larger size shoe in an attempt to accommodate a wide foot, only moves the maximal ball width of the shoe further forward, decreasing support of the foot and increasing the likelihood of tripping because of the increased length. When the shoe is too wide for a person's foot, decreasing the length of the shoe to reduce the ball width, eliminates clearance for the toes, and thus increases the likelihood of phalangeal discomfort, pain, and trauma. US Military Lasts, therefore, especially for female personnel, need to be rectified to coincide more closely with anatomical dimensions, viz., for each Last size (heel-to-toe length), the heel-to-ball length should be decreased and the ball-to-toe length increased a corresponding amount, to effectively shift the maximal ball width of the Lasts posteriorly to correspond more closely with pedal morphology.

Analysis of the scans and measurements of the project test subjects, revealed that their pedal shapes and dimensions were generally classifiable as being in one of three basic categories: (i) narrow; (ii) average; or (iii) wide, Figure 12, with only the average class evidencing good conformance with the US Military Lasts (i.e., total fit error function values ≤ 8 mm, Figure 20). It was further observed that the respective pedal shapes in these categories were bounded by: (1) "U" type shapes, that are proportionally wide across the metatarsals as well as across the heel; and (2) "V" type shapes, that are proportionally much wider at the ball than at the heel, Figures 13 and 14. The arithmetic average pedal dimensions and shape in each of these classes lay between respective "U–V" bounds, Figure 14. In addition, analysis of the scans and measurements of the subjects' heel width measured at their medial malleoli posterior distal border (W_{MalPDB}), viz, at $(x, y)_{MalPDB} = (0.333*L_B , 0.25*L_B)$, and in the same cross sectional plane at the height below $0.25*L_B$ of maximum width (W_{Max}), normalized by each subject's respective foot heel-to-ball center length (L_B), Figure 15, shows approximate Gaussian distributions with sizable dispersions (mean $W_{MalPDB}/L_B \pm\sigma_W = 0.3605 \pm 0.02785$ mm/mm, and mean $W_{Max}/L_B \pm \sigma_{Wmax} = 0.4034 \pm 0.02290$ mm/mm), Figure 16a. The differences in the distributions of W_{MalPDB} and W_{Max} reflect variations in the subjects' heel shapes. W_{MalPDB} and W_{Max} are seen to evidence reasonably strong, although not perfect, correlation, with $R^2_{W_{MalPDB}-W_{Max}} = 0.635$), Figure 16b. On the other hand, plotting the subjects' normalized proximal heel width W_{MalPDB}/L_B versus their normalized ball width W_{Ball}/L_B shows a wide dispersion of values with weak to negligible correlation, $R^2_{W_{MalPDB}-W_{Ball}} = 0.2509$, Figure 17. This reflects the fact that peoples' foot–ankle shapes and dimensions vary significantly, and are **not** algebraically scaled. Comparison of the subjects' normalized proximal heel width (W_{MalPDB}/L_B) and normalized maximal heel width (W_{Max}/L_B) with the corresponding measures for the US Military Lasts that fit the subjects the "best" with respect to heel-to-toe length and ball width, further underscores this fact. The US Military Lasts, which are algebraically scaled, have a constant heel width/ball length ratio, whereas the test subjects' feet evidence a reasonably wide range of values, that are approximately Gaussian distributed, Figure 18. Although the subjects' normalized maximal heel widths are larger than the values of the corresponding Lasts, when the midball length of the Lasts are rectified to more closely match pedal anatomical values, (i.e., moved posteriorly as previously noted) the means become closer. Figure 18 shows that to better

fit a broader range of subjects' feet, the US Military Lasts need to be augmented to incorporate multiple heel widths as well as ball widths. This is evident in Figure 19 in the plot of normalized ball width versus heel width for the test subjects' feet versus corresponding normalized widths for the US Military Lasts. The pedal widths of the test subjects are widely scattered. The respective values for the US Military Lasts, shown for ball widths AA through EEEEE, are seen to be derived as a linear least squares regression for an anthropometric sample of subjects. Although the US Military Lasts divide the pedal data well, yielding approximately equal numbers of subjects above and below the regression line, the fit afforded to subjects' feet outside of $\pm 1.0\sigma_W$ is seen to be poor. A better solution, providing a better fit around the metatarsals and ball of the foot **and** at the heel, for a much larger range of subjects can be derived by considering the "U–V" limiting pedal shapes defined in Figures 13 and 14. By defining respective "U"–shape and "V"–shape regression lines and judiciously selecting Last data points, a better fit for a much broader range of subjects can be obtained, Figure 19. This is further born out by the respective values of the total fit error function (TFE), defined as the arithmetic sum of the absolute value of the difference between the subject's foot dimensions and the corresponding dimensions of the best fitting Last with respect to the eleven most commonly used Last grading metrics given in Table 3. A comparative plot of the resulting TFE values obtained for the project test subjects and US Military Women's Lasts for: (1) a single ball width (size C); (2) for the full set of orthopedic ball widths (size AAAAA through EEEEE); and (3) for a set of ten "U–V" Lasts with multiple ball and heel widths, is shown in Figure 20. The results are plotted for the cumulative percentage of subjects with TFE less than the abscissa value shown. The "U–V" Lasts are seen to fit over 80% of the subjects with a TFE of less than 4 mm, and 95% of the subjects with a TFE of less than 9 mm. In comparison, having Lasts (and footwear) available in only a single ball and heel width is seen to accommodate only 38% of the subjects before the fit becomes unacceptable (i.e., when TFE > 8 mm), whereas the "U–V" Lasts accommodate 94% of the subjects before they reach a TFE > 8 mm, and the US Military Lasts with a full range of 13 orthopedic ball widths and a single heel width accommodate 88% of the subjects before TFE > 8 mm.

These results show that to properly accommodate and fit people's feet, footwear needs to be manufactured in several sizes of heel width, for each respective heel-to-toe length and metatarsal ball width size. Doing so significantly enhances footwear fit and functional performance, and will reduce the incidence of foot and ankle injury sustained by military personnel (particularly female personnel) during basic training and subsequent active duty. Furthermore, by employing a anthropometric "U–V" Last sizing scheme, this can be accomplished without increasing the number of Lasts required per heel-toe length size.

Footwear Biomechanical Studies — Investigations measuring pedal/footwear interface stresses, ground reaction forces, and subject body segment kinematics during stance and gait, while wearing footwear with commonly prescribed orthopedic components and modifications, were performed. Tests were conducted with five subjects measuring pedal dorsal and plantar regional interface stresses, ground reaction forces, step and stride lengths, velocities and accelerations, and limb and body segment kinematics using Tekscan FScan and Flexiforce pedal stress transducers, a CIR Systems GaitRite Electronic Walkway, a Kistler force plate, and a Qualisys 3-D Video Motion Analysis System. Studies were performed to quantify the effects of three common orthopedic footwear components — scaphoid pads (arch supports), metatarsal pads, and heel pads. The effects of variations in pad thickness and longitudinal and latitudinal dimensions were investigated and categorized as a function of resulting interface stress and subject comfort rating, Figure 21. Study results showed that the pads affected pedal loading in the regions of respective

application, as well as in adjacent regions. Although the differences in the stresses produced by the different pads often were not large, their affects on the subject's level of comfort varied markedly. Pedal sensitivity to small changes in loading evidenced by the test subjects, can thus be a major complication in pedorthic treatment, both for patients with pedal neuromusculoskeletal and vascular disorders with hypersensitivity, and for those with hyposensitivity, such as diabetics with peripheral neuropathy.

Studies were also performed on the effects of shoe outer sole modifications (sole wedges and heel wedges) on pedal/footwear interface stress magnitudes, load spatial distribution, load temporal duration, and associated lower limb kinematics. The results of variations in sole and heel wedge thickness showed that 8mm sole and heel wedges effectively reduce the loading on the respective side of the foot on which they are applied, Figure 22. Wedges of decreasing thickness were seen to evidence less effect, until at 2mm thickness their effect was negligible. The effects of rocker soles on pedal plantar stress magnitudes, load spatial distribution, temporal load duration, and lower limb kinematics, were also studied as a function of rocker radius of curvature and fulcrum position. Study results showed that rocker soles, depending upon the location of the fulcrum and the angle of inclination of the rocker, can effectively unload the metatarsal heads and shorten the heel rise-to-toe off phase of the gait cycle, but doing so increases the loading incurred in the midfoot. Similarly, the effects of variation in shoe outer sole width were investigated. As shown in Figures 23 – 25, extended width soles and heels can be used to augment the stability of subjects with neuromuscular impairments, particularly diabetics suffering peripheral neuropathy. Increased sole–heel widths of ½ inch (¼ inch per side) were found to measurably augment the stability of neuropathic subjects, smoothing the trajectory of their center of mass, enabling a more normal, less strenuous, energy efficient gait (with a more normal percentage of single limb support vs. double limb support time over the gait cycle). Further increases in width above ½ inch, although helpful for supplementation of mediolateral stability, were counter productive in some subjects with narrow base gaits, leading to striking of the contralateral heel during the swing phase of gait. Increases in width smaller than ¼ inch were found to afford minimal to negligible effects on stability.

In further biomechanical studies, the compressive creep response of the pedal plantar tissue at the heel and at the first metatarsal head of eight subjects' feet were measured using the VA NYHHS servo-optoelectromechanical tissue indentor [Houston, et al. 1998c], Figure 26. Magnetic resonance (MR) scans of two of the subjects' feet were also acquired, Figure 33, and the resulting MR images segmented with respect to tissue morphology and digitized. Corresponding nonlinear, finite element (FE) segmental models of the subjects' feet were developed at their heels and at their first metatarsal heads from the MR images and respective tissue mechanical properties. The FE models constructed were used to analyze the stresses and strains incurred at the heel and at the metatarsal heads under normal loading conditions, and in the presence of a vertical calcaneal osteocyte (heel spur), as a function of pedorthic insole treatment for a range of material stiffnesses and design geometries, Figures 27 – 31, Tables 4 and 5. Results from these studies show maximum stresses and strains in pedal plantar tissues occur directly underneath and adjacent to bone (i.e., the calcaneus and first metatarsal head). Alteration of insole material, with stiffnesses varying from 1x to 10x that of pedal tissue, was shown to have minimal effect. Alteration of insole design geometry by introduction of reliefs, either removing material or by incorporation of softer secondary materials under the center of the heel and metatarsal heads (as is common in clinical practice) was also shown to only minimally affect tissue stresses and strains. Incorporation of appropriate reliefs did, however, slightly reduce associated strain energy densities in the tissues. Because of the Dunnell effect, use of non-contoured, cylindrical reliefs was shown to cause large localized stresses, strains, and stress gradients in pedal tissues at the border of the relief. Such design geometries must, therefore, be avoided. The greatest

reductions in stress, strain, and strain energy magnitudes were achieved by custom contouring of insoles to match patients' "natural" pedal tissue geometry, in concert with proximally extending the insole borders around the fat pad to constrain its rheological displacement under load. Production of orthopedic insoles for personnel with this optimal design geometry constructed out of a viscoelastic material three to four times the stiffness of their pedal plantar tissues, was shown to enable reductions as high as 50% in maximum stresses and strains, and 90% in maximum strain energy densities, during stance. In pathologic cases with calcaneal osteophytes (heel spurs) and/or arthritic osseous deformities with vertical components, reductions of as much as 95% in tissue stresses and strains, and 98% in strain energies densities were shown to be attainable in stance with custom contoured insoles that constrain soft pedal tissue displacement.

Footwear Material Mechanical Testing — Samples of the four materials most commonly used in manufacture of orthopedic insoles (i.e., polyurethane foam, polyethylene foam, silicone, and ethyl vinyl acetate foam (EVA)) were obtained. Specimens of each material in two different densities (Shore Hardness durometers) were prepared, and mechanical tests were performed in accordance with ASTM prescribed procedures, measuring the materials' respective mechanical stiffnesses in creep and stress relaxation under normal and shear loads, Figure 32. Measurement of the respective materials' load damping response, impact response, hysteresis, and plastic deformation (set) were also measured. Results from the material creep and stress relaxation response tests were used in the project FEA pedal plantar tissue biomechanical loading studies described in the previous section. Sample insoles of the respective materials were also prepared and tested under static, axially applied loads (approximately $\frac{1}{4}^{th}$ body weight) with one experimental subject in the VA NYHHS magnetic resonance scanner, Figures 33 and 34. The MRI scan results were used to compute the values of pedal tissue strain incurred during static, axial loading as a function of pedorthic insole stiffness and design geometry.

To improve pedorthic treatment for subjects suffering metatarsalgia, plantar fasciitis, heel spurs, and/or chronic Diabetes with Charcot conditions of their feet and ankles, additional footwear design studies were conducted. Initial designs for footwear outer soles incorporating cushions under the heel, the metatarsal heads, and/or the midfoot were developed, Figure 35. As seen in Figure 33, the designs formulated mimic the anatomical structure of the pedal plantar fat pad, incorporating sealed, "honey comb" like septae, which function like miniature fluid damping cylinders to dissipate and disperse locally applied loads. Molds were made from the respective CAD design drawings, and initial prototype heel sole cushions were fabricated in a range of durometers. In addition, 3-D, sectional FE models of the cushions were generated to study the effects of cushion material stiffness, septal wall thickness, and septal cylinder internal fluid media, on load damping and dispersion performance. Unfortunately the FE models proved to be numerically conditionally stable. Slight variations in the loads applied resulted in different modes of columnar buckling, with major differences in consequent stress and strain magnitudes and distributions. This work is continuing.

Key Research Accomplishments

- Specifications were developed, components procured, and a prototype 3-D Pedorthic Optical Digitizer assembled, calibrated, and successfully laboratory and clinically tested.
- The software required for: (i) control of the digitizer; (ii) measurement acquisition, processing, analysis, visualization, and registration; and (iii) for post-processing of digitizer measurements for detection, identification, and registration of pedal fiduciary anatomical landmarks, was created and tested.

- 144 US military footwear Lasts were digitized with the optical digitizer, and the resulting measurement files entered into the VA NYHHS Pedorthic CAD System Last Library, and into the project pedorthic database.
- Optical scans and manual measurements of the feet and ankles of 51 normal, healthy female and 25 male test subjects of military service age, were acquired and used in quantitative assessment of military footwear/Last fit. Analysis of the scans and measurements showed that US Military Lasts/footwear properly fit only one third of the subjects. New Last designs incorporating multiple heel widths in addition to heel-to-toe length and metatarsal ball width sizes need to be developed and used to manufacture footwear for US military personnel. A "U–V" design scheme for such Lasts was developed based on pedal anthropometric measurements.
- The compressive creep response of eight subjects' pedal plantar tissues was measured. Magnetic resonance (MR) scans of two of the subjects' feet were acquired and digitized, and the results used to create sectional finite element models of their feet at the heel and at the first metatarsal head. The FE models developed were used in studies to optimize pedorthic insole design for prevention and treatment of podalgia, metatarsalgia, plantar fasciitis, and calcaneal osteocytes. The resulting FE model calculations of pedal plantar tissue stresses and strains, together with MR scan measurement of actual tissue strains, show only insoles custom contoured to match individuals' pedal morphological shapes, and which limit pedal soft tissue displacement, effectively reduce stresses, strains, and strain energies in pedal plantar tissues. The project FEA study results further provide convincing evidence that non-recovered (inelastic) strain energy dissipated in pedal tissues, is responsible for chronic, repetitive loading injuries, and not the magnitude of the applied stresses, as commonly assumed, (providing load magnitudes are below the yield point and critical strength of the tissue involved). Measured levels of pedal tissue plantar and dorsal stress deemed "comfortable" versus those deemed "uncomfortable" by normal, healthy test subjects show a very fine level of demarcation. This complicates pedorthic treatment, and further indicates tissue strain plays a more significant role than stress in limiting comfort/discomfort and trauma at load magnitudes below yield and critical strength levels.
- In biomechanical studies, measurements were acquired for analysis and quantification of the effects of three orthopedic components – scaphoid pads, metatarsal pads, and heel pads – on (i) pedal/footwear interface stress magnitudes, gradients, temporal duration, and spatial distribution; (ii) on ground reaction force magnitudes, locations and durations; and (iii) on lower limb kinematics. Similarly, the effects of shoe outer sole and heel wedges; rocker sole radius of curvature and fulcrum position; and of shoe outer sole and heel width, on pedal/footwear interface stresses, ground reaction forces, and limb kinematics were investigated. Results showed that orthopedic footwear components and modifications can and do affect loading in their regions of application, as well as in adjacent pedal regions. Furthermore, the differences in the stresses produced by parametric variations in the respective orthopedic components/modifications typically are not large, but their corresponding effects on subjects' level of comfort/stability can change significantly.
- The creep response and stress relaxation response (characterizing the mechanical stiffness) of four of the most commonly used pedorthic insole materials were measured; magnetic resonance scans of the feet of two test subjects statically, axially loaded wearing insoles, fabricated from the respective materials in a range of design geometries, were acquired. Measurement of tissue strains from the MR scans, together with results from the project FEA

analyses show that reductions in pedal tissue stresses, strains, and strain energies afforded by pedorthic insole materials with different durometers and elasticities are small. The greatest reductions in stress, strain, and strain energy are obtained by custom contouring insoles to match persons' "natural" pedal tissue contours and by extending the insole borders proximally around the pedal fat pad to constrain its rheological displacement under load. Production of orthopedic insoles for personnel with this optimal design geometry out of a viscoelastic material three to four times the stiffness of the person's pedal plantar tissues, enables reductions as high as 50% in maximum tissue stresses and strains, and 90% in maximum strain energy densities, to be achieved. In pathologic cases with calcaneal osteophytes (heel spurs) and/or arthritic osseous deformities, reductions of as much as 95% in tissue stresses and strains, and 98% in strain energies densities can be attained with optimally designed insoles matched to the individual's pedal morphology.

Reportable Outcomes

Manuscripts & Abstracts

- Houston VL, Luo G, Mason CP, Mussman M, Garbarini MA, Beattie AC, Cruise CM, Thongpop C. "FEA Optimization of Pedorthic Insole Design for Patients with Diabetes Mellitus." **Proc. 10th World Congress ISPO**, Glasgow, UK, July 2001; Tho10.7.
- Houston VL, Luo G, Mason CP, Mussman M, Garbarini MA, Beattie AC, Cruise CM, Thongpop C. "FEA Optimization Of Pedorthic Treatment For Podalgia," **ASME Advances in Bioengineering**, 2001; BED-Vol. 51.
- Houston VL, Luo GM, Mason CP, Beattie AC, Garbarini MA, Thongpop C. "Optimization of Pedorthic Insole Design." **Proc. 3rd Annual VA Rehabil Res & Devel Conf**, Arlington, VA, Feb 2002.

Presentations

- Houston VL, Luo G, Mason CP, Mussman M, Garbarini MA, Beattie AC, Cruise CM, Thongpop C. "FEA Optimization of Pedorthic Insole Design for Patients with Diabetes Mellitus." **Proc. 10th World Congress ISPO**, Glasgow, UK, July 2001.
- Houston VL. "Optimization Of Pedorthic Insole Designs". 2001 Annual Mtg Texas Orthotics and Prosthetics Association, Brownsville, TX, September 28, 2001.
- Houston VL. "Pedorthics Fitting & Functional Assessment." Department of Veterans Affairs Research Day, April 8, 2002, VA NYHHS, Brooklyn, NY
- Houston VL. "Tissue Biomechanical Modeling & Loading Analysis." Department of Veterans Affairs Research Day, April 8, 2002, VA NYHHS, Brooklyn, NY

Informatics

- Pedal 3-D Geometric Database established with optical scans and fiduciary manual measurements of the feet/ankles of 43 subjects of military service age.
- Optically digitized measurements of 144 US military footwear Lasts were added to the Last Library of the VA Pedorthic CAD/CAM System, and to the project pedorthic database.

Conclusions

Specifications were created, and components procured and assembled for a pedorthic optical digitizer. The prototype digitizer was calibrated, and laboratory and clinically tested. The software required for control of the digitizer, and for digitizer camera measurement acquisition, processing, visualization, and analysis, with detection, identification, and registration of fiduciary anatomical landmarks, was created and tested. 144 DLA DSPC Lasts for US Military footwear were digitized, and the resulting measurement files entered into the Last Library of the VA NYHHS Pedorthic CAD/CAM System. The feet–ankles of 51 normal, healthy female subjects of military service age and of 25 normal, healthy male veterans were optically scanned and measured. The resulting measurements were then analyzed and used in quantitative assessment of military footwear/Last fit. Analysis showed that US Military Lasts/footwear properly fit only one third of the subjects sampled. Thus, new Last designs incorporating multiple heel widths in addition to heel-to-toe length and metatarsal ball width sizes need to be developed, and used to manufacture footwear for US military personnel, in order to better fit a much broader range of personnel, and thus reduce the incidence of podalgia and pedal trauma in military personnel. A "U–V" design scheme for such Lasts based on pedal anthropometric measurements was developed. Instrumentation was procured, calibrated, and tested for measurement of pedal/footwear interface stresses, ground reaction forces, and body segment kinematics for quantification of footwear fit and function. Biomechanical studies of orthopedic footwear modifications and component designs were performed, measuring the effects of variations in design of three common orthopedic footwear components – scaphoid pads, metatarsal pads, heel pads – as well measurement of the effects of shoe outer sole and heel wedges, shoe outer sole rocker curvature and fulcrum position, and increased outer sole and heel widths, on pedal/footwear interface stresses, ground reaction forces, and body segment gait kinematics. The nonlinear mechanical stiffness characteristics of pedal plantar tissue at the heel and at the first metatarsal head, together with the external and internal geometry and morphology of the feet and ankles of eight subjects were measured, and segmental finite element models of two of the subjects' feet were created. The mechanical properties of four of the materials most commonly used in production of pedorthic insoles were measured, and the results used, together with the pedal finite element models, in pedorthic insole design optimization studies for treatment and prevention of podalgia, metatarsalgia, plantar fasciitis, and calcaneal osteophytes. In addition, an initial design for cushions to be incorporated in the mid and/or outer soles of orthopedic shoes under the metatarsal heads, the heel, and the midfoot were developed, and prototypes in a range of durometers were fabricated for use in augmented treatment of persons with pedal neuromusculoskeletal and biomechanical disorders.

The pedorthic optical digitizer developed in the project was shown to provide accurate, repeatable and consistent measurements of the 3-D spatial geometry and surface topography of peoples' feet and ankles, in natural and prescribed orthopedic alignments, in partial and full weight bearing states, registering the spatial location of fiduciary anatomical landmarks. As such, the digitizer is a powerful tool. It can have numerous applications in Pedorthics, Podiatrics, and Orthopaedics. It can be employed at military induction and training sites to provide rapid and accurate measurements of inductees' feet–ankles for issuance of properly fitting and functional footwear, especially for female personnel, whose pedal morphology and physiological conditioning makes them more susceptible to injury in improperly fitting footwear. In addition, as demonstrated in field trials of the VA Pedorthic CAD/CAM System, the optical digitizer is an essential component for rapid acquisition and input of precise, comprehensive pedal measurements needed for custom design and manufacture of well-fitting, comfortable and

functional orthopedic footwear. In addition, in medical and podiatric applications, the digitizer is a powerful quantitative tool, useful in diagnosing and monitoring treatment of pathologies and disorders that affect pedal geometry, such as vascular insufficiency; edema; tissue inflammatory response to osseous degeneration from arthritis or Charcot syndrome; musculoskeletal deformity resulting from trauma or chronic systemic diseases such as Diabetes Mellitus or arthritis. The digitizer can also be used in anthropometric surveys, compiling measurements of the pedal geometry of a statistically significant and powerful sample of persons of military service age, for use in design of new, more anatomically compliant Lasts, that will permit production of better fitting, more functional, and more comfortable footwear.

Clinical use of the digitizer, providing rapid, accurate measurement of pedal geometry, coupled with knowledge acquired from biomechanical studies of pedal tissue mechanical characteristics, and pedorthic material properties, can lead to development of new, more accurate and comprehensive metrics of footwear fit, that will contribute to increased mobility and performance, and aid in prevention of pedal trauma in military personnel, veterans, and civilian pedorthics patients. Quantitative characterization of pedal tissue and pedorthic material mechanical properties, together with characterization of the pedal/footwear interface stresses, ground reaction forces, and limb segment kinematics during stance and gait, can lead to development of new pedorthic materials and creative design geometries that provide better fitting, more comfortable, and more functional footwear. As evident in the project pedorthic insole design studies, pedal tissue stresses and strains incurred under normal walking and standing conditions, are not exceptionally large. Nonetheless, some people suffer podalgia, metatarsalgia, plantar fasciitis, and/or heel spurs from repetitive activities. The respective stress and strain magnitudes imposed on their pedal tissues typically do not change, only load duration varies. Thus the only parameter that differs appreciably in these cases is tissue strain energy density. Strain energies dissipated in pedal tissues from non-elastic deformation, can, and undoubtedly do, disrupt tissue circulation and metabolism, leading to pain and inflammation, which in turn can result in tissue structural changes and eventual mechanical failure. Development of new pedorthic insole and outer sole materials designed specifically to dissipate strain energies can alleviate this problem. New results, such as this, arising from quantitative, biomechanical studies, have the potential to significantly improve the function, comfort, and performance of footwear for military personnel, as well as that for veterans and civilians with podiatric and orthopedic pedal disorders and pathologies.

References

Boulton AJM. "Lowering the risk of neuropathy, foot ulcers, and amputations." **Diabetic Medicine**, 1998; 15 (Sup 4); S57–59.

Boulton AJM, Veves A, and Young MJ, "Etiopathogenesis and Management of Abnormal Foot Pressures," in **The Diabetic Foot,** 5th ed., Levin ME, O'Neal LW, and Bowker JH, eds., C. V. Mosby, St. Louis, MO, 1993; 234–246.

Coleman WC. "Footwear In a Management Program of Injury Prevention," in **The Diabetic Foot**, 5th ed., Levin ME, O'Neal LW, and Bowker JH, eds., C. V. Mosby, St. Louis, MO, 1993; 293–309.

D'Ambrosia RD. "Conservative Management of Metatarsal and Heel Pain in the Adult Foot," **Orthopedics**, 1987; 10: 137–142.

Donaghue VM, Sarnow MR, Giurini JM, Chrzan JS, Habershaw GM, and Veves A. "Longitudinal in-shoe foot pressure relief achieved by specially designed footwear in high risk diabetic patients," **Diabetes Res Clin Pract**, 1996; 31(1-3): 109–114.

Gould JS, "Conservative Management of the Hypersensitive Foot in Rheumatoid Arthritis," **Foot & Ankle**, 1982; 2: 224–229.

Houston VL, Mason CP, Beattie AC, LaBlanc KP, Luo G, Garbarini MA, and Cruise CM, "The VA-Cyberware Prosthetics-Orthotics-Pedorthics Optical Digitizers," in **CAD/CAM Systems in Pedorthics, Prosthetics & Orthotics**, U. Boenick and E.h.M. Nader, eds., Verlag Orthopadie-Technik, Berlin, Germany, 1998a; 133–163.

Houston VL, Mason CP, Luo G, Mussman M, LaBlanc KP, Beattie AC, Garbarini MA, and Cruise C. M. "An Overview of the VA Pedorthic CAD/CAM System," in **CAD/CAM Systems in Pedorthics, Prosthetics & Orthotics**, U. Boenick and E.h.M. Nader, eds., Verlag Orthopadie-Technik, Berlin, Germany, 1998b; 337–348.

Houston VL, Luo G, Mason CP, Arena L, Beattie AC, LaBlanc KP, Garbarini MA. "FEA for Quantification of Prosthetic/Orthotic/Pedorthic CAD," **CAD/CAM Systems in Pedorthics, Prosthetics & Orthotics**, U. Boenick and E.h.M. Nader, eds., Verlag Orthopadie-Technik, Berlin, Germany, 1998c; 254–276.

Houston VL, Mason CP, Beattie AC, LaBlanc KP, Garbarini MA, Lorenze EJ, and Thongpop CM. "The VA–Cyberware Optical Laser Digitizer," **J. Rehab. Res. & Devel.**, 1995 (February); 32(1): 55–73.

Janisse DJ. "Prescription footwear for arthritis of the foot and ankle," **Clin Orthop**, 1998; 349:100–107.

Janisse, DJ. "Pedorthic Care of the Diabetic Foot," in **The Diabetic Foot,** 5th ed., Levin ME, O'Neal LW, and Bowker JH, eds., C. V. Mosby, St. Louis, MO, 1993; 549–576.

Kelly VE, Mueller MJ, Sinacore DR. "Timing of peak plantar pressure during stance phase of walking." **J Amer Podiatric Med Assoc**, 2000 (Jan); 90 (1): 18–23.

Lord M, and Hosein R. "Pressure Redistribution By Moulded Inserts," **Proc. 7th World Congress ISPO, Chicago, IL, June 1992**; 279.

Moncur C, and Shields MN. "Clinical Management of Metatarsalgia in the Patient With Arthritis," **Clinical Management in Physical Therapy**, 1983; 3(4): 7–13.

Mueller MJ. "Application of plantar pressure assessment in footwear and insert design." **J Orthopaedic & Sports Physical Therapy**, 1999 (Dec); 29 (12): 747–755.

Mueller MJ, Sinacore DR, Hoogstrate S, and Daly L. "Hip and Ankle Walking Stratagies: Effect on Peak Plantar Pressures and Implications for Neuropathic Ulceration," **Arch Phys Med Rehabil**, 1994; 75: 1196–1200.

Parham KR, Gordon CC, Bensel CK. "Anthropometry of the Foot & Lower Leg of US Army Soldiers," US Army Natick Res, Devel, Engr Cntr Tech Rpt. TR–92/028, Natick, MA 1992.

Reinker KA, Ozbourne S. "A Comparison of Male and Female Orthopedic Pathology In Basic Training," **Military Med.**, 1979; 144: 532–536.

Riddle DL, and Freeman DB. "Management of a Patient With Diagnosis of Bilateral Plantar Fasciitis and Achilles Tendonitis," **Physical Therapy**, 1988; 68(12): 1913–1916.

Rodgers MM, and Cavanagh PR. "Pressure Distribution in Morton's Foot Structure," **Med. & Sci. in Sports & Exercise**, 1989; 21(1): 23–28.

Rose NE, Feiwell LA, and Cracchiolo A. "A Method for Measuring Foot Pressures Using a High Resolution, Computerized Insole Sensor: The Effect of Heel Wedges on Plantar Pressure Distribution and Center of Force," **Foot & Ankle**, 1992; 13(5): 263–271.

Ross J, Woodward A. "Risk Factors For Injury During Basic Military Training," **J. Occup. Med.**, 1994; 36: 1120–1126.

Schaff PS. "An Overview of Foot Pressure Measurement Systems," **Clin Podiatric Med Surg**, 1993; 10(3): 403–415.

Schaff PS, and Cavanagh PR. "Shoes for the Insensitive Foot: the Effect of a 'Rocker Bottom' Shoe Modification on Plantar Pressure Distribution," **Foot & Ankle**, 1990; 11(3): 129–140.

Tovey FI, and Moss MJ. "Specialist Shoes for the Diabetic Foot," in **The Foot in Diabetes**, Connor H, Boulton AJM, and Ward JD, eds., Wiley & Sons, New York, NY, 1987; 97–108.

van Schie C, Ulbrecht JS, Becker MB, Cavanagh PR. "Design criteria for rigid rocker shoes." **Foot Ankle Intl.**, 2000 (Oct); 21 (10): 833–844.

Wosk J, and Voloshin AS. "Low Back Pain: Conservative Treatment With Artificial Shock Absorbers," **Arch. Phys. Med. & Rehabil.**, 1985; 66: 145–148.

Wunderlich RE, Cavanagh PR. "Gender Differences in Adult Foot Shape: Implications for Shoe Design." **Med Sci Sports Exerc**, 2001; 33(4): 605–611.

Young CR. "The FScan System of Foot Pressure Analysis." **Clin Podiatric Med Surg**, 1993; 10(3): 455–461.

APPENDICES

FIGURES 1-35

TABLES 1-5

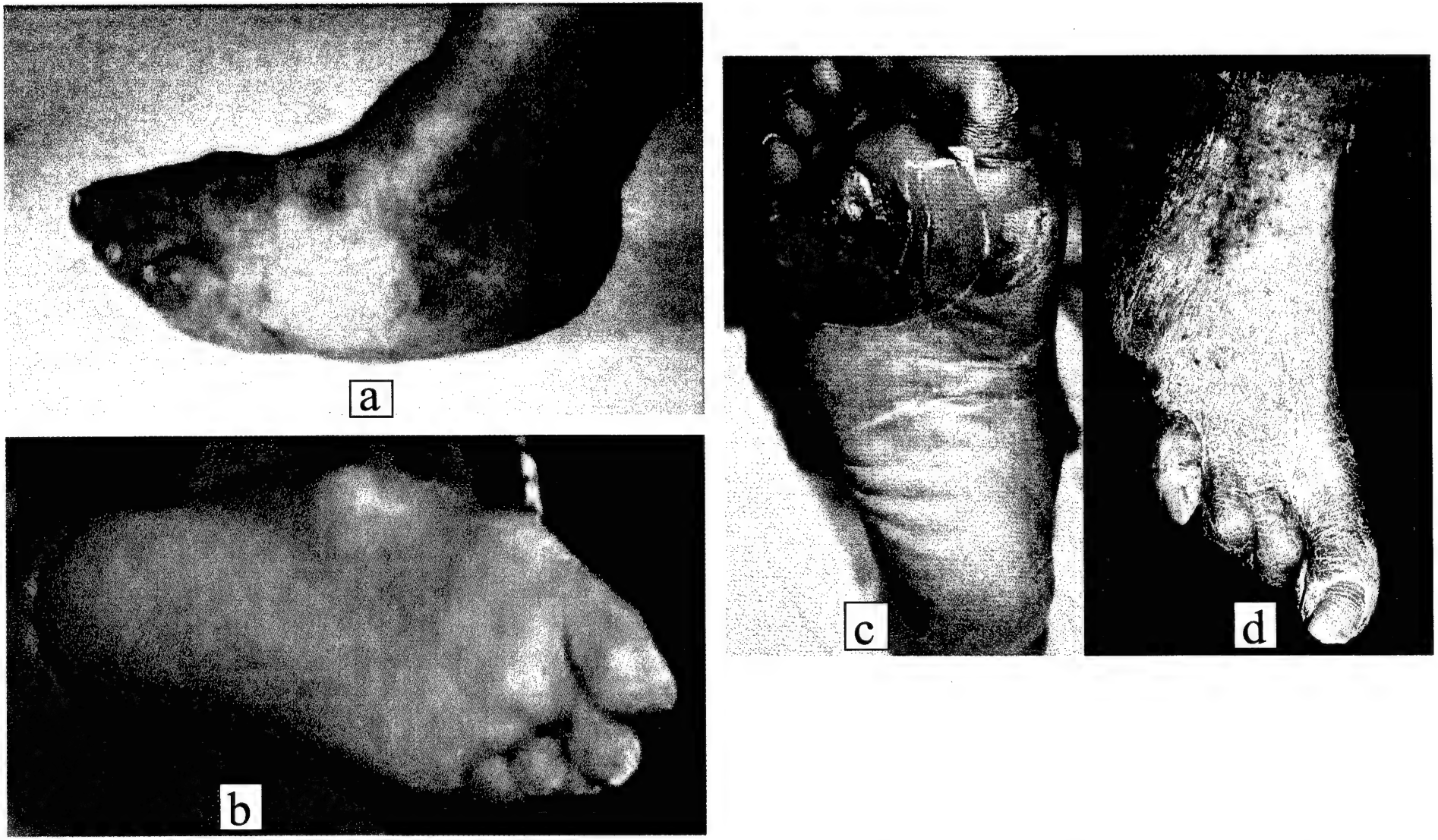

Figure 1. The feet–ankles of US Veterans requiring custom orthopedic footwear. (a) Veteran paratrooper with impact injury to mid-foot; (b) Veteran with pedal deformity from Diabetes Mellitus Charcot neurothropathy; (c) Veteran with stage 3 decubitus ulcer from chronic Diabetic Mellitus; (d) Veteran with peripheral vascular disease and resected fifth ray of forefoot from repetitive stress injury and consequent tissue necrosis and gangrene.

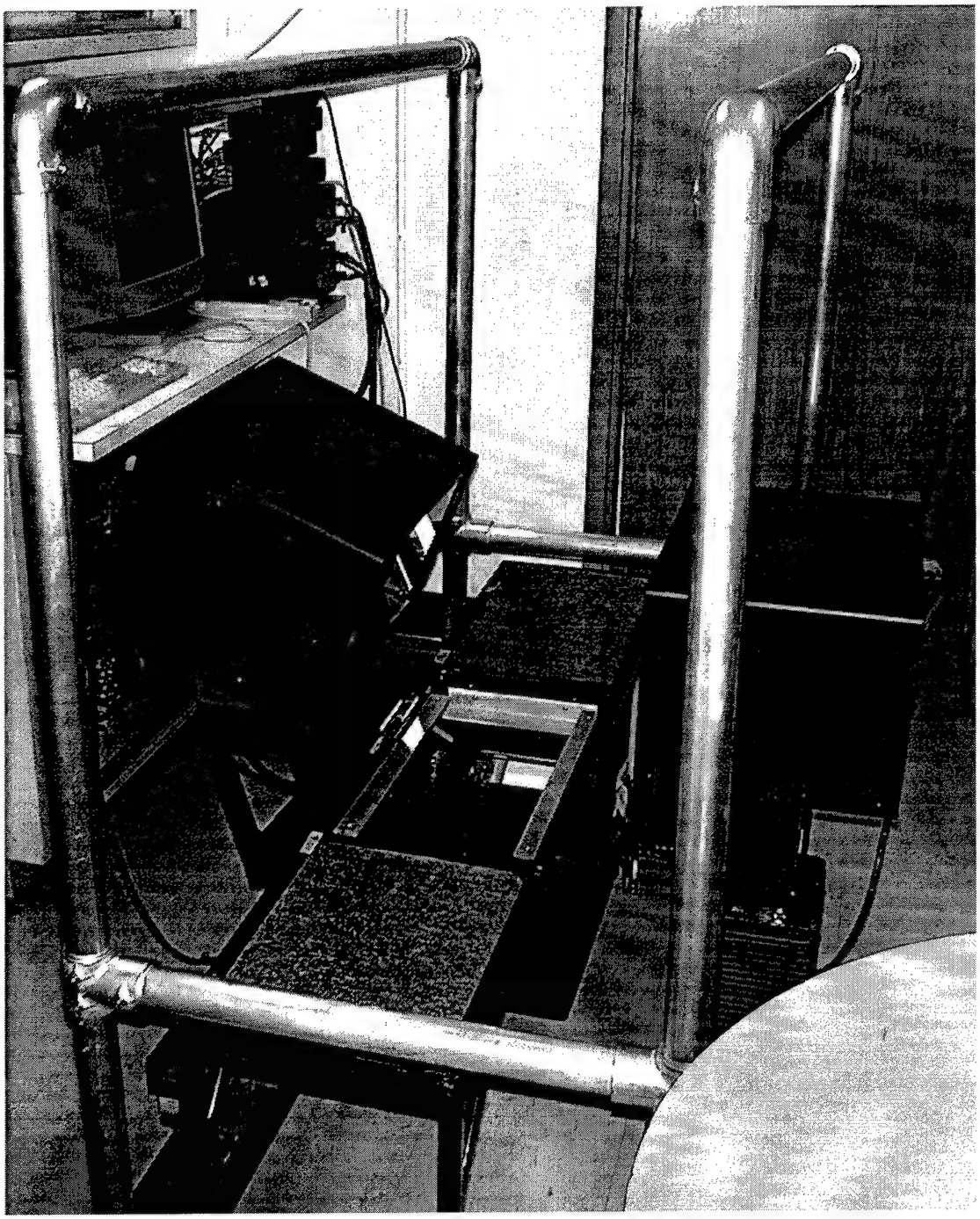

Figure 2. VA NYHHS Pedorthic Optical Digitizer.

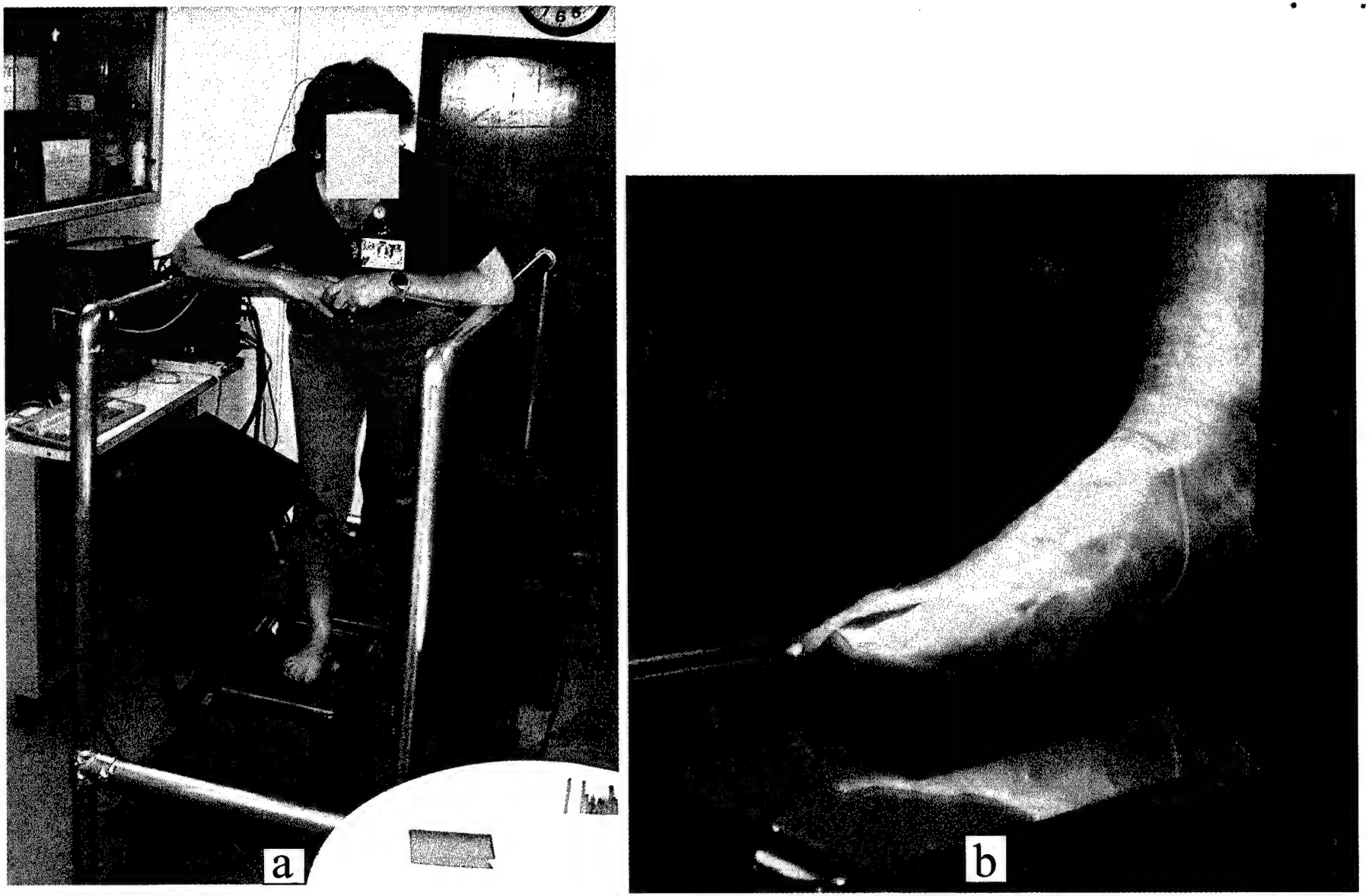

Figure 3. (a) Digitization of the foot and ankle of a test subject in the Pedorthic Optical Digitizer. The subject stands on the digitizer walkway, balanced in the support rails, with her foot in neutral alignment, resting on a transparent lucite platen, bearing approximately 1/3rd body weight, as the scan heads are driven along the translation rails, digitizing the cross-sectional contours of the foot and ankle from the crest of the heel to the distal end of the toes. (b) Close-up of the subject's foot being digitized, showing circumferential coverage of a pedal cross section with the incident plane of laser light, including in the arch.

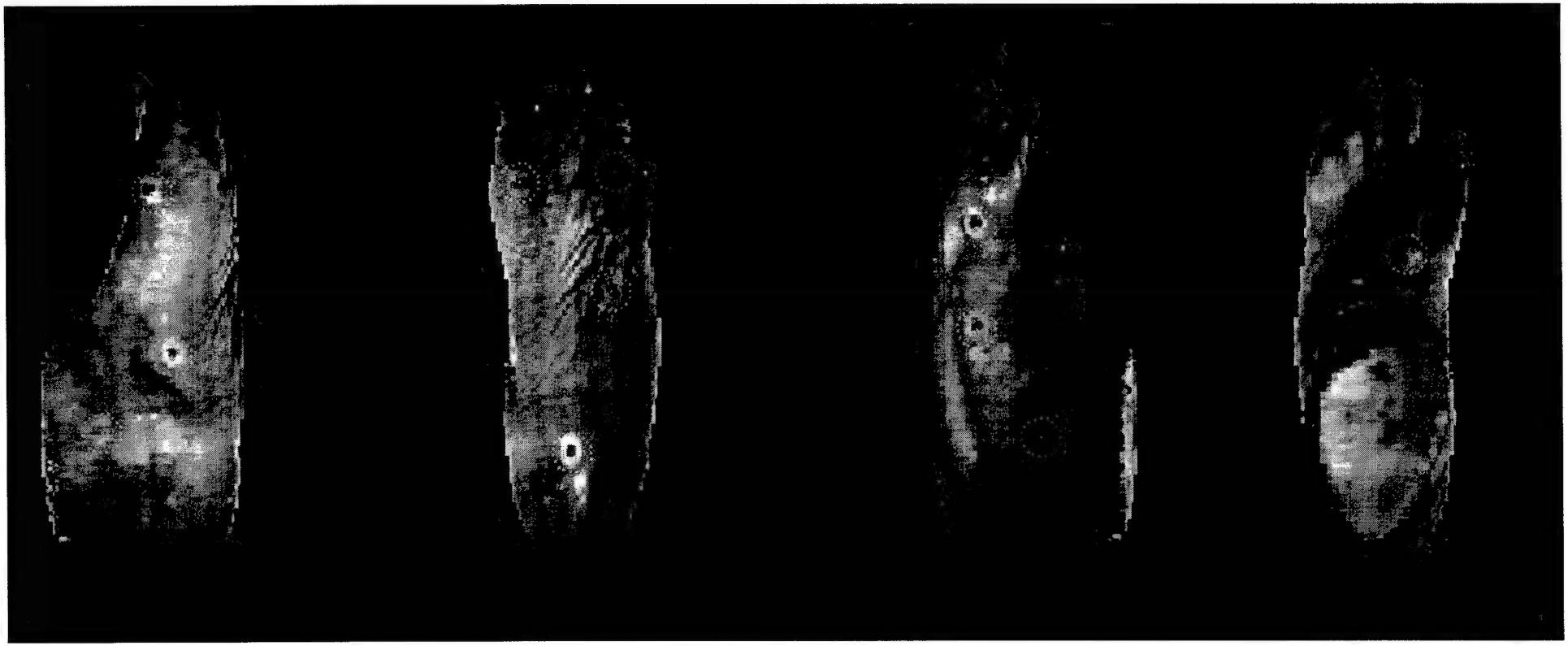

Figure 4A. Images of the scan of a test subject's foot-ankle with the VA NYHHS Pedorthic Optical Digitizer after post-processing of the camera output intensity and range data with the automatic landmark detection, identification, and registration (ALDIR) algorithm. Differences in the intensity of the laser signal reflected from the pedal surface and from the fiduciary landmarks are evident in the scan data. The encircled points are the landmarks detected by the ALDIR neural network algorithm.

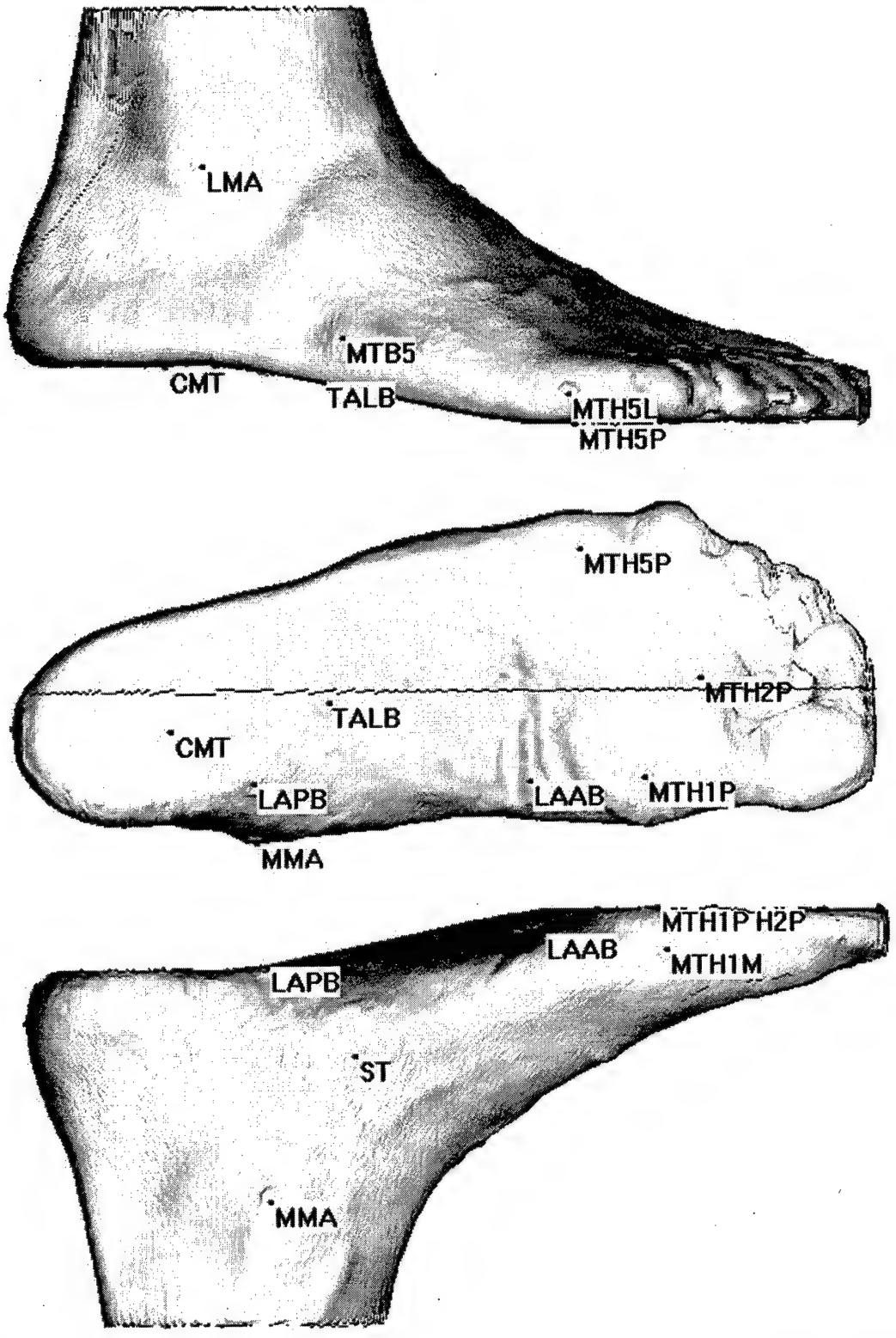

Figure 4B. Principal orthogonal views of the shaded solid image of a test subject's foot-ankle, shown after post-processing the optical scan measurements with the ALDIR algorithm and import of the resulting data into the VA NYHHS Pedorthic CAD/CAM System for design and manufacture of custom orthopedic footwear.

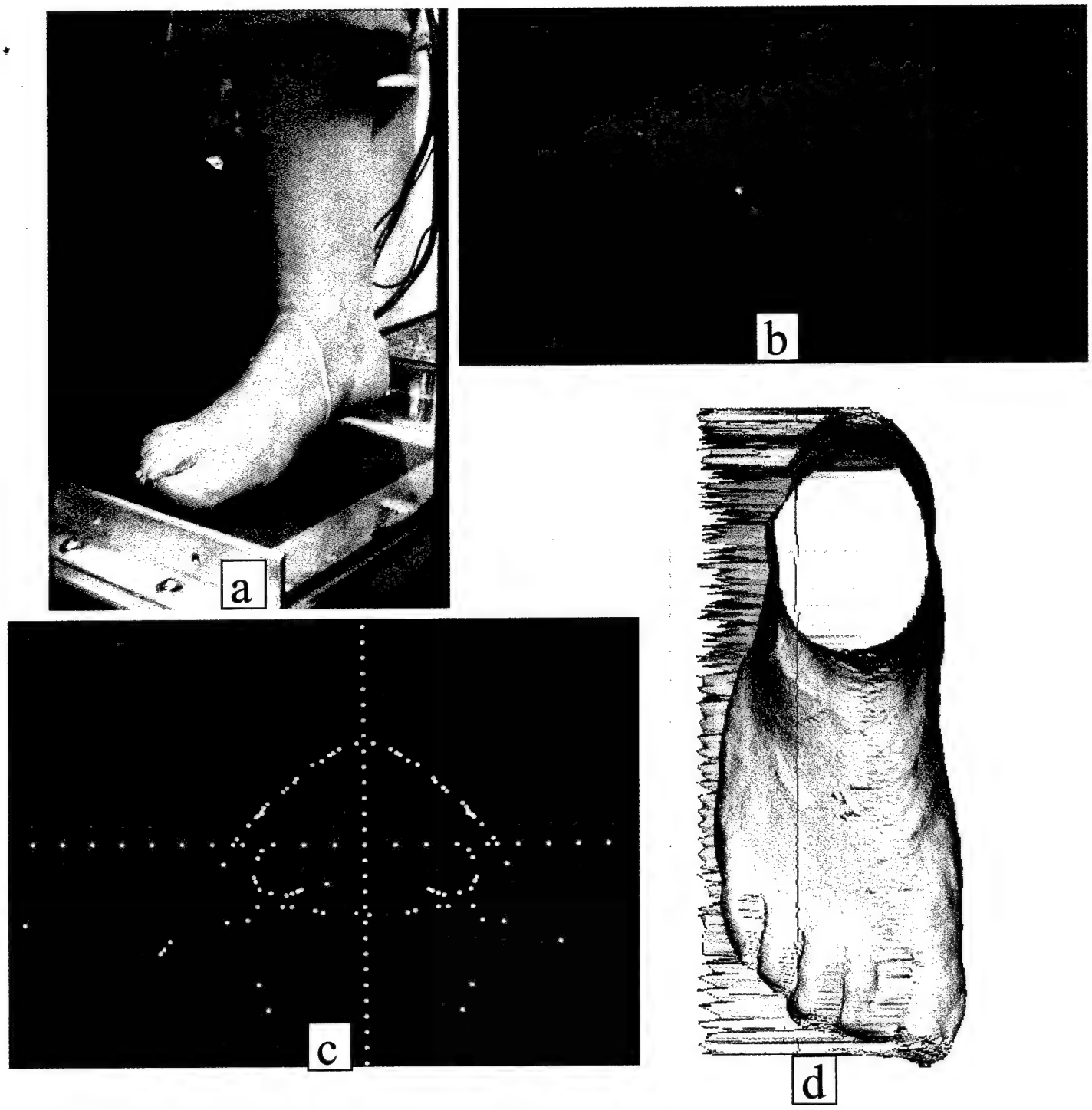

Figure 5. Scan measurement corruption from refractive distortion and multiple reflections of the incident laser signal. (a) Scan of a test subject's foot showing refractive distortion of the incident laser signal in the contoured support platen. (b) Scan experiment showing near-infrared laser source signal (large red dot) and spurious secondary, tertiary, and quaternary multiply reflected signals from in the support platen (small red dots). (c) Composite digitizer camera output signals for the scan of a pedal cross-section, showing measurement corruption from refractive distortion and multiple reflections at the mediodistal, laterodistal, and plantar borders. (d) Pedorthic CAD/CAM shaded solid model of the subject's foot resulting from the corrupted measurements.

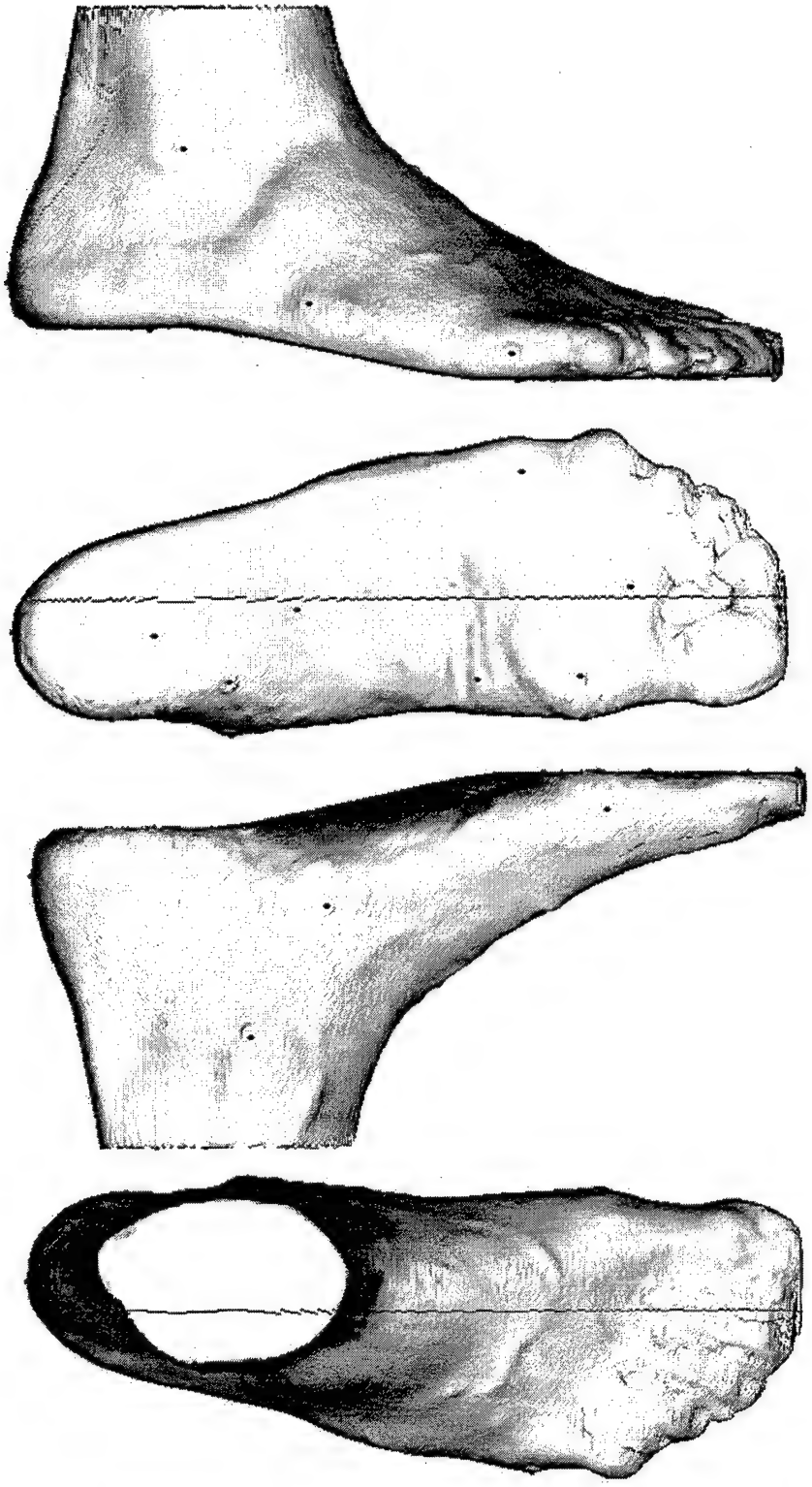

Figure 6. Four principal orthogonal views of the optical scan of a test subject's foot-ankle displayed in the VA NYHHS Pedorthic CAD/CAM System. Scan measurements were acquired with the VA NYHHS Pedorthic Optical Digitizer employing the "workarounds" developed to mitigate signal distortion and corruption from refractory effects and spurious noise from multiple reflections. In addition, Play-Doh filler has been inserted between the subject's toes to prevent multiple segmentation of the phalangeal data, and thus allow representation of the scan data in cylindrical coordinates.

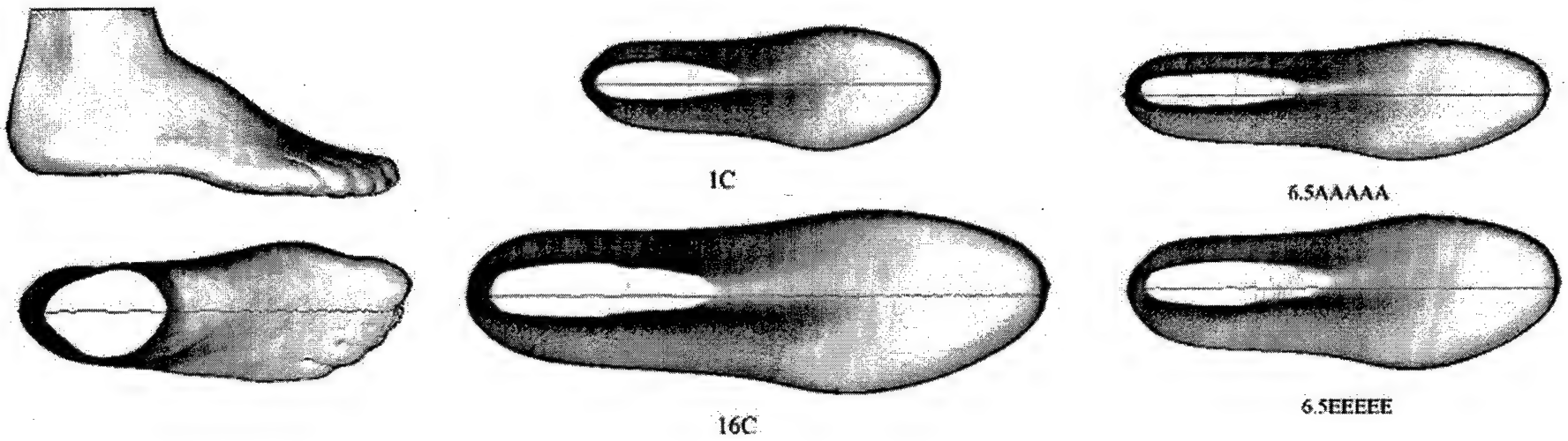

Figure 7A. DLA DPSC US Military Lasts in the range of sizes (heel-to-toe lengths and metatarsal ball widths) nominally available for fabrication of custom and orthopedic footwear for US military personnel.

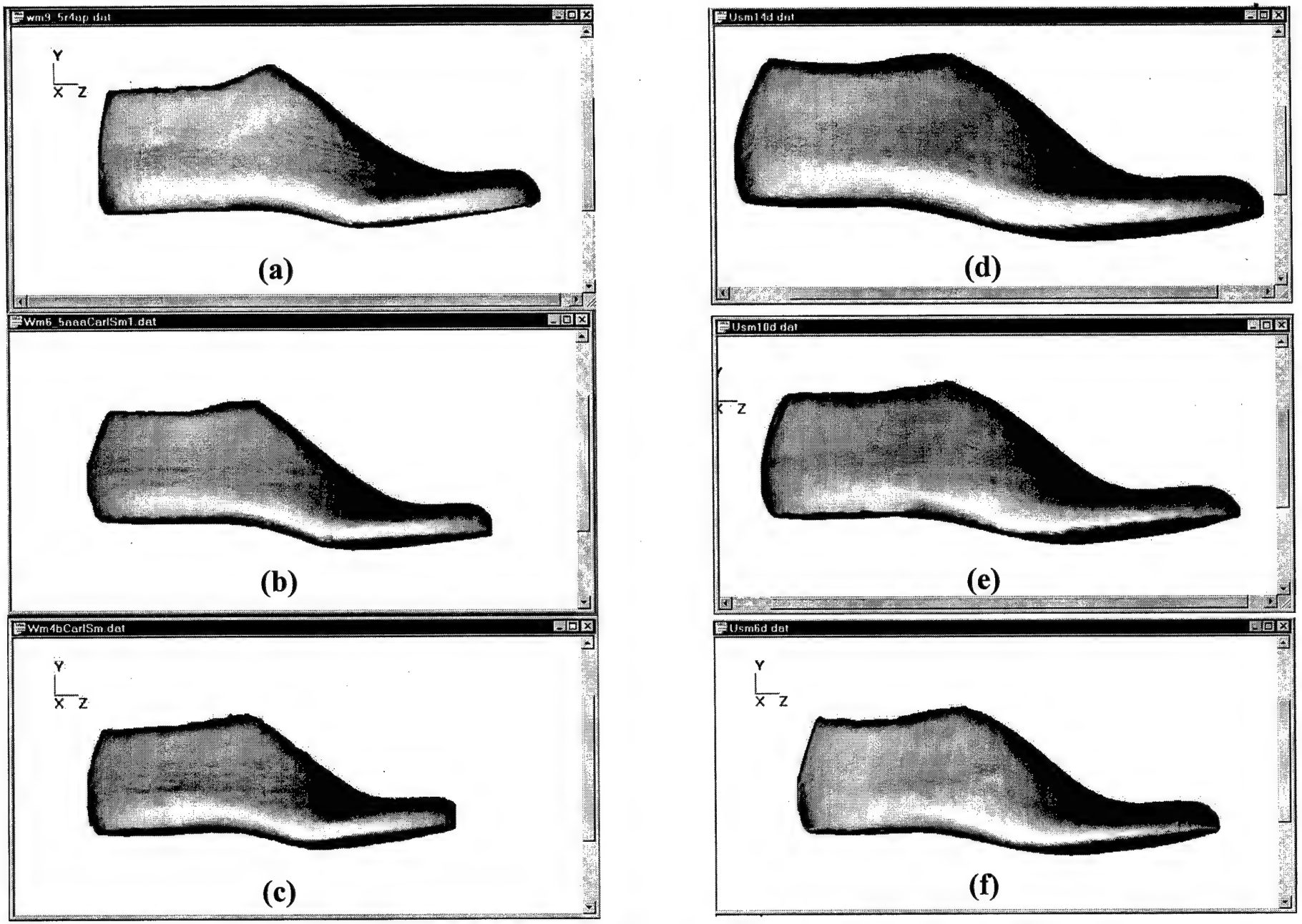

Figure 7B. Lateral sagittal views of digitized DLA DPSC US Military Lasts for female military personnel (a – c) and for male military personnel (d – f). Shaded solid models of small, mid-sized, and the largest Lasts available in the respective sets are shown. The algebraic (non-anatomical) scaling of the Lasts is evident.

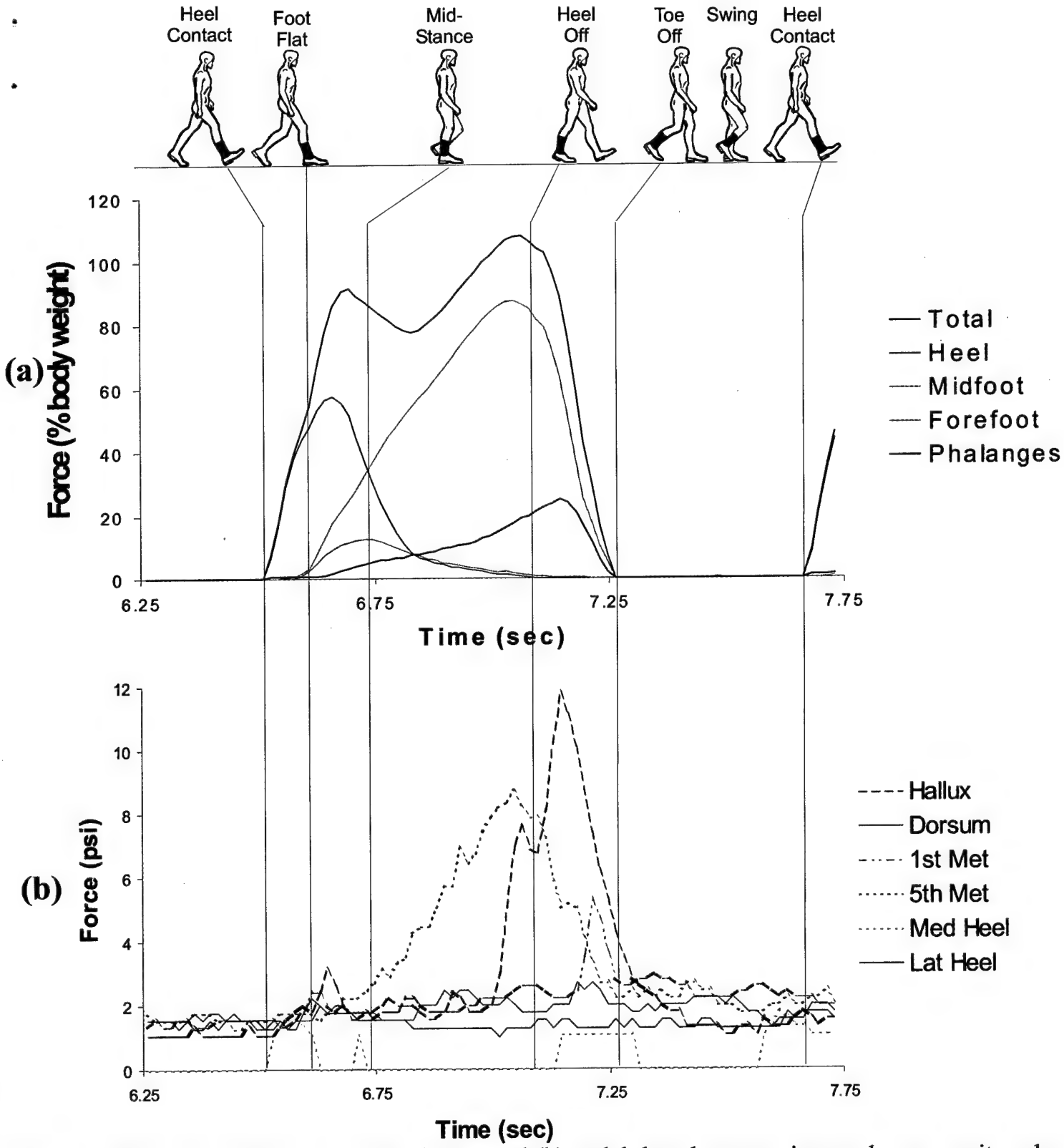

Figure 8. Total and regional (a) pedal plantar, and (b) pedal dorsal stresses incurred over a gait cycle during normal, level walking by a test subject wearing shoes judged "too tight" across the metatarsal heads, but otherwise deemed to be acceptably fitting. The subject evidence reduced heel and midfoot loading relative to that in the forefoot. The largest stresses applied on the dorsal aspect of the foot were evidenced on the dorsal medial aspect of the hallux and the lateral dorsal aspect of the fifth metatarsal head. A (considerably smaller) peak was also observed to occur on the medial dorsal aspect of the first metatarsal head between heel rise and toe off as weight was transferred to the contralateral limb. These results indicate that stresses above 4 psi in magnitude that are routinely applied to the dorsum of the foot over regions with prominent underlying bony structures are excessive, and can lead to discomfort and potential trauma.

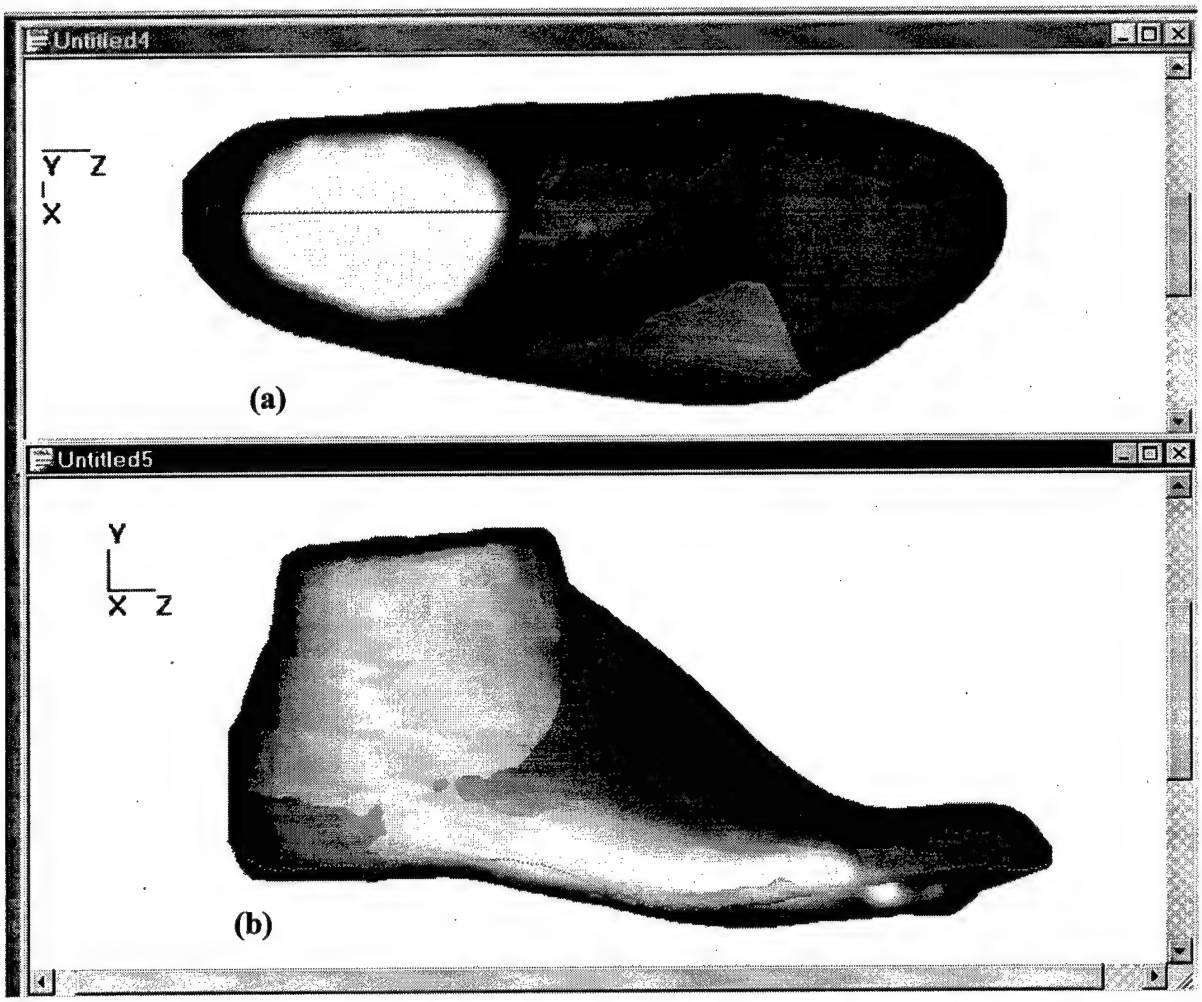

(c) Pedorthic Foot/Ankle and Footwear Last Grading Parameters

Pedorthic Grading Parameters *(mm)*	Parametric Dimension Test Subject Foot/Ankle	Parametric Dimension Military Footware Last	Dimensional Differences (Subj Foot/Ankle – Last)
Heel to toe length	243	254	–11
Heel to ball length	170	178	–8
Heel to crest length	108	117	–9
Ball width	95	87	+8
Heel width	69	61	+8
Span circumference	326	325	+1
Ball circumference	232	217	+15
Instep circumference	260	243	+17
Waist circumference	242	230	+12
Toe box height	23	26	–3
Total Volume *(cm^3)*	924	670	254

Figure 9. VA Pedorthic CAD System shaded solid **(a)** dorsal and **(b)** lateral sagittal views of the foot and ankle of a normal, healthy female subject of military service age with the "best" fitting DLA DPSC US Military Last superimposed. Non-compliant regions between the subject's foot/ankle and the Last, which are at potential risk of injury, are evident. **(c)** Set of eleven pedorthic "grading" parameters, only two or three of which are typically clinically used to assess fit, are shown for the subject's foot and the Last.

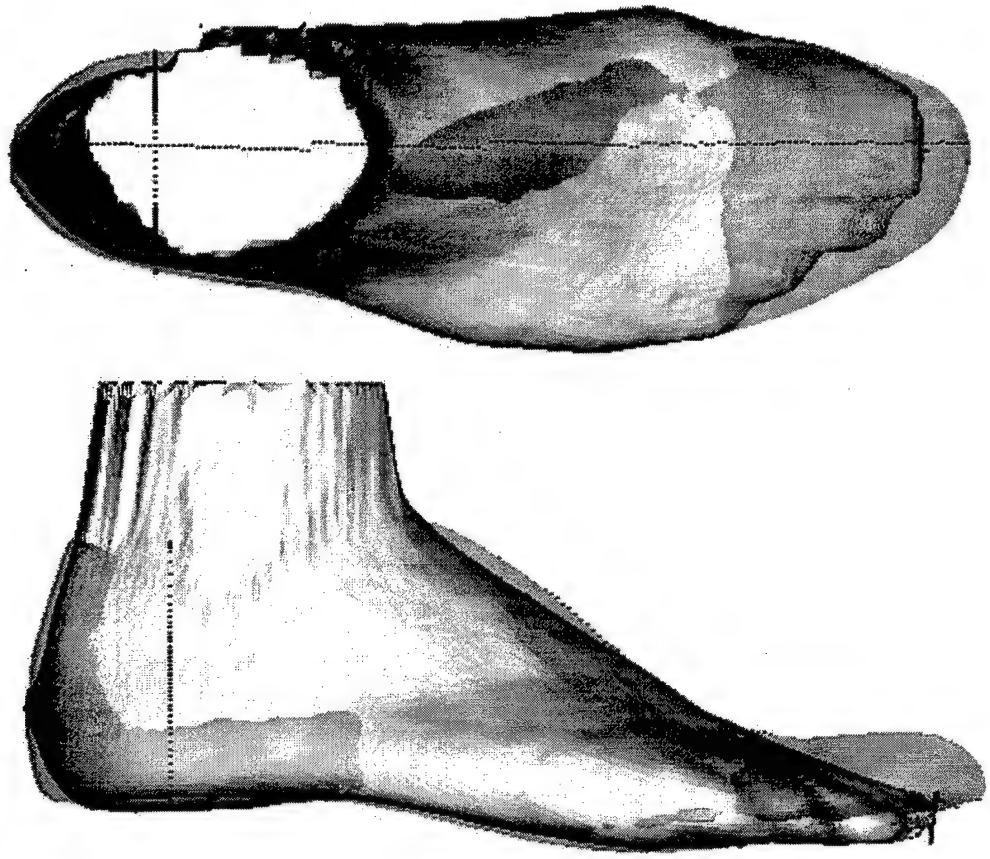

Pedorthic Foot/Ankle and Footwear Last Grading Parameters

Pedorthic Grading Parameters *(mm)*	Parametric Dimension Test Subject Foot/Ankle	Parametric Dimension Military Footware Last	Dimensional Differences (Subj Foot/Ankle – Last)
Heel to toe length	232	243	-11
Heel to ball length	162	170	-8
Heel to crest length	104	113	-9
Ball width	87	79	8
Heel width	52	57	-5
Span circumference	285	293	-8
Ball circumference	214	187	27
Instep circumference	225	212	13
Waist circumference	222	207	15
Toe box height	19	24	-5
Total Volume *(cm^3)*	717	532	185

Figure 10. Shaded solid dorsal and lateral views of the scan of the foot–ankle of a normal, healthy female subject of military service age, shown with the "best" fitting DLA DPSC US Military Last superimposed. The values of the eleven most common parameters used in Last grading are also given for the subject's foot and the Last, respectively. Regions of compliance and non-compliance between the foot and the Last are evident. The subject is representative of the substantial percentage of females with narrow heels, in contrast to the subject shown in Figure 9, whose foot has a larger heel width to metatarsal ball width ratio. For the project sample population, the heel widths to ball widths measured for the subjects, normalized with respect to heel-to-ball length, evidenced weak to negligible correlation (R^2 = 0.2509). This reflects the significant variation that exists among peoples' pedal structure and dimensions, and thus the resulting difficulty inherent in providing properly fitting and functioning footwear for **all** personnel.

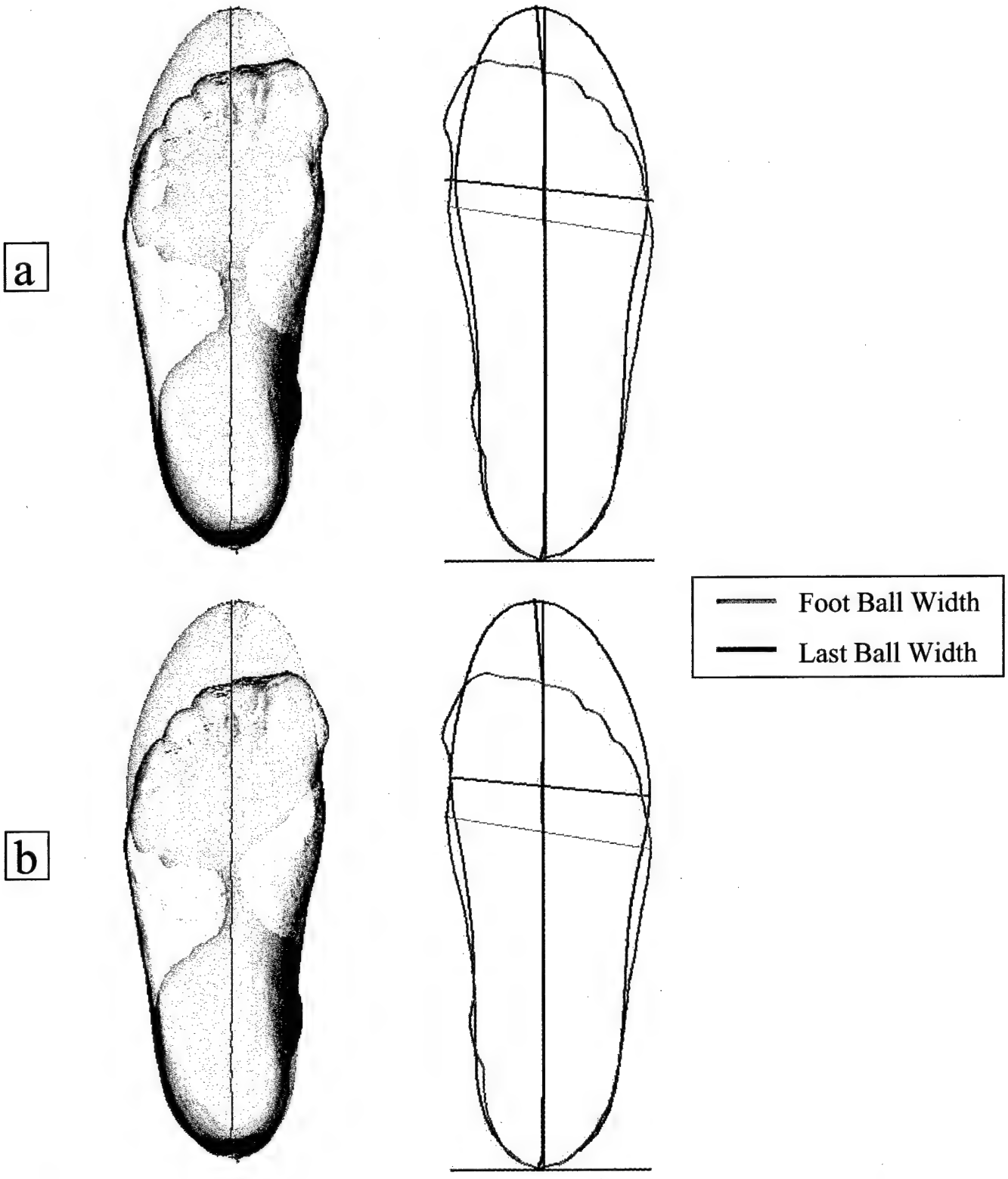

Figure 11. US Military Last-Foot Ball Width Mismatch. (a) Dorsal view and corresponding transverse cross section of the shaded solid model of a female test subject's foot superimposed on a size 6.5EE US Military Last. 8mm of distal clearance is allowed for the toes. The discrepancy in the spatial location of the maximal ball width of the subject's foot and the maximal ball width of the Last is evident. (b) Shaded solid model and corresponding transverse cross section of the subject's foot with a size 7.5EE US Military Last superimposed. Although the compliance between the foot and the shoe is slightly better with respect to width, the mismatch between the maximal ball width of the foot and the Last is seen to be exacerbated, as is the discrepancy between the distal end of the toes and the end of the shoes.

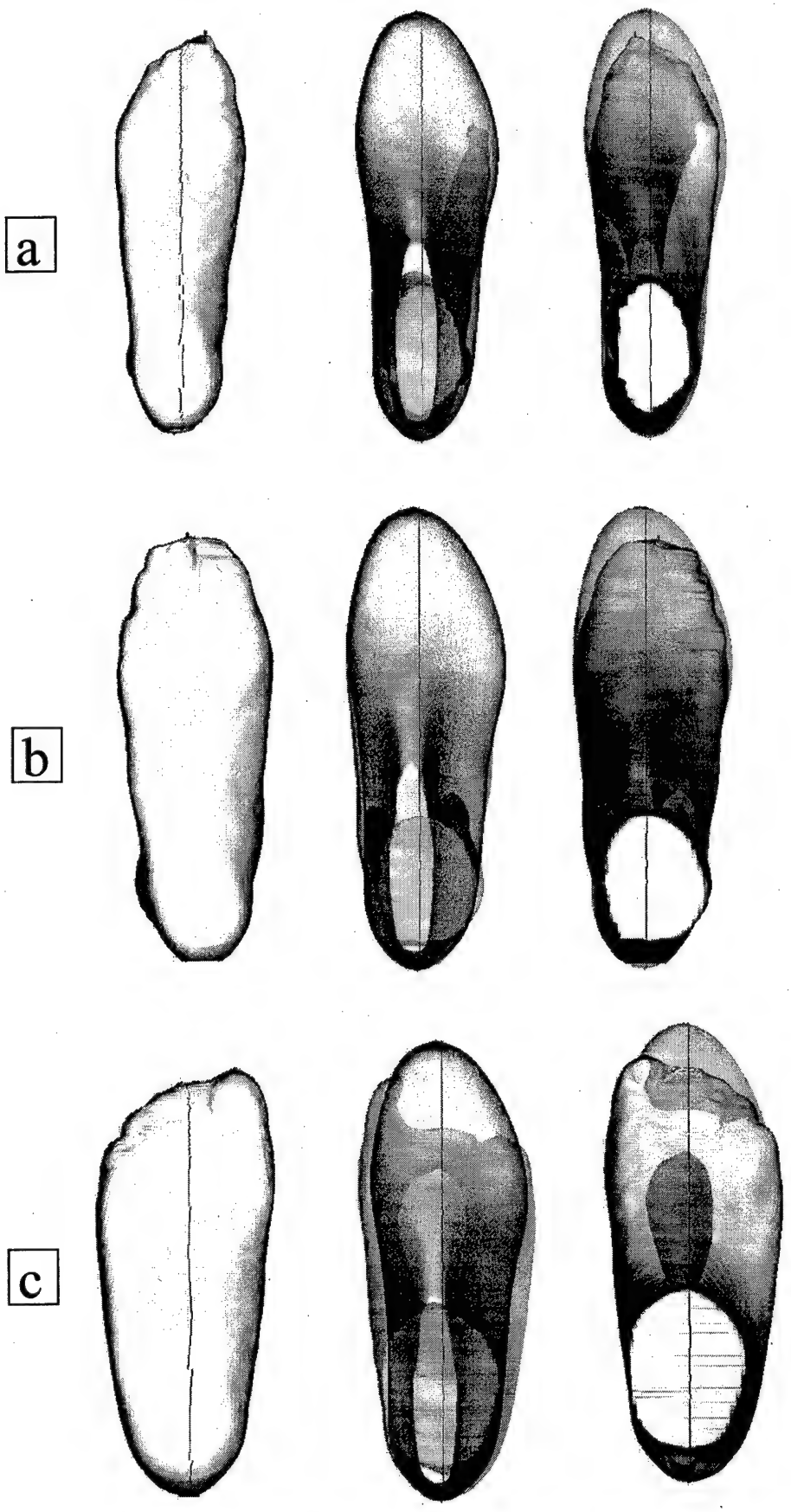

Figure 12. Variation in the shape of test subjects' feet, leading to their classification into three general categories with respect to width – (a) Narrow; (b) Average; and (c) Wide .

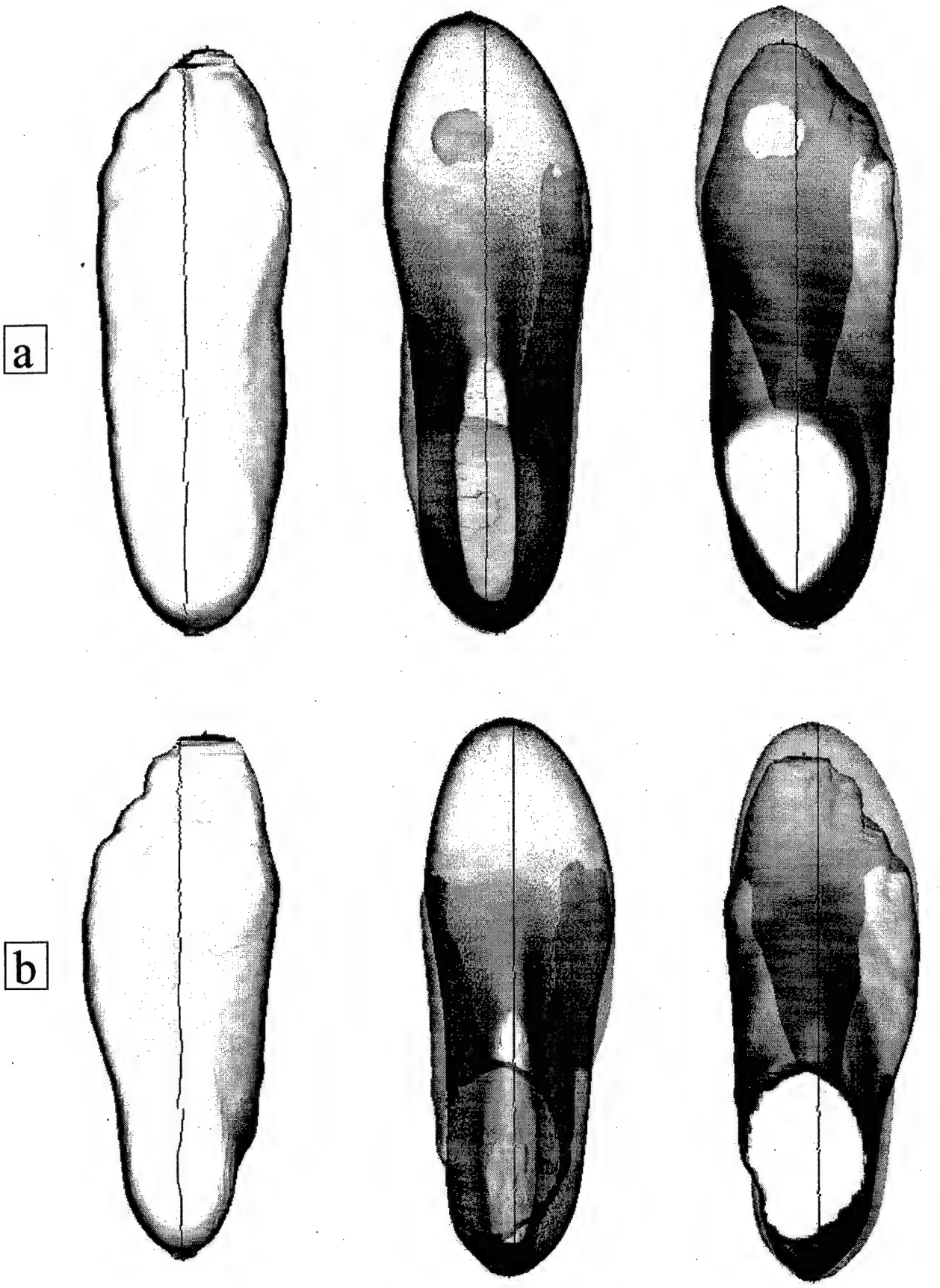

Figure 13. Pedal shape and width limiting classes. (a) "U"–shaped feet are proportionally wide through both the metatarsals and the heel. (b) "V"–shaped feet are relatively wide at the metatarsal heads but narrow at the heel.

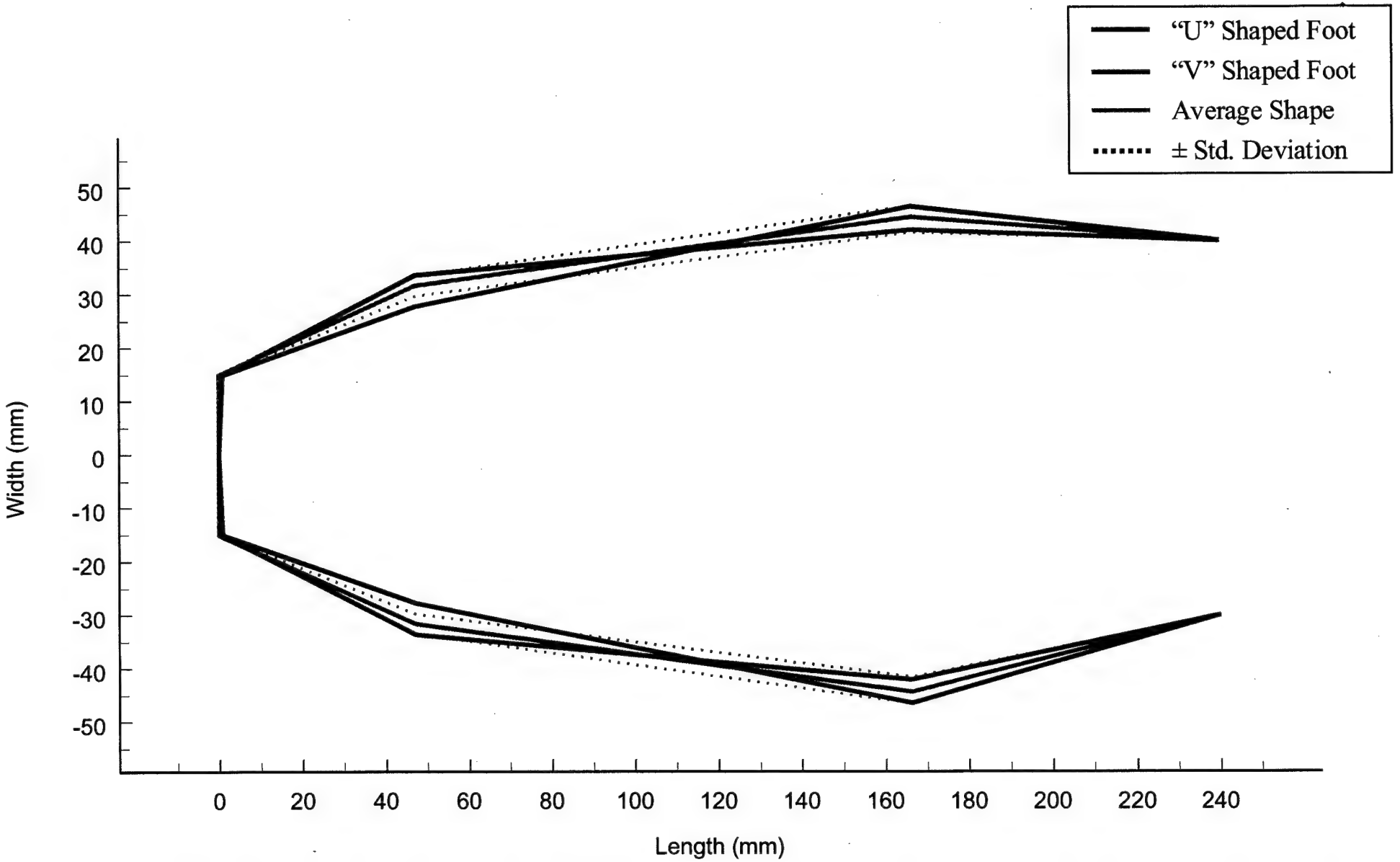

Figure 14. Pedal length–width dimensions and "U"–shaped and "V"–shaped limiting bounds. The mean length and width dimensions, normalized with respect to heel-to-midball length, of the feet of the 51 normal, healthy female test subjects are shown bounded by the "U"–shaped and "V"–shaped limiting cases. Variations of up to 12 mm (6 mm per side) in heel width are evidenced among the subjects sampled. This underscores the need to incorporate heel width as a key parameter in shoe sizing to ensure proper fit and function of footwear.

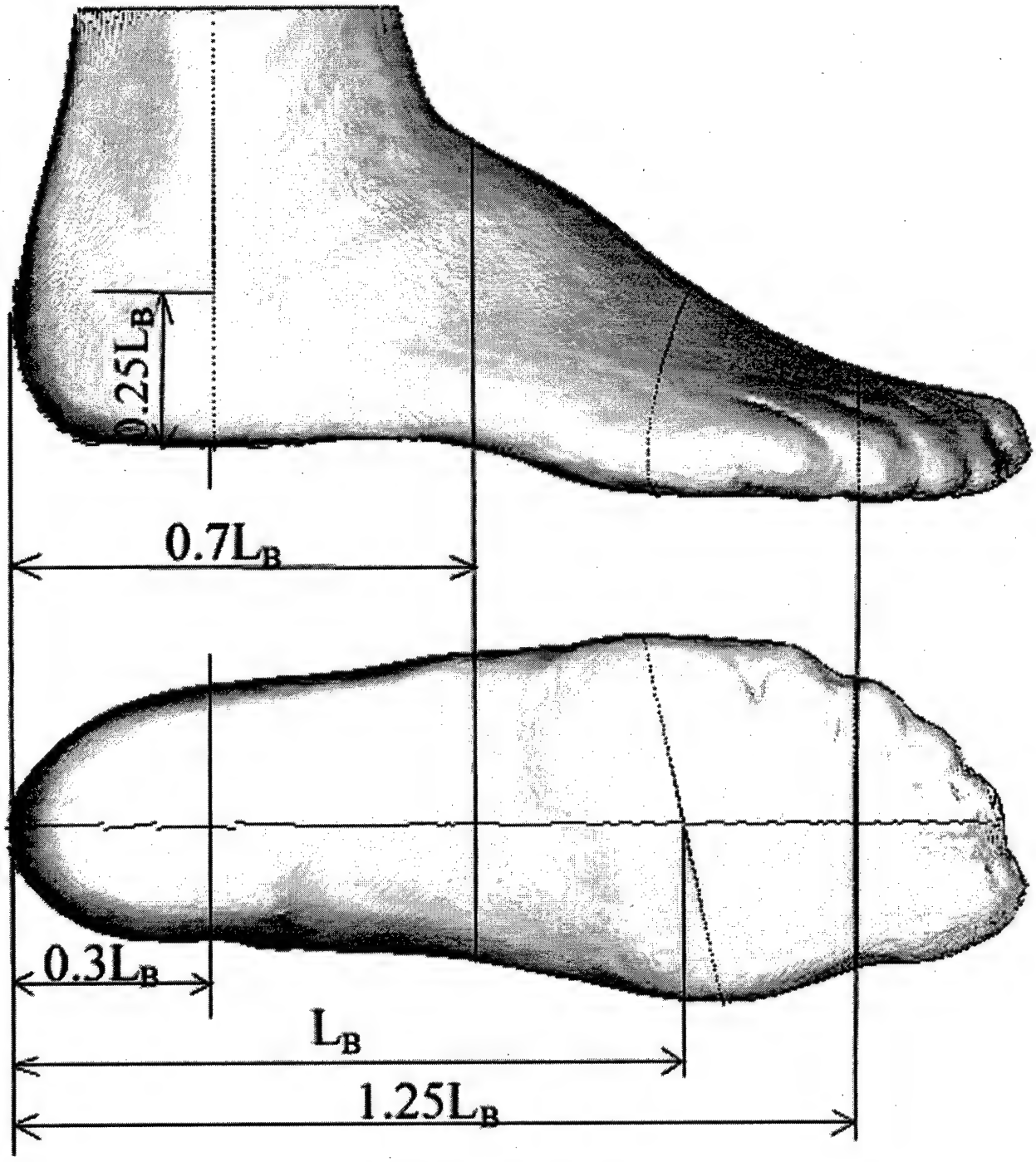

Figure 15. Normalized, standard locations for measurement of fiduciary dimensions of the foot and ankle. For consistency in anthropometric measurement and morphological comparative analyses, locations are chosen as a function of heel-to-midball center length, L_B.

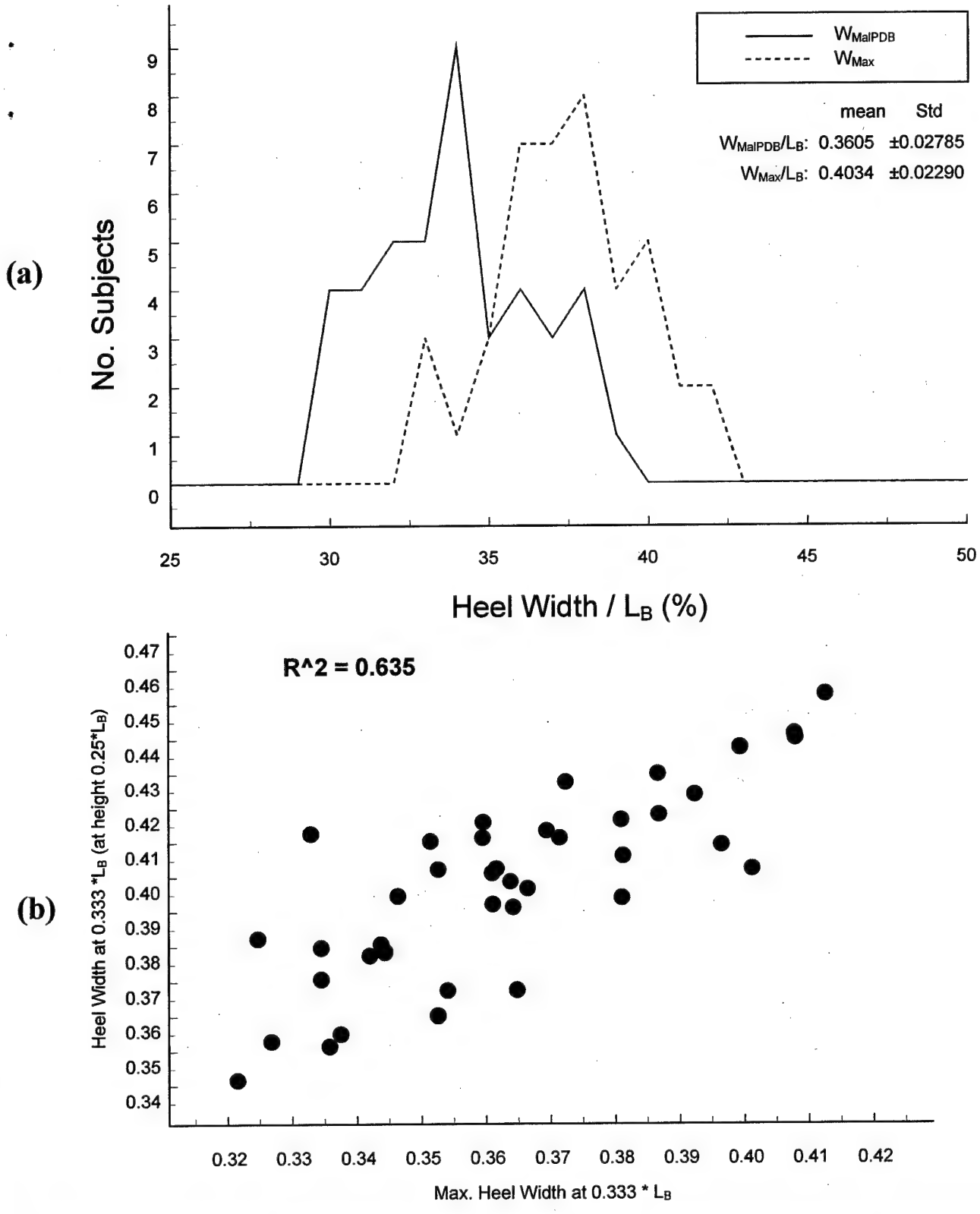

Figure 16. Heel width measurements for 51 normal, healthy female test subjects of military service age. **(a)** Heel widths for the subjects measured posterior to the distal border of the medial malleolus at a distance of $0.333*L_B$ anterior to the crest of the heel (W_{MalPDB}), together with the maximal heel width measured in the same cross-sectional plane (W_{Max}), normalized with respect to the subject's heel-to-ball center length (L_B). The resulting distributions are approximately Gaussian, and have sizable dispersions ($\pm\sigma_W$). Differences between the distributions of W_{MalPDB} and W_{Max} reflect variations in the heel widths and contours between the subjects. (b) Scatter plot showing the correlation of W_{MalPDB} and W_{Max} . Although the two widths are strongly correlated $R^2_{W_{MalPDB}-W_{Max}} = 0.635$, they are not identical, and therefore both dimensions need to be considered in design of Lasts and footwear.

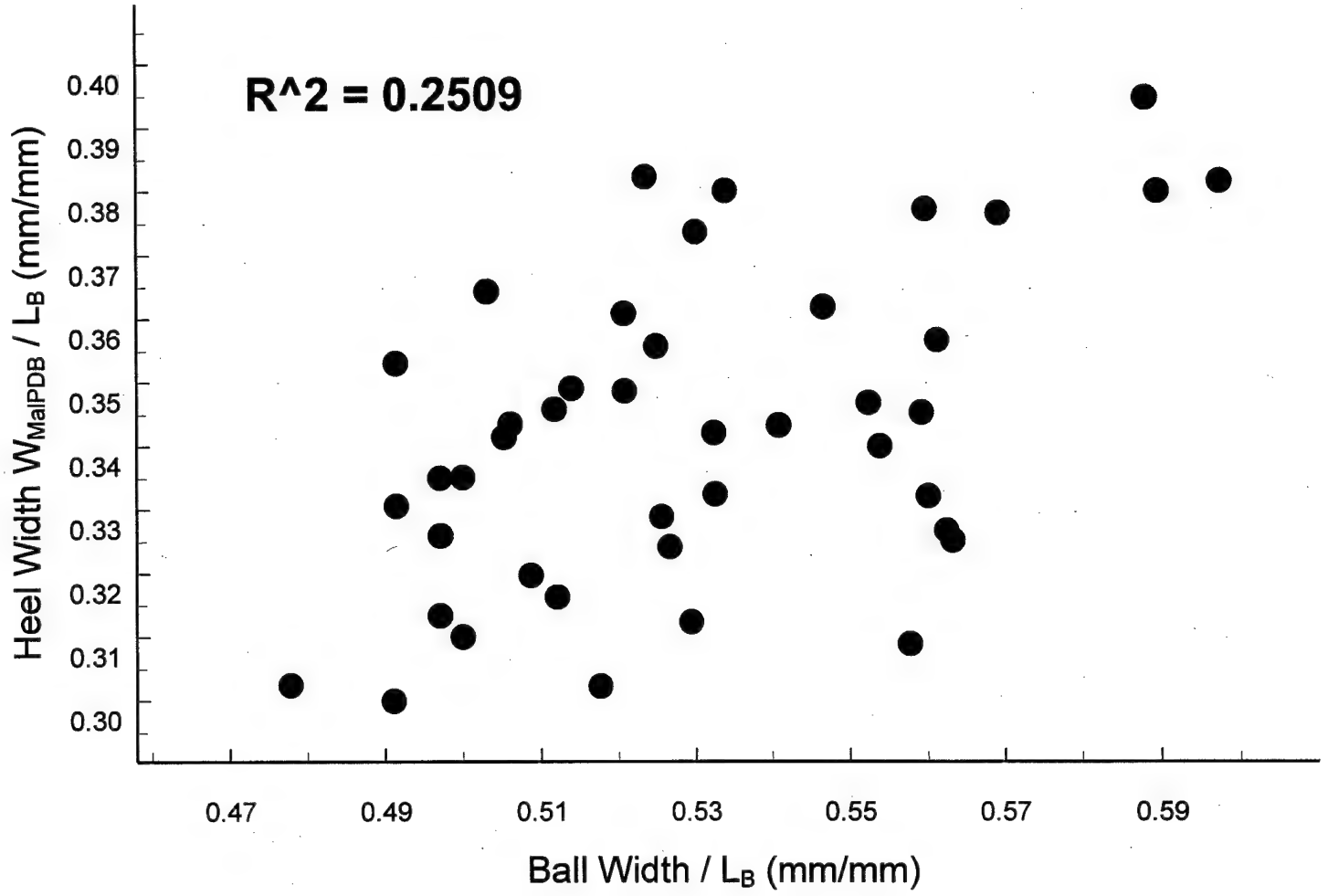

Figure 17. Regression plot of the 51 normal, healthy female test subjects' normalized heel width W_{MalPDB}/L_B versus their normalized ball width W_{Ball}/L_B . The wide dispersion evidences weak to negligible correlation ($R^2_{W_{MalPDB}\text{-}W_{Ball}} = 0.2509$) between the two parameters, reflecting the fact that peoples' foot–ankle shapes and dimensions vary significantly and are **not** algebraically scaled.

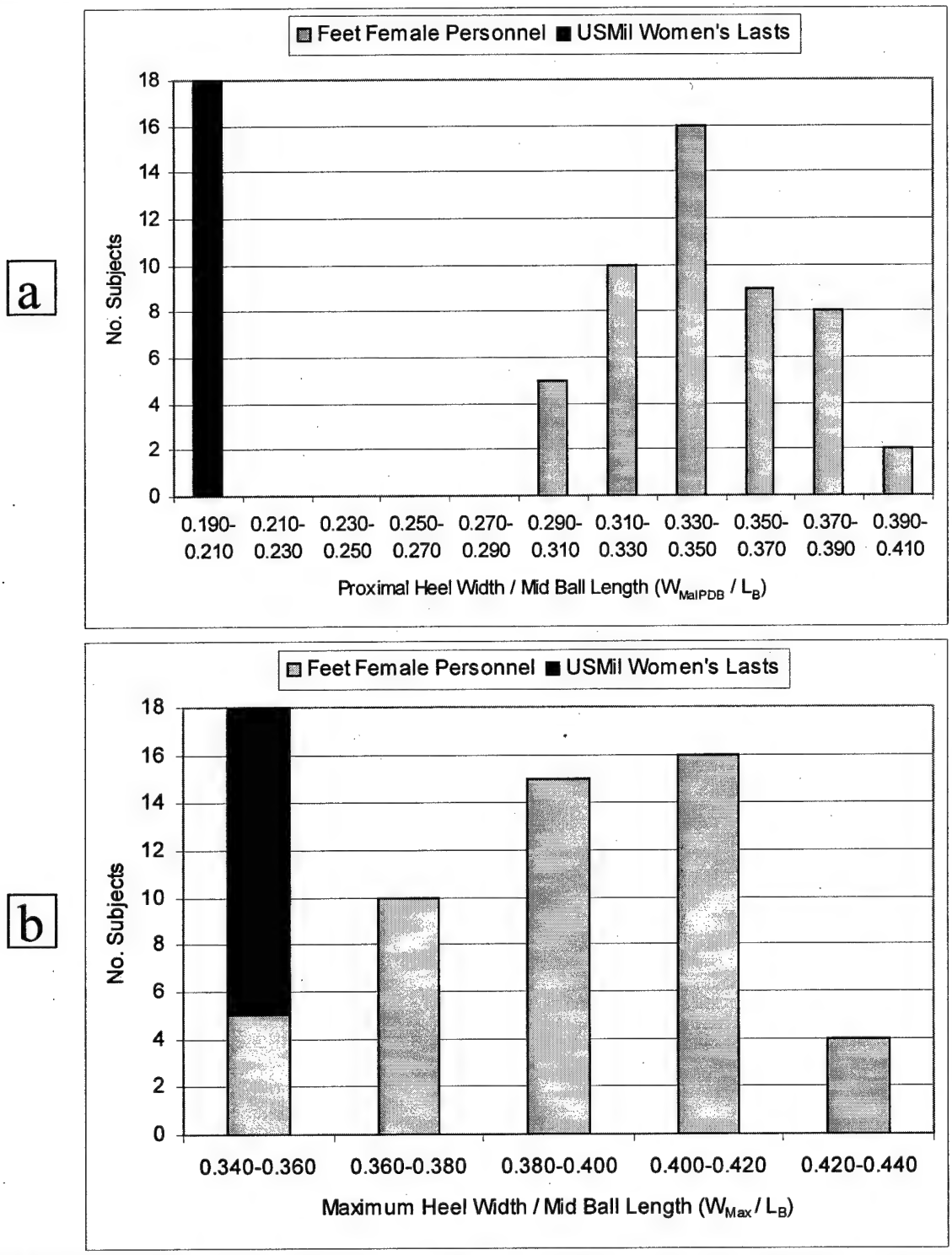

Figure 18. Distribution of heel widths of 51 normal, healthy female test subjects of military service age, compared to that of US Military Lasts. **(a)** Proximal heel widths (W_{MalPDB}) for the subjects, measured posterior to the distal border of the medial malleolus at a distance of $0.333*L_B$ anterior to the posterior crest of the heel at a height of $0.25*L_B$ above the plantar surface, are shown normalized with respect to midball length (L_B). **(b)** Maximal heel widths (W_{Max}), measured in the same cross sectional plane at the widest part of the heel below a height of $0.25*L_B$, are shown normalized with respect to midball length. The subjects' heel widths are Gaussian distributed with reasonably wide dispersions, and are larger than the corresponding normalized widths of the US Military Lasts. (Correction for the mismatch between the midball lengths of the Lasts and the subjects' feet, however, brings the respective means much closer together.) The dispersion in the widths measured for the subjects underscores the non-algebraic structure of peoples' feet, and highlights the need for Lasts with a range of heel widths.

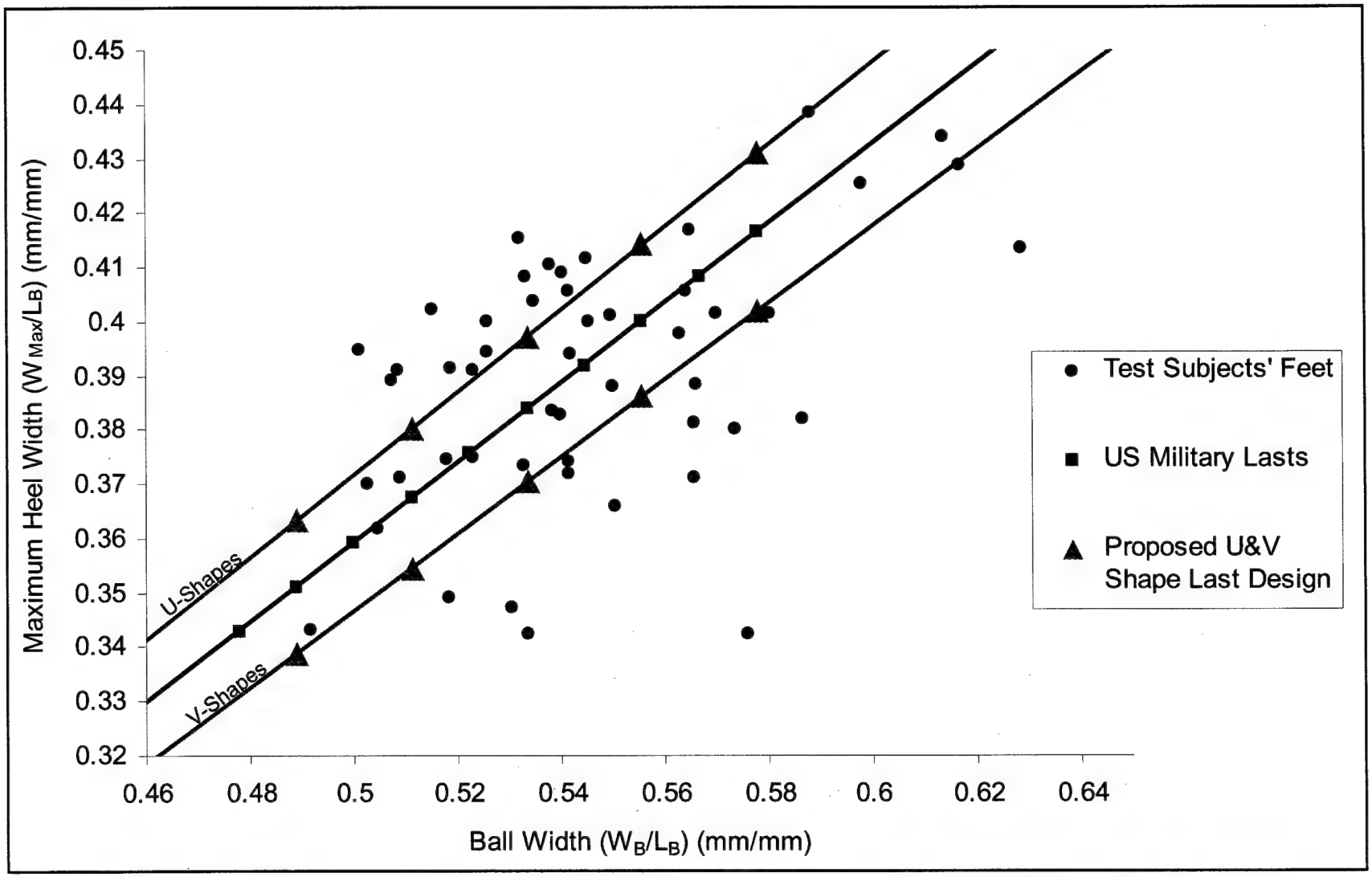

Figure 19. Foot–Last Total Fit Error — the arithmetic sum of the absolute value of the deviation between a person's foot and the corresponding best fitting Last evaluated for the eleven Last grading metrics in Table 3. Results are plotted versus the cumulative percentage of subjects with a total fit error less than a specified value: (1) for US Military Women's Lasts with a single (size C) ball width; (2) for US Military Women's Lasts with ball widths in size AAAAA through EEEEE; and (3) for a set of "U–V" Lasts with ten ball and heel widths. The "U–V" Lasts are seen to fit the feet of a greater percentage of subjects with less error than the current US Military Women's Lasts.

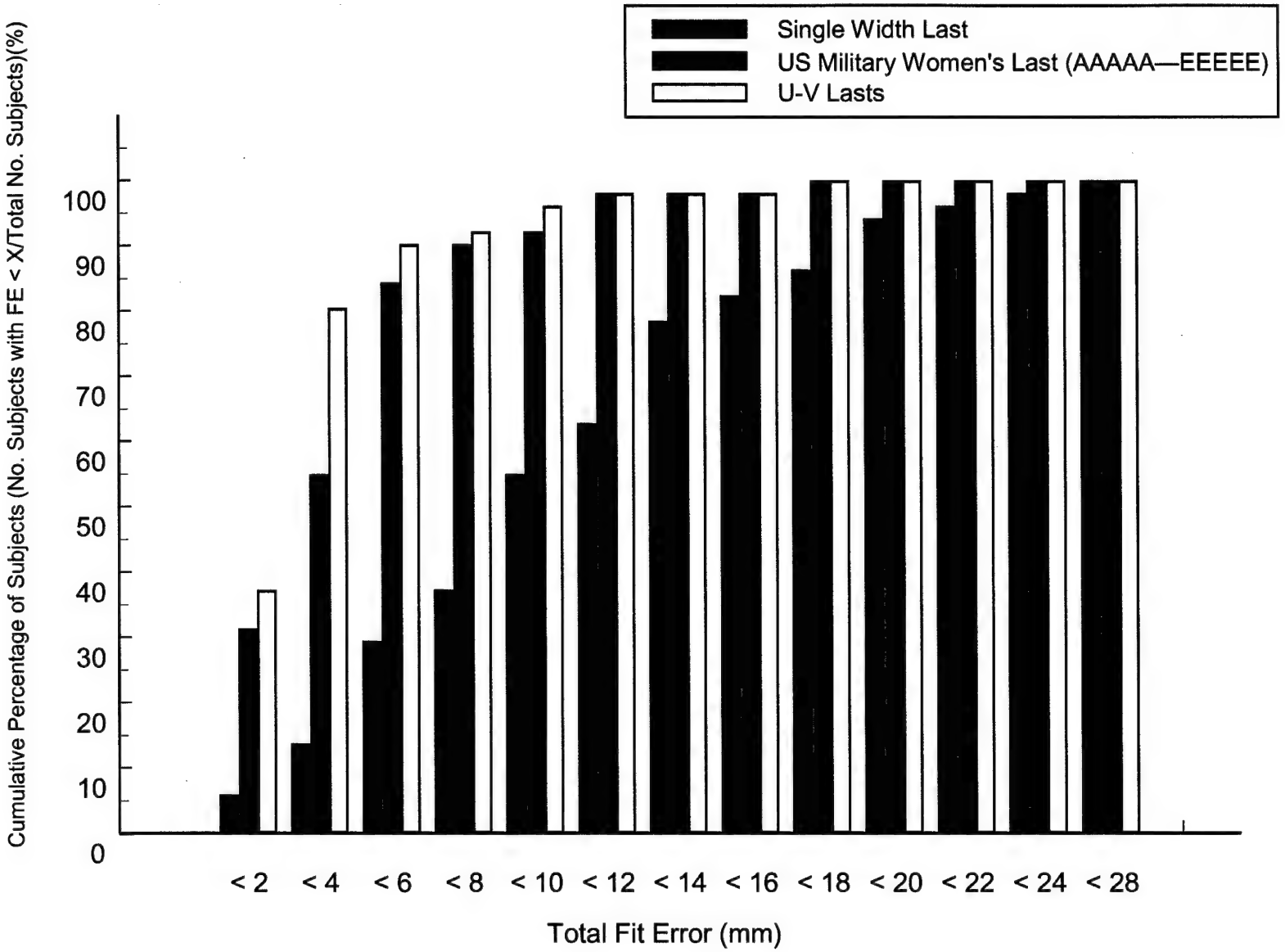

Figure 20. Foot–Last Total Fit Error — the arithmetic sum of the absolute value of the deviation between a person's foot and the corresponding best fitting Last evaluated at the eleven Last grading metrics given in Table 3. Total fit errors are plotted versus the cumulative percentage of subjects with an error less than the specified value: (1) for US Military Women's Lasts with a single (size C) ball width and heel width; (2) for US Military Women's Lasts with ball widths in size AAAAA through EEEEE and a single heel width; and (3) for a set of "U–V" Lasts with a total of ten ball and heel widths. The "U–V" Lasts are seen to fit the feet of a greater percentage of subjects with less error than the current US Military Women's Lasts with multiple ball widths and a single heel width. Approximately two and a half times as many peoples' feet can be accommodated by "U–V" Lasts before fit becomes unacceptable (TFE > 8 mm), than by Lasts with a single ball width and a single heel width.

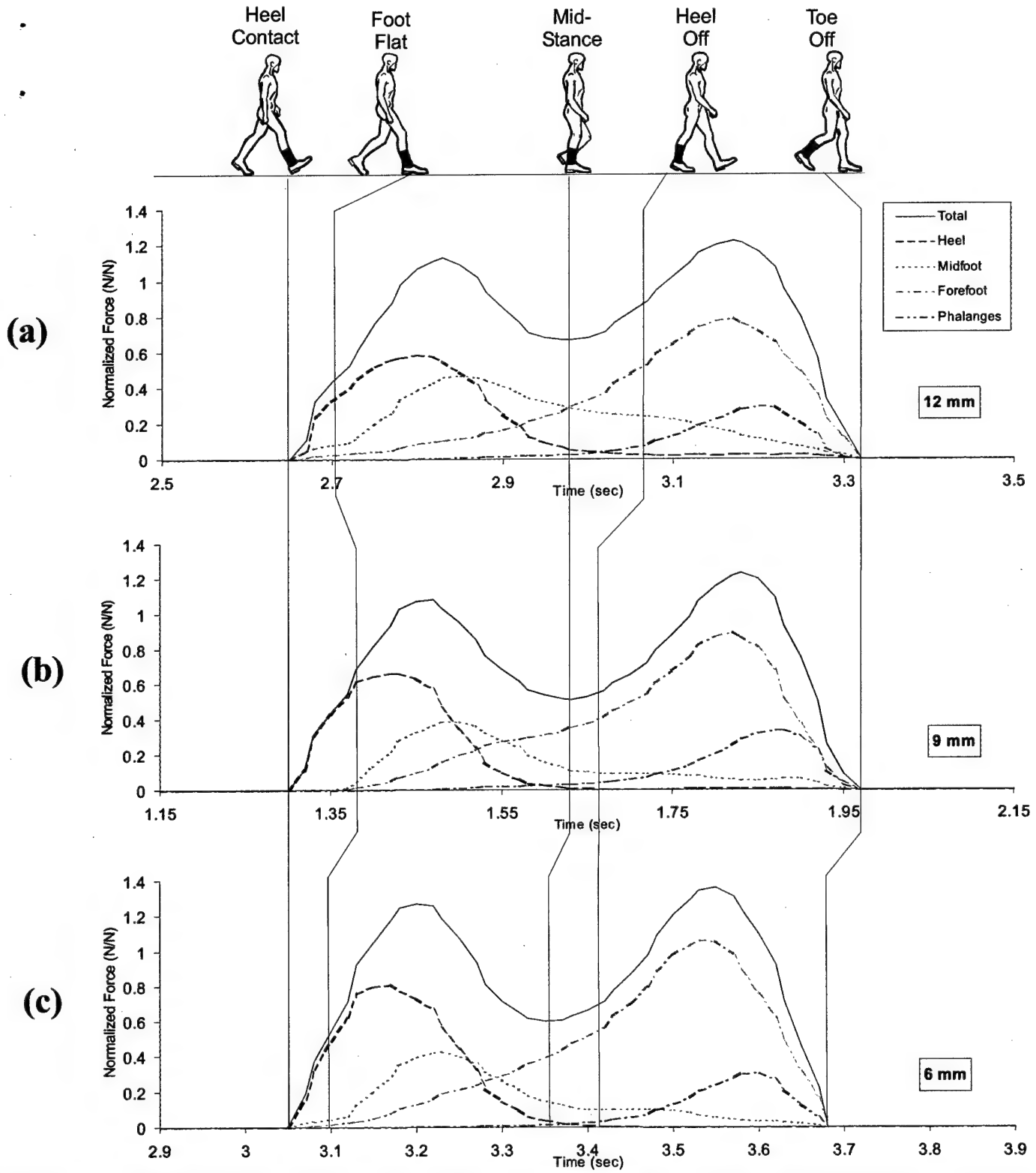

Figure 21. Biomechanical studies of the effects of arch supports on pedal plantar stresses. Total and regional plantar stresses over a typical gait cycle during normal, level walking at a subject selected speed of 1.8 m/sec, are shown for a normal, healthy test subject of military service age wearing well-fitting oxford shoes with 50 Shore hardness durometer RTV rubber scaphoid pads (arch supports). The pads were matched to the subject's longitudinal and transverse arch dimensions, with thickness as a parameter. The resultant stresses incurred in the subject's foot are shown for pad thicknesses of: **(a)** 12 mm; **(b)** 9 mm; and **(c)** 6 mm, respectively. The subject rated the level of comfort afforded by the respective pads as: **(a)** "uncomfortable/painful;" **(b)** "somewhat uncomfortable-to-tolerable;" and **(c)** "comfortable." The resultant segmental loads, show that with the 12 mm thickness pad, appreciable loading could be offset from the forefoot to the arch. This correspondingly was reduced as the pad thickness was decreased. The differences in pressures measured for the 9 mm versus 6 mm thickness pads were not large, however, their effects on the subject's level of comfort were significant.

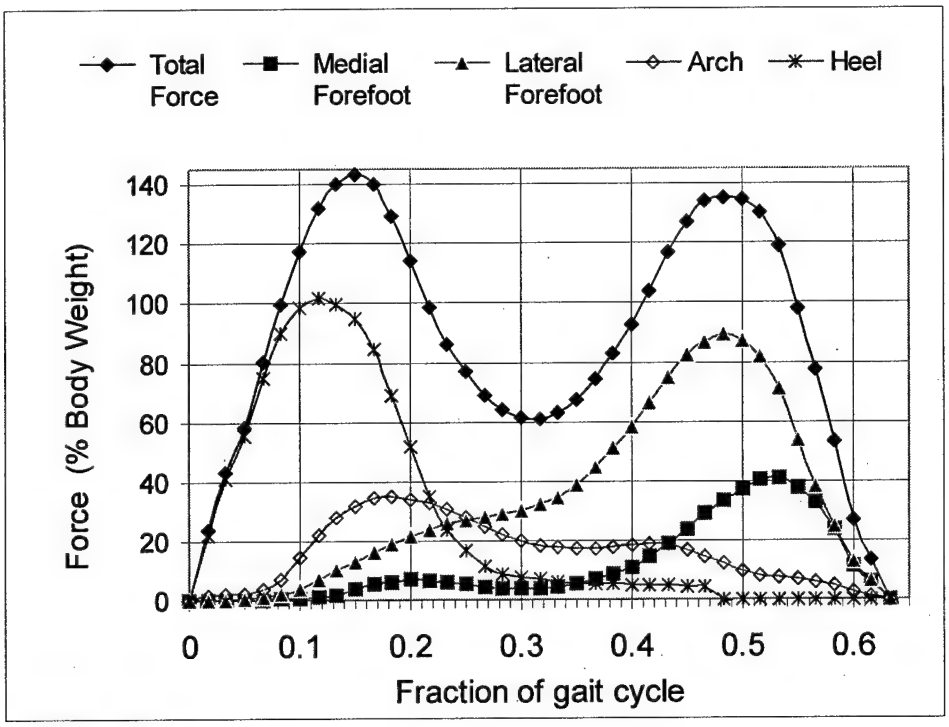

(a)

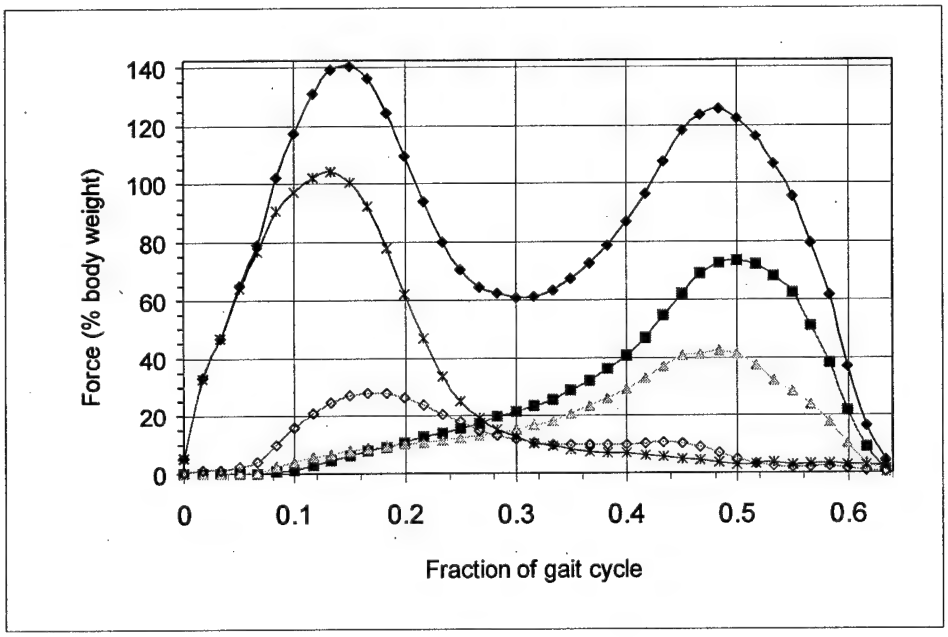

(b)

Figure 22. Biomechanical studies of the effects of shoe outer sole wedges on pedal/footwear interface stress magnitudes, spatial distribution, temporal duration, and lower limb kinematics. Total and regional plantar stresses over a typical gait cycle during normal, level walking at a subject selected speed of 1.8 m/sec, are shown for the right foot of a normal, healthy test subject of military service age wearing well-fitting oxford shoes with a lateral sole wedge. Results are shown for wedges of: **(a)** 0 mm in thickness (no wedge); **(b)** 8 mm in thickness;

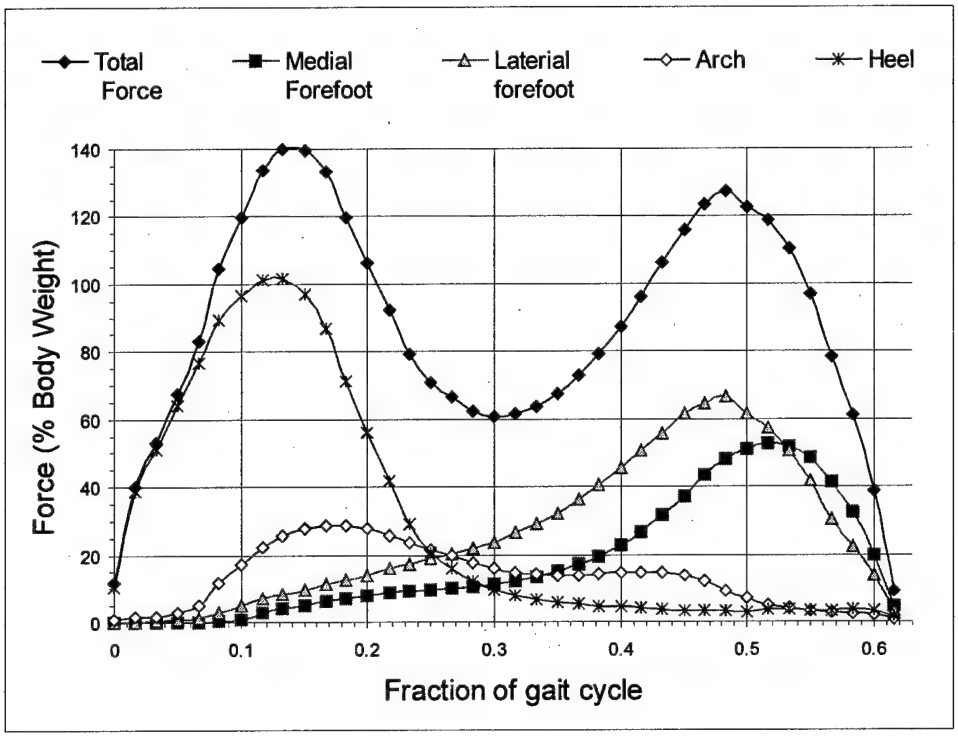

(c)

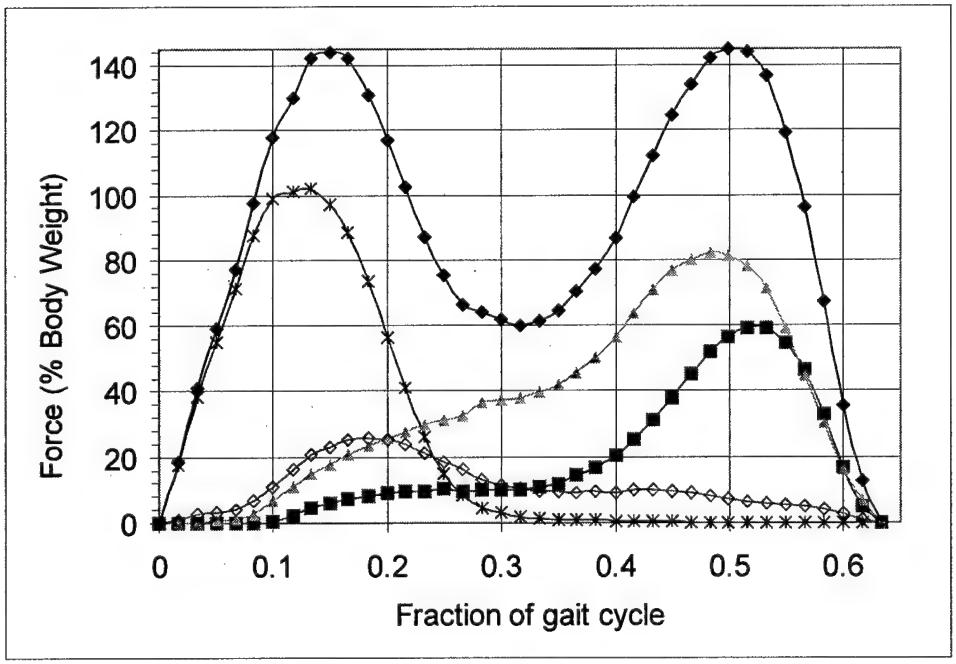

(d)

Figure 22. (cont.) (c) 4 mm in thickness; and **(d)** 2 mm in thickness. As seen, an 8mm sole wedge effectively reduces forefoot loading on the respective side of application. Wedges of decreasing thickness were found to correspondingly produce reduced effects on loading, until at 2mm thickness their effect was negligible.

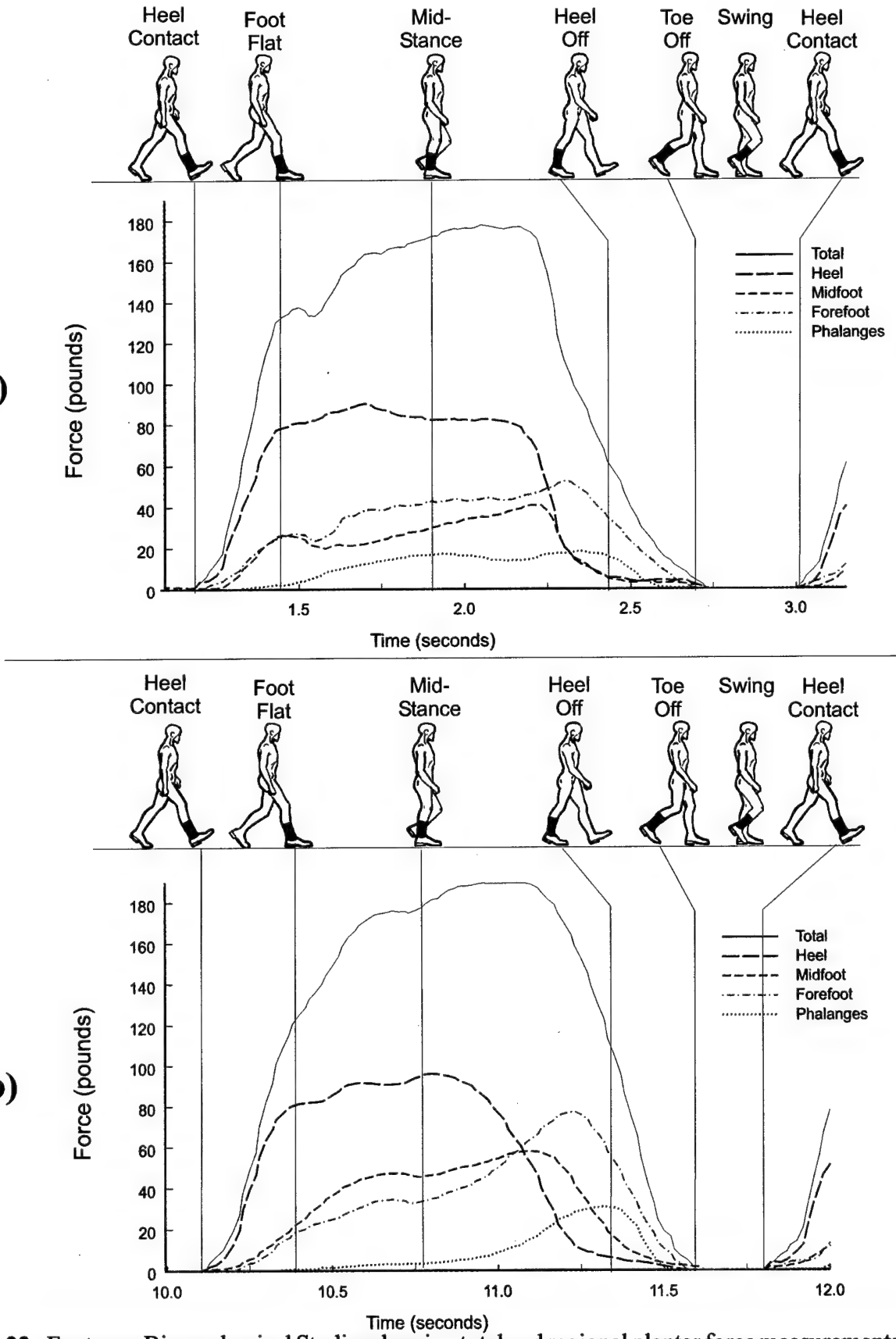

Figure 23. Footwear Biomechanical Studies showing total and regional plantar force measurements versus time from the central gait cycle in a 10 m level walking trial at user selected walking speed, for the right foot of a test diabetic subject with a peripheral neuropathy wearing oxford style shoes with: **(a)** "normal" width outer soles and heels; and **(b)** ½" extended width outer soles and heels. Non-demarcated heel contact-to-foot flat, with prolonged loading of the heel and mid-foot regions, and lengthened and reduced amplitude loading of the forefoot, indicative of a festinating gait is evident in the "normal" width sole and heel shoes. In the extended width sole and heel shoes the subject's gait is slightly improved, with heel contacttofoot flat, midstance, and heel risetotoe off gait phases being more clearly defined, and the duration of heel and midfoot loading reduced, indicating a more controlled, stabler, energy efficient gait.

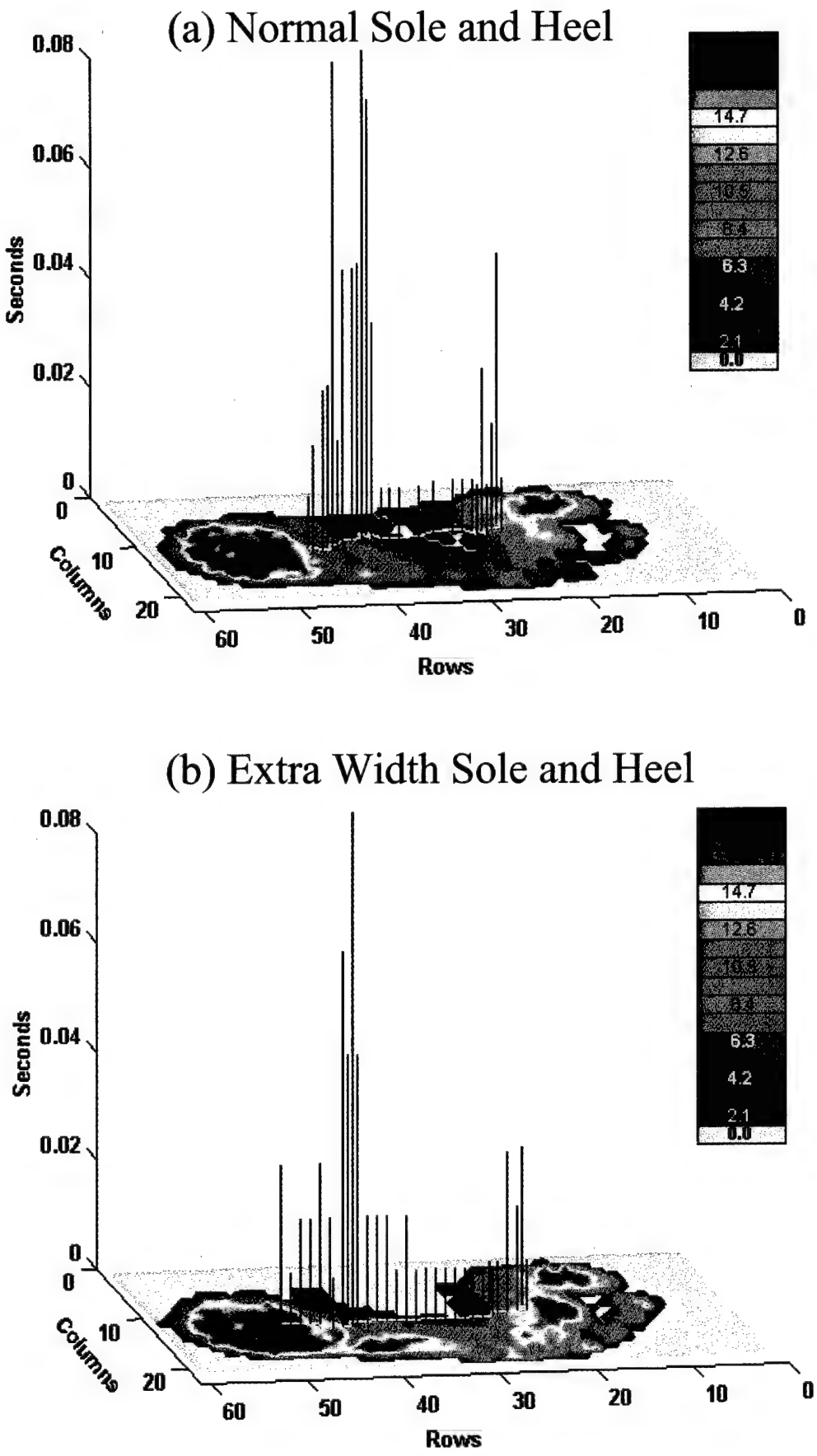

Figure 24. Peak plantar pressures over a gait cycle in the 10 m level walking trial of the neuromuscular test subject shown in Figure 23. Measurements were acquired using individual sensel calibrated, 960 element, FScan FVR insole transducers, sampled at 100 Hz. Pressures are shown color encoded by magnitude. Center of pressure (COP) trajectories are shown as a white line in the (x,y)–plane, with corresponding segmental temporal loading durations plotted along the z–axis. **(a)** In the shoes with standard width outer soles and heels, the subject is seen to initiate floor contact flatfooted, maintaining much of his body weight back on his heel throughout the weight transfer and midstance phases of gait. The subject's COP is seen to wander erratically, reflecting difficulty in neuromuscular control, and decreased stability. **(b)** With the extended width sole and heel shoes, loading is seen to be distributed more evenly over the subject's foot; he has more clearly demarcated heel contact and heel rise–to–toe off gait phases; and his COP trajectory is much smoother, indicating a stabler gait.

PARAMETER	tot/Left	Right
Leg Length(cm)	89.	89.
Step Time(sec)	.992	.972
Step Length(cm)	28.444	31.469
Step Extremity(ratio)	.32	.35
Cycle Time(sec)	1.963	1.982
Stride Length(cm)	59.94	61.359
HH Base Support(cm)	15.073	15.139
Swing Time(sec)	.565	.492
Stance Time(sec)	1.398	1.49
Single Supp. Time(sec)	.492	.565
Double Supp. Time(sec)	.912	.898
Swing % of Cycle	28.8	24.8
Stance % of Cycle	71.2	75.2
Single Supp % Cycle	25.1	28.5
Double Supp % Cycle	46.5	45.3
Toe In / Out	18.1	21.3

PARAMETER	
Step Count	24.
Distance	718.95
Ambulation Time	23.56
Velocity	30.5
Normalized Velocity	61.1
Cadence	.34
Step Time Differential	.02
Step Length Differential	3.025
Cycle Time Differential	.019
Functional Amb. Profile	55.

(a) Standard Shoes

PARAMETER	tot/Left	Right
Leg Length(cm)	89.	89.
Step Time(sec)	.978	1.09
Step Length(cm)	29.106	32.063
Step Extremity(ratio)	.33	.36
Cycle Time(sec)	2.082	2.078
Stride Length(cm)	62.3	61.063
HH Base Support(cm)	10.536	10.332
Swing Time(sec)	.554	.58
Stance Time(sec)	1.528	1.498
Single Supp. Time(sec)	.58	.554
Double Supp. Time(sec)	.948	.945
Swing % of Cycle	26.6	27.9
Stance % of Cycle	73.4	72.1
Single Supp % Cycle	27.9	26.7
Double Supp % Cycle	45.5	45.5
Toe In / Out	16.8	24.1

PARAMETER	
Step Count	23.
Distance	701.97
Ambulation Time	23.74
Velocity	29.6
Normalized Velocity	58.1
Cadence	.33
Step Time Differential	.112
Step Length Differential	2.957
Cycle Time Differential	.004
Functional Amb. Profile	56.

(b) Wide Soles

Figure 25. GaitRite Electronic Walkway measurements over the 10 m level walking trial at user selected speed for the neuromuscular test subject in Figures 23 and 24: **(a)** in standard width sole and heel shoes, and **(b)** in extended width sole and heel shoes. In the extended width sole and heel shoes the subject's stride length is slightly increased; his mediolateral gait base decreased, and his COM mediolateral accelerations decreased — all indicative of an improved, more stable gait.

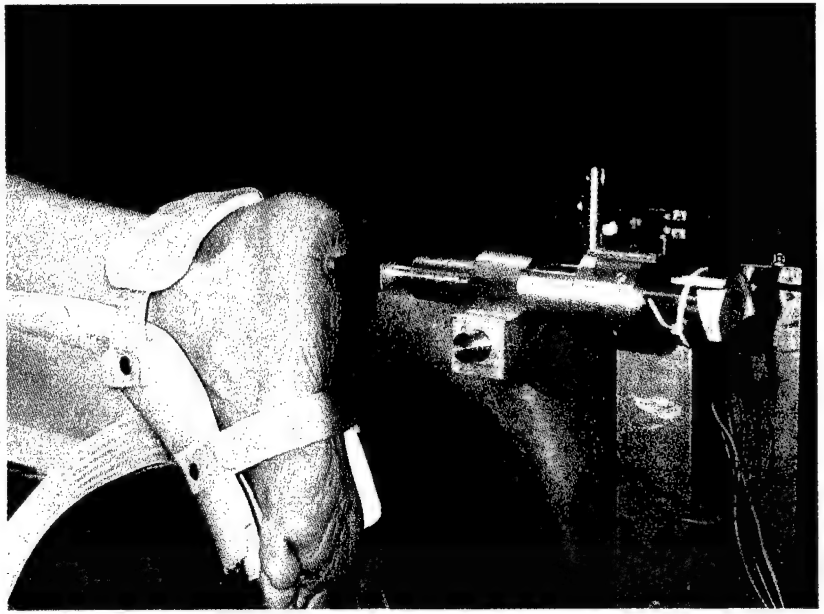

(a)

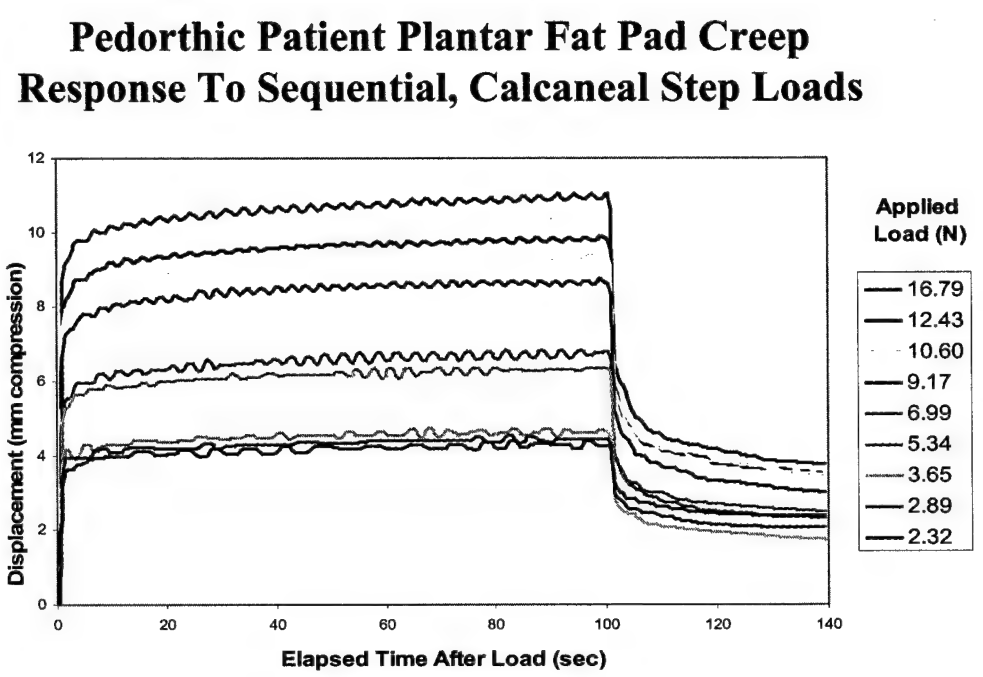

(b)

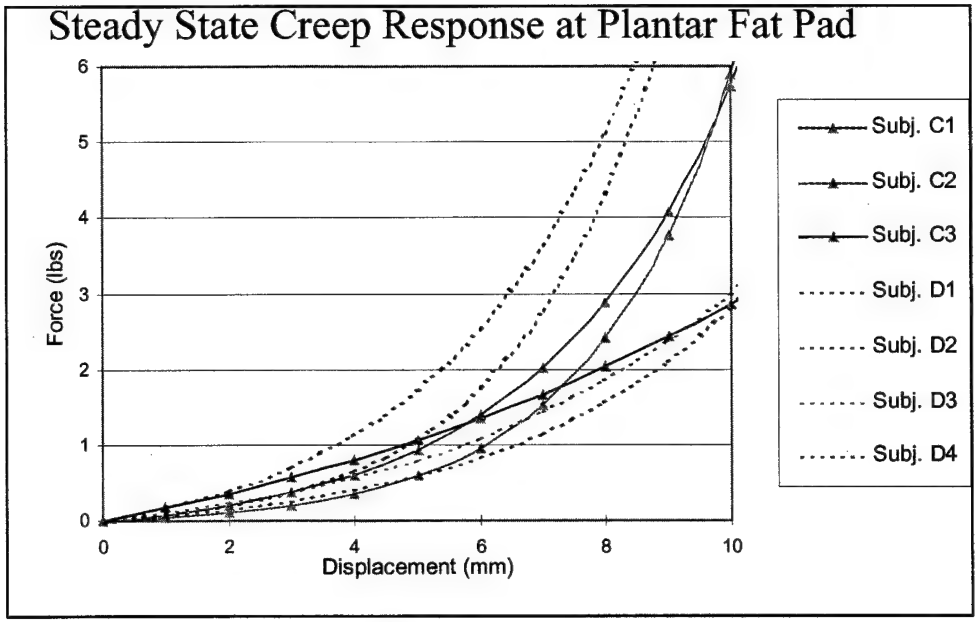

(c)

Figure 26. (a) Measurement of the mechanical properties of a test subject's pedal fat pad with the VA NYHHS optoelectromechanical tissue indentor. As shown, subjects are mechanically "locked" in place relative to the indentor frame to mitigate "movement noise". **(b)** Tissue creep responses at nine step force loads of increasing magnitude, sequentially applied to the plantar fat pad. **(c)** Resulting Force-Displacement plots of the steady state creep response of the pedal plantar fat pads for 3 normal subjects, and 4 neuropathic diabetic subjects.

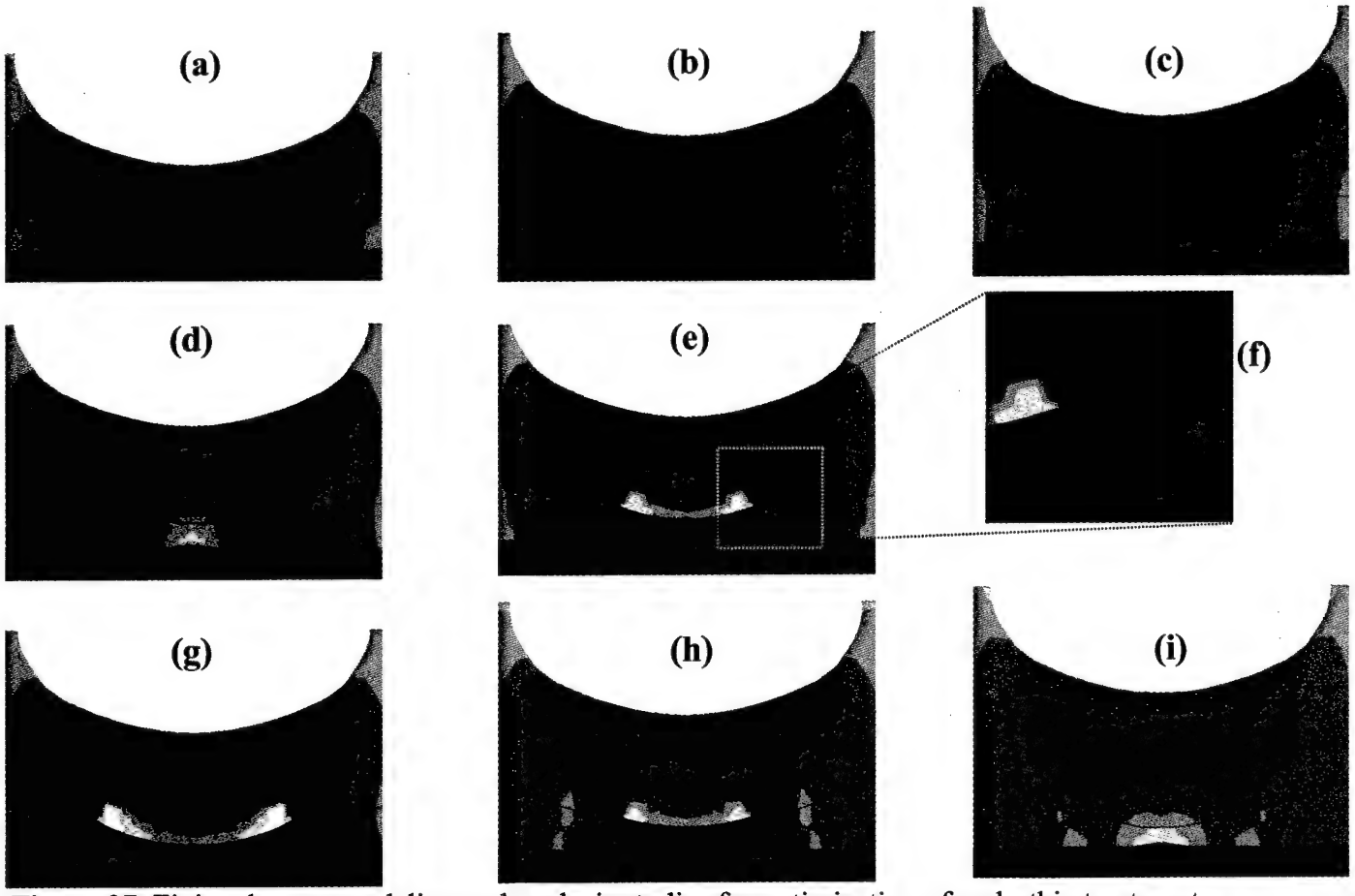

Figure 27. Finite element modeling and analysis studies for optimization of pedorthic treatment of podalgia/plantar fasciitis. Mid-calcaneal, frontal cross sections of the foot of a test subject showing FEA predicted vertical stress incurred, as a function of pedorthic insole material stiffness and design geometry, when the subject stands on a flat, rigid surface, applying a vertical load of 200 Newtons (approximately ¼ body weight) through his talus and calcaneous. All insoles in their unloaded state are 5 mm thick at center. **(a)** Tissue stress distribution incurred with the subject standing barefoot without a pedorthosis. **(b)** Tissue stress distribution incurred with the subject standing on a non-contoured, generic insole, with material stiffness equivalent to that of his pedal tissues. **(c)** Stress distribution incurred when standing on a non-contoured insole with material stiffness six times that of his pedal tissue. **(d)** Stress distribution produced by standing on a non-contoured, generic insole, six times pedal tissue stiffness, with a conical relief 25 mm in base diameter and 2.5 mm deep cut out of the bottom of the insole under the heel. **(e)** Stress distribution produced by standing on a non-contoured insole, six times pedal tissue stiffness, with a 14 mm diameter cylindrical relief cut out of the insole under the heel. **(f)** Enlarged inset of case (e) showing the increase in stress magnitudes due to the Dunnel effect from large gradients in stiffness of adjoining materials at the tissue–insole–relief junction. **(g)** Stress distribution produced with a non-contoured insole, six times pedal tissue stiffness, with a 20 mm diameter cylindrical relief cut out under the heel. **(h)** Stress distribution produced with an insole six times pedal tissue stiffness, and custom made to match the subject's pedal contours, with a 14 mm diameter cylindrical relief cut out under the heel. **(i)** Stress distribution produced with a custom contoured insole, six times the pedal tissue stiffness, with a conical relief 25 mm in base diameter and 2.5 mm deep cut out under the heel, and with the additional condition that rheological displacement of pedal soft plantar tissues relative to the calcaneous is constrained (as achieved by extending the borders of the insole proximally around the fat pad to hold it in place). As clearly evident, only in this latter case are tissue stresses and stress gradients reduced appreciably. *(See Table 4 for a quantitative tabulation of results.)*

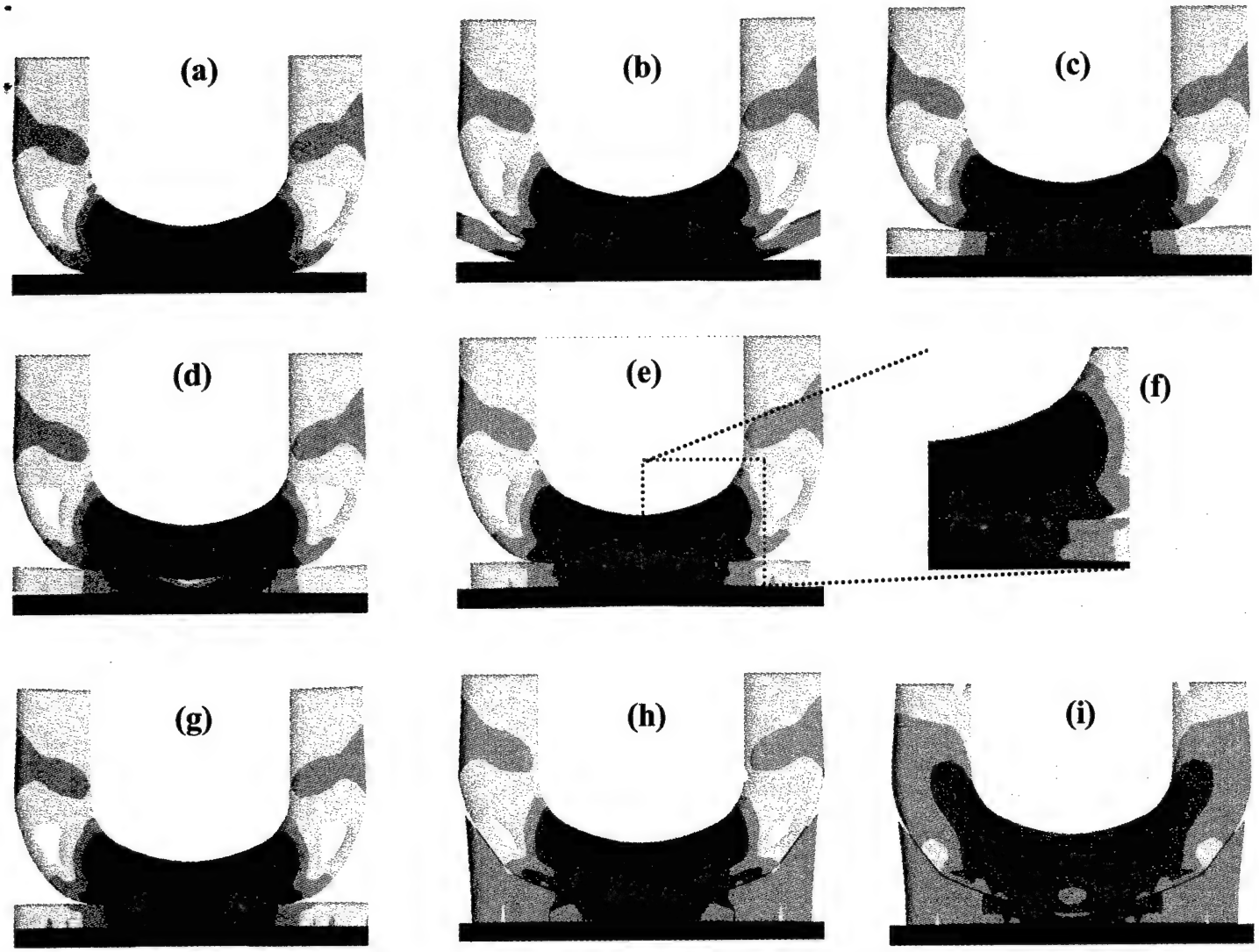

Figure 28. Finite element modeling and analysis studies for optimization of pedorthic treatment of podalgia/plantar fasciitis. FEA predicted tissue total vertical strains at the mid-calcaneal, frontal cross section of the test subject's foot in Figure 27, standing on a flat, rigid surface supporting a 200 Newton vertical load through his calcaneous and talus. **(a)** Tissue strains incurred standing barefoot without a pedorthosis. **(b)** Tissue strains incurred when standing on a non-contoured, generic insole with material stiffness equivalent to that of the subject's pedal tissues. **(c)** Strains incurred when standing on a non-contoured insole with material stiffness six times that of pedal tissue. **(d)** Tissue strains produced by standing on a non-contoured insole, six times pedal tissue stiffness, with a conical relief 25 mm in base diameter and 2.5 mm deep cut out of the bottom of the insole under the heel. **(e)** Strains produced by standing on a non-contoured insole, six times pedal tissue stiffness, with a 14 mm diameter cylindrical relief cut out of the insole under the heel. **(f)** Enlarged inset of case (e) showing the strains and strain gradients produced adjacent to the insole relief border. **(g)** Strains produced with a non-contoured insole, six times pedal tissue stiffness, with a 20 mm diameter cylindrical relief cut out under the heel. **(h)** Strains produced with an insole six times pedal tissue stiffness, and custom fabricated to match the subject's pedal contours, with a 14 mm diameter cylindrical relief cut out under the heel. **(i)** Strains produced with a custom contoured insole, six times pedal tissue stiffness, with a conical relief 25 mm in base diameter and 2.5 mm deep cut out under the heel, and with the additional condition that rheological displacement of pedal soft plantar tissues relative to the calcaneous is constrained (as achieved by extending the borders of the insole proximally around the fat pad to hold it in place). As evident, only in this latter case are tissue strains reduced appreciably.

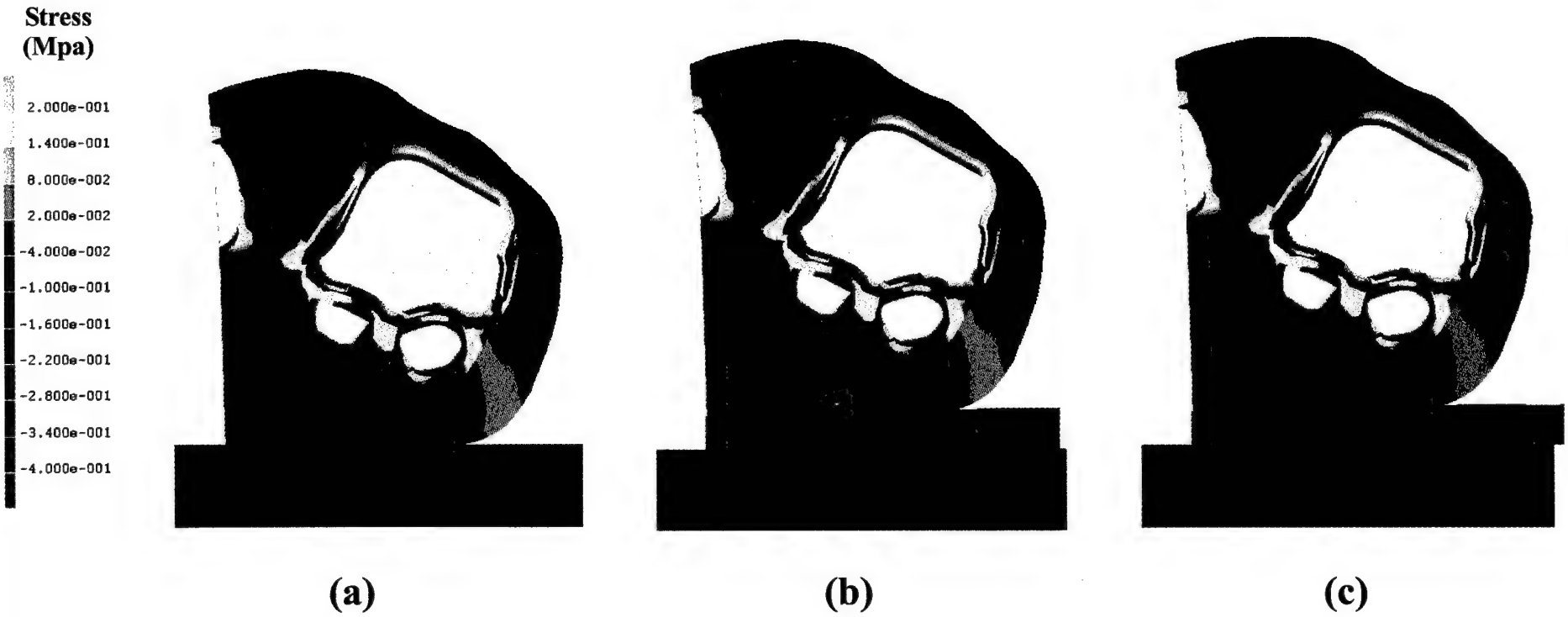

Figure 29. FEA predicted vertical Cauchy stresses produced at the 1st metatarsal head of a test subject standing: **(a)** barefoot on the floor; **(b)** on an insole made from Latex impregnated cork (with 80 Shore hardness durometer); and **(c)** on a poron insole of 30 Shore hardness durometer. Differences in the resulting peak stresses produced in the pedal tissues are seen to be minimal, with the spatial distribution of the stress in the pedal tissues supported on the softer poron being generally slightly lower in magnitude and more dispersed.

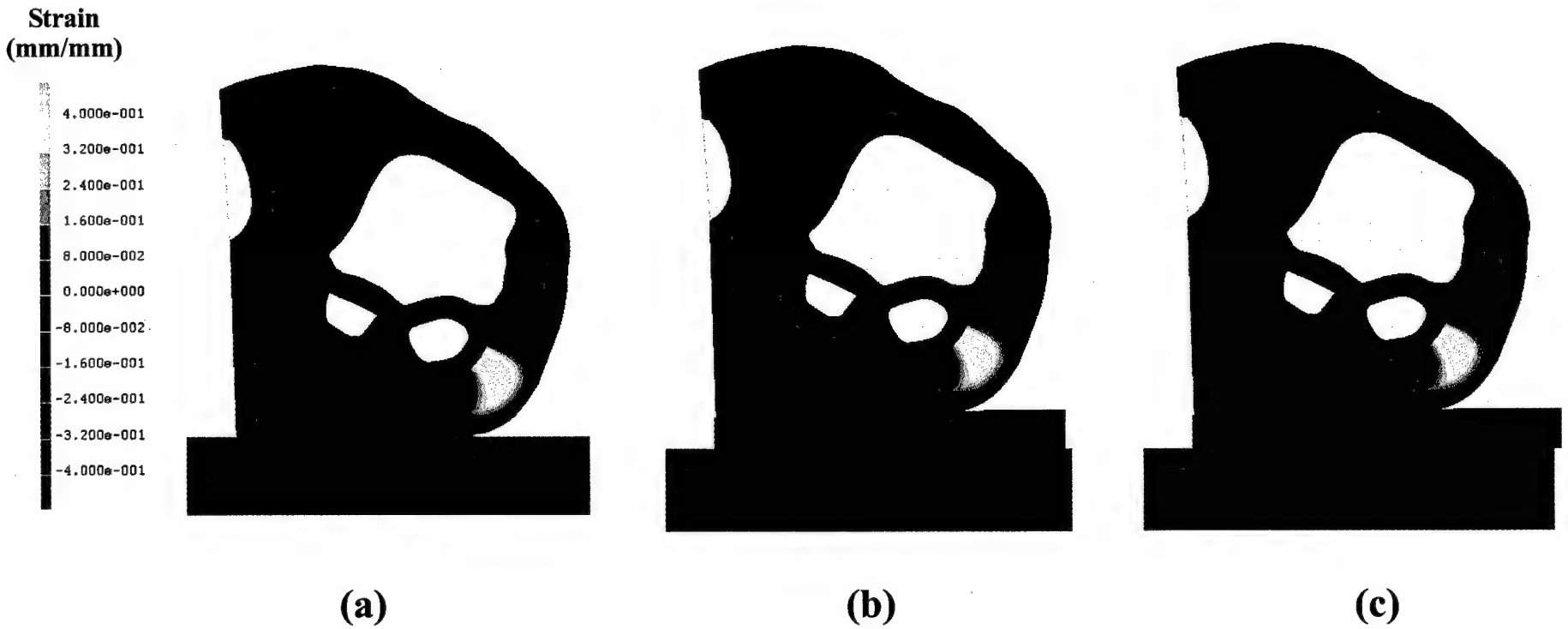

Figure 30. FEA predicted vertical Green strains produced at the 1st metatarsal head of a test subject standing: **(a)** barefoot on the floor; **(b)** on an insole made from Latex impregnated cork (with 80 Shore hardness durometer); and **(c)** on a poron insole of 30 Shore hardness durometer. The strains produced in the pedal tissues supported by the insoles are slightly smaller than in the barefoot case. The pedal tissue strains supported on the softer poron are generally slightly lower in magnitude and more dispersed.

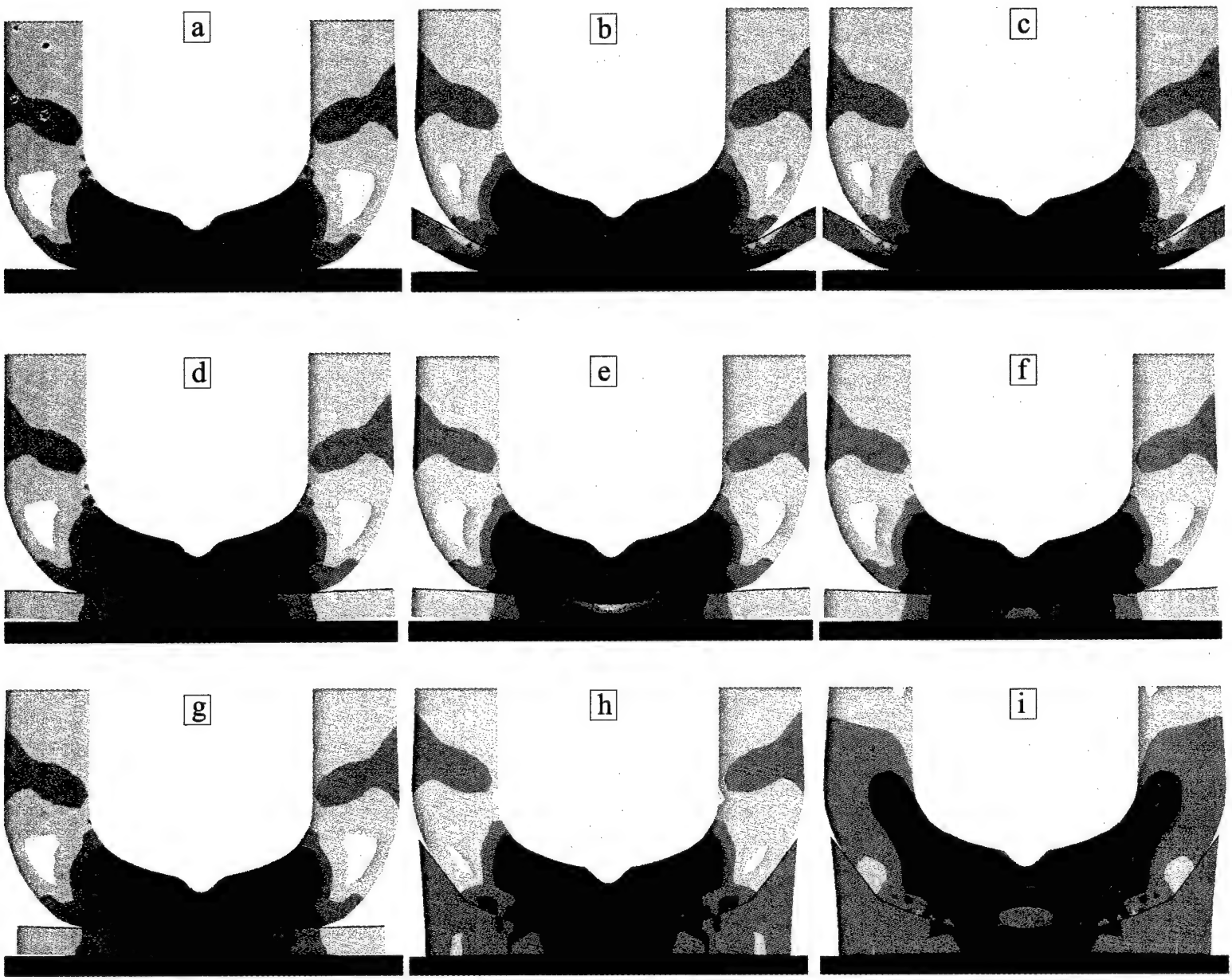

Figure 31. Finite element modeling and analysis studies for optimization of pedorthic treatment for calcaneal osteophytes. FEA predicted tissue total vertical strains at the mid-calcaneal, frontal cross section of the foot of a test subject with a vertical heel spur, standing on a flat, rigid surface, applying a 200 Newton vertical load through his talus and calcaneous. Tissue strains are shown as a function of pedorthic insole material stiffness and design geometry. All insoles are 5 mm thick at center in their unloaded state. **(a)** Tissue strains incurred with the subject standing barefoot without a pedorthosis. **(b)** Tissue strains incurred when standing on a non-contoured, generic insole with material stiffness equivalent to that of the subject's pedal tissues. **(c)** Strains incurred when standing on a non-contoured insole with material stiffness 2.5 times that of pedal tissue. **(d)** Tissue strains produced by standing on a non-contoured insole, six times pedal tissue stiffness. **(e)** Tissue strains produced by standing on a non-contoured insole, six times pedal tissue stiffness, with a conical relief 25 mm in base diameter and 2.5 mm deep cut out of the top of the insole under the heel. **(f)** Tissue strains produced by standing on a non-contoured insole, six times pedal tissue stiffness, with a conical relief 25 mm in base diameter and 2.5 mm deep cut out of the bottom of the insole under the heel. **(g)** Strains produced by standing on a non-contoured insole, six times pedal tissue stiffness, with a 14 mm diameter cylindrical relief cut out of the insole under the heel. **(h)** Strains produced with an insole six times pedal tissue stiffness, and custom fabricated to match the subject's pedal contours, with a 14 mm diameter cylindrical relief cut out under the heel. **(i)** Strains produced with a custom contoured insole, six times pedal tissue stiffness, with a 14 mm diameter cylindrical relief cut out under the heel, and with the additional condition that rheological displacement of pedal soft plantar tissues relative to the calcaneous is constrained (as achieved by extending the borders of the insole proximally around the fat pad to hold it in place). Only in the latter case are pedal tissue strains reduced appreciably. *(See Table 5 for a quantitative tabulation of results.)*

Plastic Insole Material Stress-Strain Characteristics

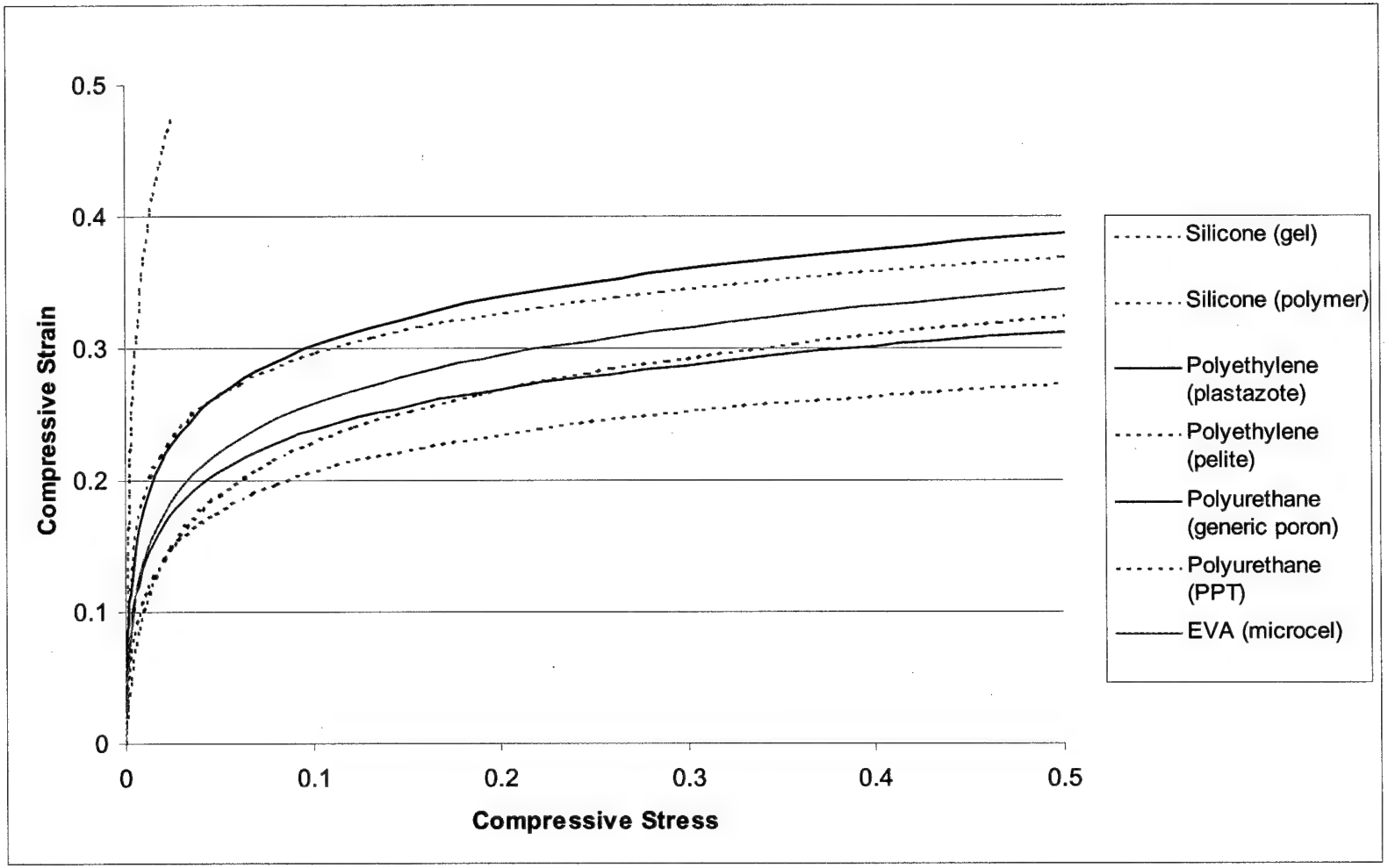

Figure 32. Nonlinear stress-strain characteristics of seven plastic materials commonly used in fabrication of orthopedic insoles.

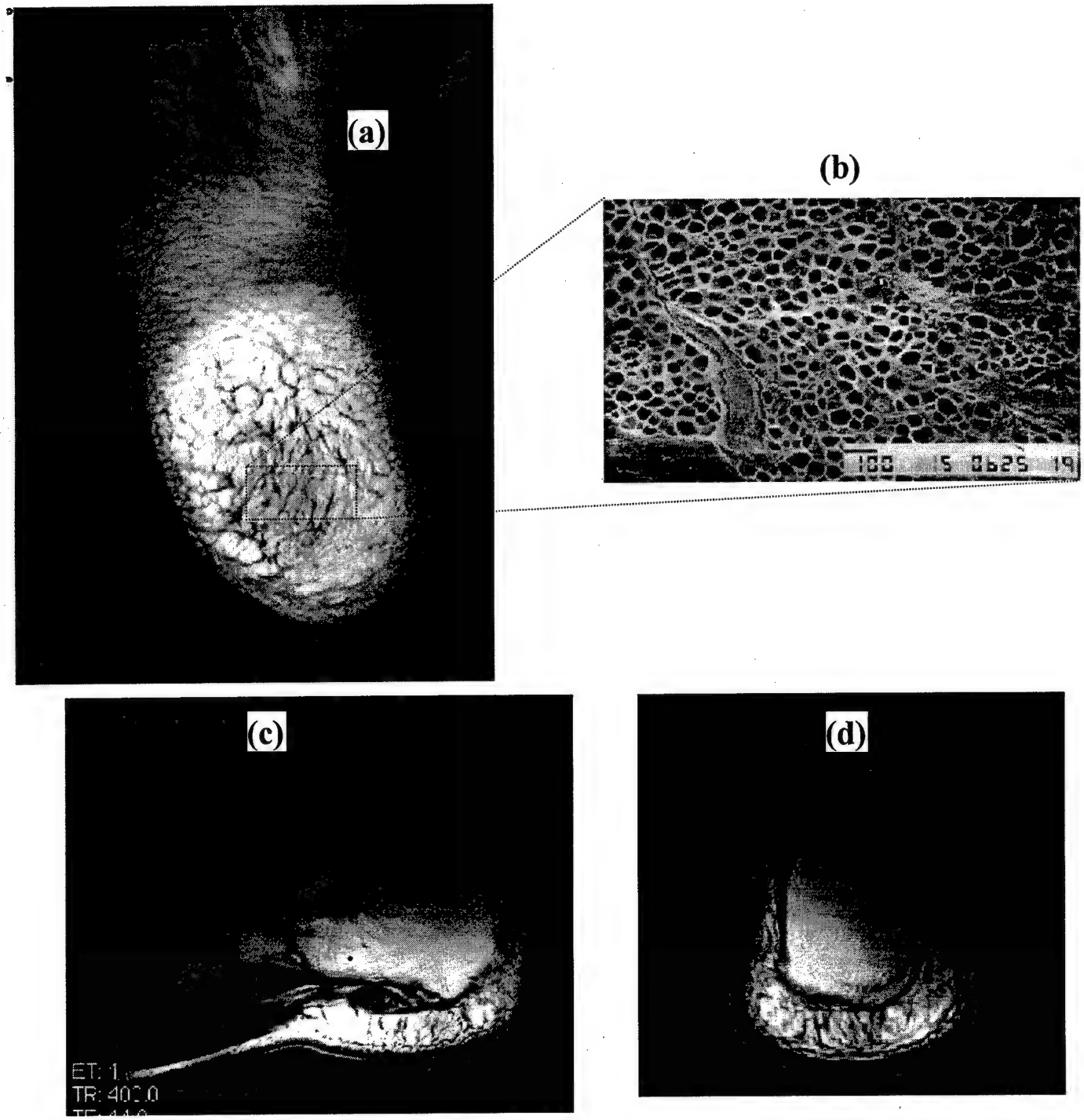

Figure 33. Magnetic resonance images of the test subject's foot in Figure 26 in an unloaded state, showing: **(a)** a longitudinal cross section distal to the calcaneous; **(b)** a magnified histological section of the plantar fat pad under the calcaneous, showing the individual, "honey comb" like septae that dampen and disperse pedal loads; **(c)** a sagittal cross section through the mid-foot showing the morphology of the fat pad, plantar aponeurosis, calcaneous, and talus; and **(d)** a frontal cross section through the mid-calcaneous showing the relative structure of the fat pad, with axial alignment of the septae directly under the calcaneous for damping of impact loads, and gradual transition of the septal alignment to a convoluted pattern near the calcaneal borders serving to disperse plantar loading.

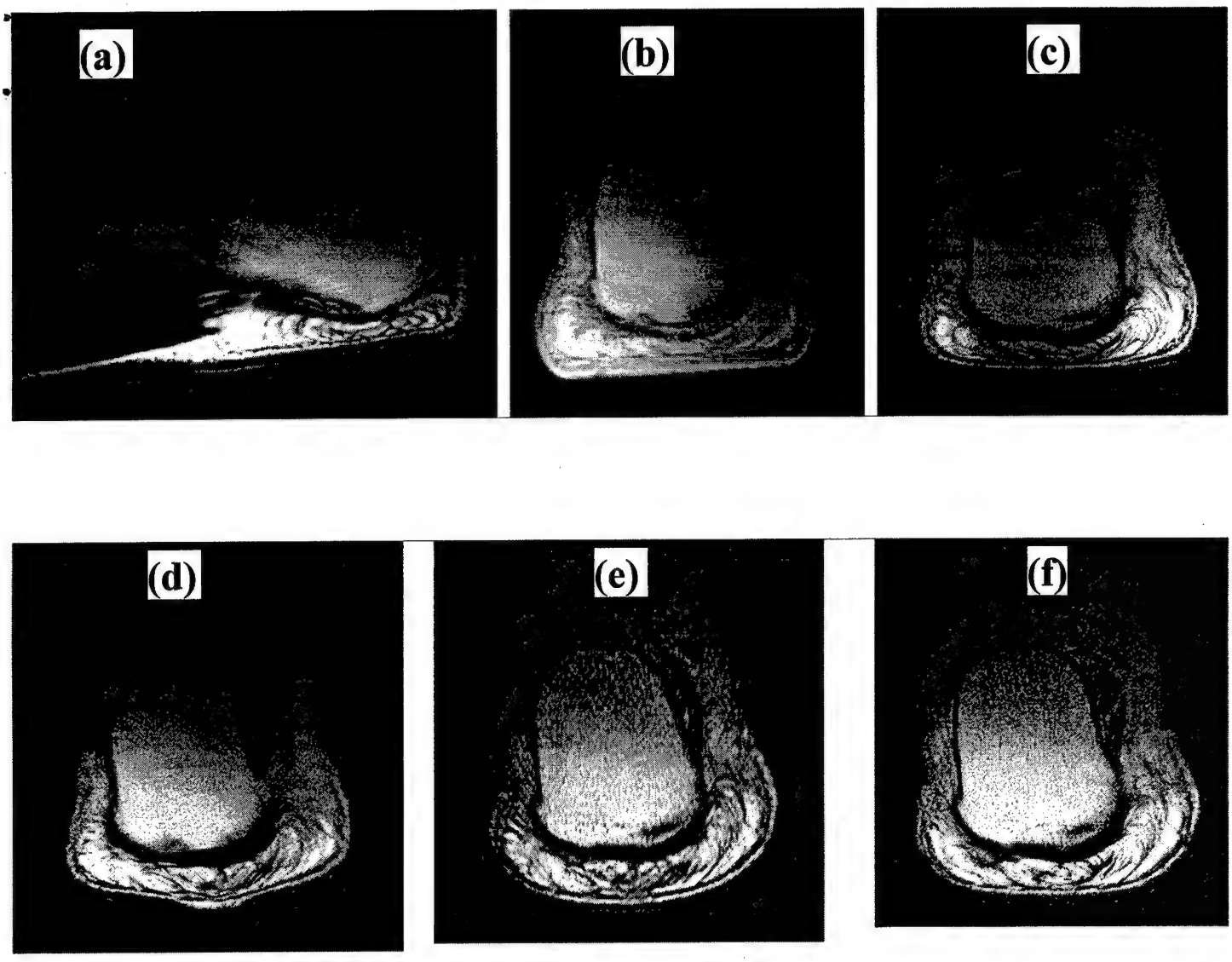

Figure 34. Magnetic resonance images of the test subject's foot in Figure 26 with a 200 Newton load applied axially through the tibia, talus, and calcaneous. **(a)** Sagittal cross section of the subject's foot axially loaded without a pedorthosis. **(b)** Frontal cross section through the mid-calcaneous of the subject's bare foot under axial load. **(c)** Frontal cross section of the subject's foot under axial load while supported on a generic, non-contoured insole, approximately six times his pedal tissue stiffness. **(d)** Frontal cross section of the subject's foot under axial load while supported on a generic, non-contoured insole, approximately six times his pedal tissue stiffness, with a 14 mm diameter cylindrical relief cut out under the heel. **(e)** Frontal cross section of the subject's foot under axial load while supported on a custom contoured insole designed to match his unloaded pedal tissue shape, approximately six times his pedal tissue stiffness. **(f)** Frontal cross section of the subject's foot under axial load while supported on an insole approximately six times his pedal tissue stiffness, custom contoured to match his unloaded pedal shape, with borders extending proximally, constraining displacement of his pedal plantar fat pad. The tissue strains incurred with the custom contoured insoles are seen to be measurably less than with the non-contoured, generic insoles.

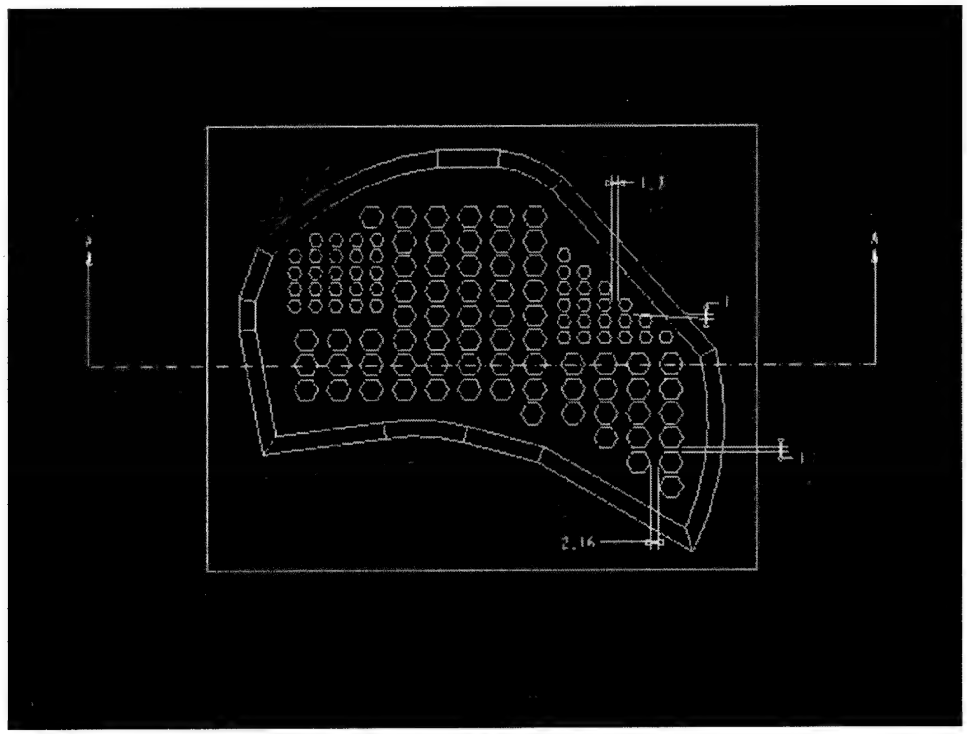

(a)

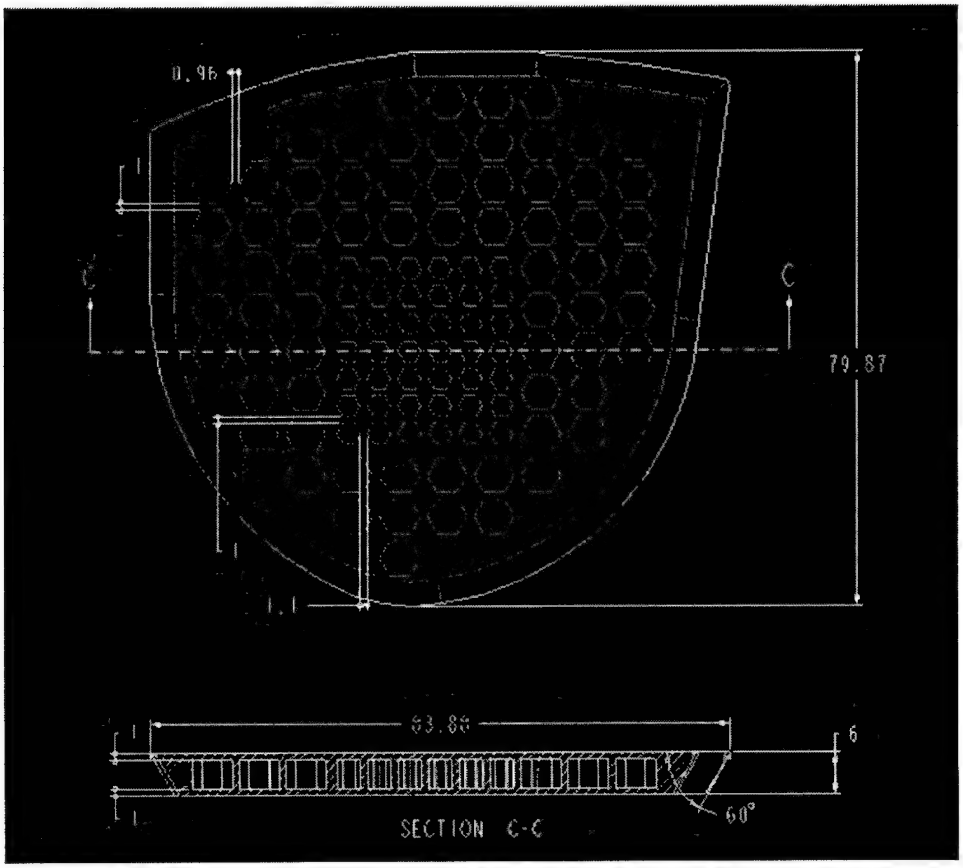

(b)

Figure 35. Initial design for **(a)** metatarsal head, and **(b)** heel cushions to be incorporated in the outer soles of footwear for treatment of metatarsalgia, plantar fasciitis, and heel spurs. As seen in Figure 33, the design mimics the anatomical structure of the pedal plantar fat pad, incorporating sealed, "honey comb" like septae, which serve as miniature hydraulic/pneumatic damping cylinders that dissipate and disperse locally applied loads.

Table 1. VA OSS ORTHOPEDIC SHOE LAST SURVEY MODIFICATION CODE LOG

	LAST REGION	MOD CODE	MAGNITUDE AND/OR DIRECTION OF MODIFICATION		LAST REGION		MAGNITUDE AND/OR DIRECTION OF MODIFICATION
1	TOE BOX AREA	A	RAISED 0 TO 1/4" DORSAL	6	FOREFOOT POSITION	A	ADDUCTED
		B	RAISED 1/4 TO 1/2" "			B	ABDUCTED
		C	RAISED 1/2/ TO 1" "			C	BUNION SHAPE
		D	WIDER WIDTH 0 TO 1/4 "			D	STRAIGHT
		E	WIDER WIDTH 1/4 TO 1/2 "				
		F	WIDER WIDTH 1/2 TO 1"	7	TONGUE/VAMP	A	BUILDUP 0 TO 1/4 "
		G	ADDITION TO PLANTAR AREA 0 TO 1/4 "			B	BUILDUP 1/4 TO 1/2 "
		H	ADDITION TO PLANTAR AREA 1/4 TO 1/2"			C	BUILDUP 1/2 TO 1 "
		I	ADDITION TO PLANTAR AREA 1/2 TO 1"				
				8	HEEL AREA	A	PLANTAR AREA DEPRESSION 0 TO 1/4 "
2	HALLUX AREA	A	RAISED DORSAL 0 TO 1/4 "			B	PLANTAR AREA DEPRESSION 1/4 TO1/2 "
		B	RAISED DORSAL 1/4 TO 1/2 "			C	PLANTAR AREA DEPRESSION 1/4 TO 1 "
		C	RAISED DORSAL 1/2 TO1 "			D	PLANTAR AREA RAISED 0 TO 1/4 "
		D	WIDEN AREA 0 TO 1/4 " MED SIDE			E	PLANTAR AREA RAISED 1/4 TO1/2 "
		E	WIDEN AREA 1/4 TO 1/2 " MED SIDE			F	PLANTAR AREA RAISED 1/2 TO 1 "
		F	WIDEN AREA 1/2 TO 1 " MED SIDE			G	LATERAL WEDGE 0 TO 1/4"
		G	PLANTAR AREA RAISED 0 TO 1/4 "			H	BUILDUP AROUND HEEL M/L 1/4"
		H	PLANTAR AREA RAISED 1/4 TO1/2 "				
		I	PLANTAR AREA RAISED 1/2 TO 1 "	9	HEEL POSITION	A	STRAIGHT
						B	INVERSION
3	5TH TOE AREA	A	RAISED DORSAL 0 TO 1/4 "			C	EVERSION
		B	RAISED DORSAL 1/4 TO 1/2 "				
		C	RAISED DORSAL 1/2 TO1 "	10	PLANTAR SURFACE	A	RAISE UNDER TOES (S,M,L)
		D	WIDEN AREA 0 TO 1/4 " LAT SIDE			B	RAISE UNDER METHEADS (S,M,L)
		E	WIDEN AREA 1/4 TO 1/2 " LAT SIDE			C	DEPRESSION UNDER TOES (S,M,L)
		F	WIDEN AREA 1/2 TO 1 " LAT SIDE			D	DEPRESSION UNDER METHEADS (S,M,L)
		G	PLANTAR AREA RAISED 0 TO 1/4 "			E	WEDGE LATERAL SIDE OF FOOT (S,M,L)
		H	PLANTAR AREA RAISED 1/4 TO1/2 "			F	WEDGE MEDIAL SIDE (S, M, L)
		I	PLANTAR AREA RAISED 1/2 TO 1 "			G	(S) 1/4SMALL , (M) 1/2MED (L) 3/4 LARGE
						H	OTHER THAN ABOVE
4	METATARSAL AREA	A	PLANTAR AREA DEPRESSION 0 TO 1/4 "				
		B	PLANTAR AREA DEPRESSION 1/4 TO1/2 "	11	ANKLE	A	BUILDUP MED 0 TO 1/2"
		C	PLANTAR AREA RAISED 0 TO 1/4 "			B	BUILDUP LAT 0 TO 1/2"
		D	PLANTAR AREA RAISED 1/4 TO1/2 "			C	BUILDUP BILATERALLY 0 TO 1/2"
						D	BUILDUP > 1/2" M(MED, L(LAT) B(BOTH)
5	ARCH AREA	A	PLANTAR AREA DEPRESSION 0 TO 1/4 "				
		B	PLANTAR AREA DEPRESSION 1/4 TO1/2 "				
		C	PLANTAR AREA DEPRESSION 1/4 TO 1 "				
		D	PLANTAR AREA RAISED 0 TO 1/4 "				
		E	PLANTAR AREA RAISED 1/4 TO1/2 "				
		F	PLANTAR AREA RAISED 1/2 TO 1 "				

Table 2. Female Test Subjects — Foot/Ankle Measurements (mm)

Subj No	Body H	Calf C	Heel Toe L	Heel Ball L	Heel Ant. Ankle L	Heel Lever	Toe Lever	Ball W Horiz	Ball W Dia	Heel to 5MTH	Heel W	Ball C	Waist C	Heel to Instep L	Instep C	Span C	Heel Toe Semi-C	Max Toe H	Ankle H	Ankle AP W	Ankle ML W	Ankle C	Malle-olus L-R	M Malle-olus H	L Malle-olus H	Dorsal Foot H	M Plan Arch H
1	168	37	24.5	17	10.5	6.2	17.3	9.5	10.5	16.2	7.37	26.9	26.5	10.5	29	34.5	27	3	10	9.37	6.8	26.5	6.9	8.5	7	7.8	1.85
2	178	30	25.8	18.3	9.3	6	20	9.6	10.1	17.5	6.3	24.4	24	11	24.1	34	28	2.6	11	8.9	7	24.3	6.8	9	7.8	7.6	4
3	160	27	24	17.5	8	4.6	18.5	8.9	9	16.1	6.2	20.6	21.5	9.5	21.8	30.8	25.7	2.5	9.28	7.1	6.2	19.4	6.6	7.83	6.13	6.62	2.3
4	164	28	22.6	17.1	8	5.7	16.9	8.1	8.2	14.36	5.9	21	19.7	11	20.4	29	25	2.2	9.1	7.3	5.3	19.7		7.28	5.58	5.89	2.86
5	161	32	24.2	17.4	8.6	4.5	19.7	9.2	9.53	14.14	6.1	24.5	22.8	10.1	24	31.3	25.3	2.3	10.5	8.2	5.4	21.9	6.7	7.7	6.68	6.54	2.68
6	159	32	23	16.5	10	5.1	13	9.1	9.5	14	6.4	23	23.1	10.6	24.2	31.1	26	2.7	10	7.6	6.1	21.2	6.2	8.25	7.4	7.3	2.6
7	155	38	23.2	17.3	10.5	6.5	16.7	9.6	10	14.5	5.8	23.6	23.8	12	24.1	31.9	25.6	2.8	9.7	8.1	7	23.3	6.7	8.38	6.84	7.22	4
8	157	31	22.9	16.7	9	4.5	18.4	8.2	8.9	14.5	5.9	21.1	20.7	11	21.8	30.3	26.2	2.8	8.54	7	5.6	20.9	6	7.28	6.4	6.51	2.89
9	157	34	23.6	16.9	8.5	4.7	18.6	8.9	9.1	14.7	5.7	21.2	21.1	11.4	22	31.2	25.6	2.8	10.3	6.7	5.2	19.8	5.8	8.77	6.55	7.22	3.41
10	171	30	23.4	17.1	7.7	5.7	17.7	8.5	8.6	15.6	5.2	21.3	20.7	9.3	21.9	31.5	26.5	2.4	10.8	6.5	4.9	19.8	6.4	8.63	6.8	6.99	3.65
11	165	32	25	18.4	8.8	5.4	19.6	9	9.1	16.6	5.9	22.1	21.9	10	22.9	31.4	31.4	2.4	10.2	6.6	5.5	20.3	6.8	8.24	6.98	6.47	3.13
12	154	32	22.8	17.1	9	5.5	17.3	8	8.2	14.9	5.5	20	19.8	9.9	21.9	28.4	25.5	2.2	9.43	6.8	5.2	19.7	6	7.38	6.61	6.15	3.05
13	163	33	24.1	17.4	9	5	15	8.8	8.9	15.5	6.1	22.1	22.5	11	23.4	32.4	27.1	2.7	10.4	6.8	6	20.5	6.1	8.08	7.1	7	3.35
14	165	30	22.6	17	8.5	5.5	17.1	8	8.1	14.3	5.1	20	20.4	10.4	20.5	31.1	25.6	2.5	10.3	6.6	5	19.1	5.8	7.86	6.2	6.1	2.73
15	160	33	22.6	16.9	7.8	6.3	16.3	8.3	8.6	14.4	5.5	21.6	21.4	9.9	22.8	30.3	25.7	2.1	9.71	6.5	5.5	20.1	6.4	7.42	6.53	6.46	2.8
16	173	38	25.9	19.4	10	6.4	19.5	9.6	9.8	17.1	6.5	24.5	25	11.6	25.1	36.8	29.1	3.7	12	7.9	6.1	23.6	7	9.67	7.62	7.03	3.36
17	165	29	24.7	18.1	10	6.3	18.4	9	9.1	16.4	6.8	22.9	22.7	12.3	23	33.9	29.2	3.1	9.95	7.6	5.6	21.3	6.3	8.43	6.87	6.84	3.06
18	160	31	22.6	16.4	8.5	5.5	17.1	9.3	9.4	14.5	5.5	22.1	21.1	10.6	21.8	30.9	25.1	2	9.3	6.4	5.1	19	6	7.3	6.53	6.04	2.1
19	165	32	24.9	17.8	9	5.5	19.4	9.6	9.3	15.5	6.2	23.1	23	11	23.6	31.6	27.1	2.6	9.91	7.5	5.8	21.7	6.3	8.17	6.92	6.69	2.43
20	173	32	24.5	18.2	9.7	6	18.5	8.9	9.2	15.4	6.5	23	22.3	11.6	24	34.3	26.6	3.2	10.5	7.8	6.2	22.8	6.3	8.58	7	7.5	3.88
21	152	35	22.5	16.2	8.7	5.2	17.3	8.9	9	13.8	5.7	23.4	22.8	9.6	23.9	31.3	24.5	2.9	10.3	7.5	5.9	21.8	6.8	8.32	6.66	7.01	3.06
22	163	37	23.7	17.6	8.8	6	17.7	8.7	8.8	14.9	6	22.7	22.4	11.5	23.4	33.2	27	2.5	10.8	8.5	6.6	24.5	6.5	8.97	6.76	7.2	3
23	160	32	24	17.9	8.9	6.4	17.6	8.6	8.9	15.2	5.8	22	21.6	10.9	23	32.7	26.9	2.9	10	7.1	5.4	21	6.3	7.67	7.23	7.28	2.3
24	175	32	25.4	18.5	9.6	6.4	19	9.2	9.3	16.6	5.7	23.4	22.5	12.5	23.5	32.4	27.7	2.4	10.9	7.5	5.4	21.3	7.3	8.58	6.49	7.16	2.29
25	161	31	24.5	17.8	8.2	6	18.5	9.1	9.5	14.5	6.5	22.6	22.6	12	24.1	33.9	27.3	2.7	10.9	7.3	5.2	21	6	8.59	6.36	7.58	2.8
26	171	40	25.4	19.7	9.4	7.6	17.8	10.2	10.4	16.6	7.6	25.9	26.7	12.9	26.6	35.8	29.5	3.7	10.2	8.6	6.8	25.4	7.5	8.03	7.07	6.73	1.51
27	157	34	23.4	17.4	8.6	5.6	17.8	9.7	9.8	14.6	5.5	23.7	22.3	10.7	23.2	32.8	27	2.8	10.9	7.6	5.9	21.5	6.4	8.3	7.39	7.5	3.48
28	165	29	24.8	18.1	7.8	4.9	19.9	8.9	9	16.1	5.5	22	22.4	10.7	23.9	32.2	27.3	2.2	9.9	6.9	5.5	20.3	6.6	7.59	7.31	6.83	1.56
29	171	27	26.5	19.6	10.5	7.4	19.1	9.5	9.8	17.6	7.3	25	25	13.1	26.3	38.8	30.8	2.8	11	7.5	5.6	21.8	6.6	9.12	7.07	8.36	3.22
30	168	32	24.6	18	7.1	5.5	19.1	9.2	9.3	15.4	6.2	23.4	22.7	11.9	24.5	33.6	28.1	2.6	10.8	7.7	6.5	22.8	6.6	9.1	7.73	7.65	3
31	165	31	24.4	17.6	8.6	6.4	18	8.8	8.9	15.6	6	22.8	22.2	11.8	23	31.2	27.1	2.8	9.9	7.5	5.8	21	6.8	8.3	6.79	7.18	2.69
32	160	29	23.8	17.8	8.8	5.9	17.9	9.2	9.3	15	6.3	22.1	22	10.5	22.8	31.5	26	2.3	9.68	6.9	5.9	20.8	6.5	7.88	7.56	6.56	2.05
33	157	34	22.6	16.6	7.8	5.9	16.7	8.9	9.1	13.4	6.4	22.5	22	10.9	22.7	30.3	26.1	2.6	9.28	6.8	5.6	20.5	6.3	7.55	5.88	6.29	2.56
34	157	36	22.5	16	8.1	5.5	17	8.7	8.9	13.9	5.2	22.3	22	10.4	22	30.1	24.6	2.4	9.83	7.1	5.4	20.1	6.6	7.98	6.5	7.03	2.65
35	165	32	24.8	18.1	9.8	6.5	18.3	8.5	8.9	15	5.7	33.5	22	10.9	25	32.1	26	2.3	10.5	7.5	5.1	19.9	6.5	8.5	6.78	7.79	2.96
36	163	34	24.3	18.2	9.8	7.7	1.6	9.4	9.5	15	6.7	24.5	25	11	24.1	33.1	27.5	3.6	11.5	8	5.8	28	7.11	9.32	7.83	7.5	2.37
37	168	29	24.2	17.6	8.1	5.5	18.9	8.8	8.9	15.5	5.8	22.4	21	11.4	23.2	37.1	26.8	2.3	9.81	6.7	5.2	20.1	6.1	7.98	6.46	6.5	2.53
38	163	36	26.1	19.3	6.5	7	19.1	9.7	10.1	17.1	6.7	24.3	24.7	11	28	34.9	29.2	2.4	9.37	8.3	6.4	24.8	7.1	7.87	6.9	7.4	2.73
39	157	26	22.6	16.6	8.2	4.3	18.9	8	8.2	14	4.9	20.4	19.6	9.5	21	27.9	25.2	2.1	9.26	5.8	4.6	17.2	6.1	7.28	7.14	5.96	2.83
40	173	29	25.8	19.1	10	6.5	19.3	9.5	9.6	15.5	6.3	22.5	22.7	11	25	32.3	28.1	2.4	9.05	7.3	5.4	20.5	6.7	7.23	5.62	6.89	2.31
41	162	35	24.7	18.4	10	6	18.7	8.9	9	15.3	6.1	23	21.3	11	22.8	31	26.2	2.6	11.6	6.8	5.5	21.7	6.2	9.07	6.62	7.65	2.94
42	156	33	22.2	16.5	7.4	5.6	16.6	8.6	8.7	13	5.8	21.8	20.8	10.5	22	30.2	25.9	2	11	6.2	5.1	19	6.1	7.8	7.3	6.53	3.35
43	169	26	25.7	19.1	9.9	5.5	20.2	8.9	9	16	6.3	20	22.6	12.6	23	32	29	2.9	11.2	6.9	5.4	20.4	6.5	8.26	6.97	6.71	3.52
44	142	32	20.5	14	7.1	4.5	16.5	8.5	8.6	23	5.5	19.9	20.2	8.5	21.1	26.8	24	2.2	9.6	6.7	4.9	18.4	6.2	7	6.4	6.2	2.1
45	160	30	24.2	17.5	9.5	5.9	18.3	9.6	9.7	15.3	5.9	22.4	21.9	13	23.5	30.5	26.5	2.2	8.4	7.8	5.6	20.9	6.5	8.7	6.2	5.5	3.4
46	157	31	23.8	17.2	9.4	5.9	17.9	9	9.2	15.3	6.4	22.7	22	9.2	23.5	29.4	26.1	2.7	11.7	7.3	5.5	26	6.5	10.5	9.3	6.8	3.1
47	168	37	23.8	17.5	9.5	6.5	17.3	8.8	8.7	14.7	6.2	22.5	21.1	10.1	23.9	30.8	26.3	2.5	11.2	8.1	5.6	21.2	6.6	9.1	7	5.8	3.3
48	163	37	24.6	18	10	5.8	18.8	9.1	9.2	15	6.5	21.9	21.8	11.5	22.9	30.4	28	2.1	11	7.6	5.8	20.8	6.5	9.1	6.4	6.5	2.6
49	165	34	23.4	17.4	7.7	5.1	18.3	8.5	8.6	14.8	6.1	22	20.6	8.7	24.2	29.9	27.9	2.5	10.6	7.2	5.7	21.8	6.3	8.6	7.4	6.7	2.7
50	173	35	26.9	20.5	9.9	8.9	18	10.1	10.2	16.2	8.2	26.2	25.9	11.3	27.5	35.1	30.8	3.6	11.6	9.1	7	25.8	7.7	9	8.2	7.3	1.9
51	163	32	23	17.4	9.5	6.1	16.9	8.1	8.3	13	5.4	21.3	20.6	9.2	24.1	29.9	25.6	2.5	11	8.6	6.9	21.7	7.6	8.6	7.2	6.7	2.7

H = height L = length W = width C = circumference

Table 3. ORTHOPEDIC FOOTWEAR LAST GRADING PARAMETERS

Parameter	Description	Grading Weight
Heel–to–Toe Length	AP distance crest of heel to end of (1^{st}–2^{nd})toes	1.0
Heel–to–Waist Length	AP distance crest of heel to Waist	1.0
Heel–to–Ball Length	AP distance crest of heel to Ball Center	1.0
Heel Width	ML distance across heel at posterior border of medial malleolus	1.0
Ball Width	ML distance apex 1^{st} metatarsal head to apex 5^{th} metatarsal head	1.0
Ball Circumference	Circumferential distance around ball of foot/Last	0.75
Span Circumference	Circumferential distance around span of foot/Last	0.75
Instep Circumference	Circumferential distance around foot/Last at navicular–cuboid level	0.75
Maximal Toe Height	Maximal vertical distance from plantar surface foot/last to dorsal surface 1^{st}–2^{nd} toes or 3^{rd}–4^{th} toes at IP joint	0.4
Waist Circumference	Circumferential distance around foot/Last at 1^{st} –2^{nd} cuneiform level	0.25
Heel–to–Toe Semi– Circumference	Circumferential distance from heel crest mid point medially around foot/Last at dorsal border to distal end of (2^{nd}) toe	0.75

Table 4. Optimization of Pedorthic Treatment for Podalgia

Stresses–Strains in Heel Pad Soft Tissue vs Pedorthic Insole Stiffness & Geometry

Pedorthic Insole	Heel Pad Maximum Cauchy Stress (*MPa*)	Heel Pad Maximum Green Strain (*mm/mm*)	Heel Pad Maximum Strain Energy Density ($x10^{-3}$ *Joule / mm*^{3})
(a) No Insole	–0.412	–0.459	53.06
(b) Standard flat insole with 1x stiffness of heel pad tissue	–0.354	–0.445	33.77
(c) Standard flat insole with 2.5 x stiffness of heel pad tissue	–0.378	–0.452	40.90
(d) Standard flat insole with 6 x stiffness of heel pad tissue	–0.394	–0.455	46.27
(e) Standard flat insole with 6 x tissue stiffness & 25mm base diameter 2.5mm deep conical relief on bottom surface	–0.342	–0.438	30.44
(f) Standard flat insole with 6 x tissue stiffness & 25mm base diameter 2.5mm deep conical relief on top surface	–0.341	–0.436	30.06
(g) Standard flat insole with 6 x tissue stiffness & 20mm diameter cylindrical relief	–0.277	–0.400	13.08
(h) Standard flat insole with 6 x tissue stiffness & 14mm diameter cylindrical relief	–0.344	–0.434	30.87
(i) Custom contoured insole with 6 x tissue stiffness & 14mm diameter cylindrical relief	–0.236	–0.384	8.91
(j) Custom contoured insole with 2.5 x tissue stiffness & 14mm diameter cylindrical relief	–0.234	–0.381	8.84
(k) Custom contoured insole with 6 x tissue stiffness, 20mm diameter cylindrical relief	–0.197	–0.344	5.76
(l) Custom contoured insole with 6 x tissue stiffness, 25mm base diameter 2.5mm deep conical relief on top surface	–0.222	–0.373	7.80
(m) Custom contoured insole with 6 x tissue stiffness, 14mm diameter cylindrical relief, & constrained tissue movement	–0.167	–0.252	13.51
(n) Custom contoured insole with 2.5 x tissue stiffness, 14mm diameter cylindrical relief, & constrained tissue movement	–0.171	–0.249	14.47
(o) Custom contoured insole with 6 x tissue stiffness, 20mm diameter cylindrical relief, & constrained tissue movement	–0.172	–0.256	14.06
(p) Custom contoured insole with 6 x tissue stiffness, 25mm base diameter 2.5mm deep conical relief on top surface, & constrained tissue movement	–0.168	–0.254	13.52
(q) Custom contoured insole with 6 x tissue stiffness, 25mm base diameter 3 mm deep conical relief on bottom surface, & constrained tissue movement	–0.169	–0.254	13.69
(r) Custom contoured insole with 2.5 x tissue stiffness, 25mm base diameter 3 mm deep conical relief on bottom surface, & constrained tissue movement	–0.170	–0.250	14.36

Table 5. Optimization of Pedorthic Treatment for Vertical Calcaneal Osteophyte Stresses–Strains in Heel Pad Soft Tissue vs Pedorthic Insole Stiffness & Geometry

Pedorthic Insole	Heel Pad Maximum Cauchy Stress *(MPa)*	Heel Pad Maximum Green Strain *(mm/mm)*	Heel Pad Maximum Strain Energy Density *($x10^{-3}$ Joule / mm^3)*
(a) No Insole	–6.538	–0.497	822.9
(b) Standard flat insole with 1x stiffness of heel pad tissue	–5.160	–0.4916	529.0
(c) Standard flat insole with 2.5 x stiffness of heel pad tissue	–5.808	–0.495	671.7
(d) Standard flat insole with 6 x stiffness of heel pad tissue	–6.170	–0.496	748.8
(e) Standard flat insole with 6 x tissue stiffness & 25mm base diameter 2.5mm deep conical relief on bottom surface	–4.634	–0.486	430.2
(f) Standard flat insole with 6 x tissue stiffness & 25mm base diameter 2.5mm deep conical relief on top surface	–4.544	–0.486	415.0
(g) Standard flat insole with 6 x tissue stiffness & 20mm diameter cylindrical relief	–2.796	–0.458	216.5
(h) Standard flat insole with 6 x tissue stiffness & 14mm diameter cylindrical relief	–4.563	–0.485	423.8
(i) Custom contoured insole with 6 x tissue stiffness & 14mm diameter cylindrical relief	–2.270	–0.445	160.1
(j) Custom contoured insole with 2.5 x tissue stiffness & 14mm diameter cylindrical relief	–2.186	–0.440	152.8
(k) Custom contoured insole with 6 x tissue stiffness, 20mm diameter cylindrical relief	–1.470	–0.3972	72.3
(l) Custom contoured insole with 6 x tissue stiffness, 25mm base diameter 2.5mm deep conical relief on top surface	–1.946	–0.4353	119.5
(m) Custom contoured insole with 6 x tissue stiffness, 14mm diameter cylindrical relief, & constrained tissue movement	–0.351	–0.252	13.4
(n) Custom contoured insole with 2.5 x tissue stiffness, 14mm diameter cylindrical relief, & constrained tissue movement	–0.318	–0.249	14.5
(o) Custom contoured insole with 6 x tissue stiffness, 20mm diameter cylindrical relief, & constrained tissue movement	–0.184	–0.256	14.0
(p) Custom contoured insole with 6 x tissue stiffness, 25mm base diameter 2.5mm deep conical relief on top surface, & constrained tissue movement	–0.317	–0.254	13.5
(q) Custom contoured insole with 6 x tissue stiffness, 25mm base diameter 3mm deep conical relief on bottom surface, & constrained tissue movement	–0.304	–0.254	13.7
(r) Custom contoured insole with 2.5 x tissue stiffness, 25mm base diameter 3mm deep conical relief on bottom surface, & constrained tissue movement	–0.391	–0.264	14.3